

2002

Diaphragm bolt loosening retrofit for web gap fatigue cracking in steel girder bridges

David Joseph Tarries
Iowa State University

Follow this and additional works at: <https://lib.dr.iastate.edu/rtd>



Part of the [Civil Engineering Commons](#), and the [Structural Engineering Commons](#)

Recommended Citation

Tarries, David Joseph, "Diaphragm bolt loosening retrofit for web gap fatigue cracking in steel girder bridges" (2002). *Retrospective Theses and Dissertations*. 17270.
<https://lib.dr.iastate.edu/rtd/17270>

This Thesis is brought to you for free and open access by the Iowa State University Capstones, Theses and Dissertations at Iowa State University Digital Repository. It has been accepted for inclusion in Retrospective Theses and Dissertations by an authorized administrator of Iowa State University Digital Repository. For more information, please contact digirep@iastate.edu.

Diaphragm bolt loosening retrofit for web gap fatigue cracking in steel girder bridges

by

David Joseph Tarries

A thesis submitted to the graduate faculty
in partial fulfillment of the requirements for the degree of
MASTER OF SCIENCE

Major: Civil Engineering (Structural Engineering)

Program of Study Committee:
Terry J. Wipf (Co-major Professor)
Lowell F. Greimann (Co-major Professor)
Lester W. Schmerr

Iowa State University

Ames, Iowa

2002

Copyright © David Joseph Tarries, 2002. All rights reserved.

Graduate College
Iowa State University

This is to certify that the master's thesis of

David Joseph Tarries

has met the thesis requirements of Iowa State University

Co-major Professor

Co-major Professor

For the Major Program

Table of Contents

List of Figures	v
Chapter 1. General Introduction.....	1
Introduction	1
Steel Girder Bridge Literature Review.....	3
Health Monitoring Literature Review	5
Chapter 2. Bolt Loosening Retrofit for Fatigue Cracking in Steel Girder Bridges with I-beam Diaphragms	6
Abstract	6
Introduction	6
Previous Research	7
Bridge Description	8
Bridge Behavior and Condition.....	12
Instrumentation.....	15
Field Test Description	19
Experimental Results.....	21
Conclusions	27
Implementation Issues	27
References	28
Chapter 3. Bolt Loosening Retrofit for Fatigue Cracking in Steel Girder Bridges with Channel Diaphragms	30
Abstract	30
Introduction	31
Previous Research	31
Bridge Description	33
Bridge Behavior and Condition.....	37
Instrumentation.....	40
Experimental Approach.....	43
Experimental Results.....	46
Conclusions	52
Implementation Issues	52
References	53
Chapter 4. IA 17 Continuous Remote Monitoring of Bolt Loosening in an X-type Diaphragm Steel Bridge	55
Abstract	55
Introduction	56
Previous Research	57
Bridge Description	58
Experimental Approach.....	63
Test Procedure.....	68
Short-Term Experimental Results.....	71
Long-Term Experimental Results	76
Conclusions	78
Implementation Issues	79

References.....	80
Chapter 5. General Conclusions	81
General Discussion	81
Recommendations for Future Research	82
References.....	84
Acknowledgements.....	87
Appendix.....	88

List of Figures

Figure 1. Photograph of test bridge looking northwest.....	9
Figure 2. Bridge cross section looking toward direction of traffic.	10
Figure 3. Plan view of bridge superstructure.	10
Figure 4. Profile illustration of original interior girder.	11
Figure 5. Photograph of underside of the bridge looking northwest.....	11
Figure 6. Diagram of a typical diaphragm/girder connection in the negative moment region.	12
Figure 7. Photograph of typical web gap.	12
Figure 8. Exaggerated illustration of diaphragm bending due to differential deflection.	13
Figure 9. Depiction of web gap double bending.	13
Figure 10. Locations of confirmed cracks and drilled hole retrofits.	14
Figure 11. Photograph of typical drilled hole retrofit in a web.	14
Figure 12. Plan view of gage placement.	15
Figure 13. Web gap gradient instrumentation.	16
Figure 14: D1 strain instrumentation looking east and south.	17
Figure 15. Out-of-plane displacement instrumentation.	18
Figure 16. Test truck configuration.	19
Figure 17. Test truck placement on bridge deck.	20
Figure 18. Illustration of bolt loosening condition with bottom row tight.	21
Figure 19. G1 south gradient strain plots.	22
Figure 20. G2 north gradient strain plots.	23
Figure 21. D1 bending strain plots.	24
Figure 22. G1 and G2 out-of-plane displacement plots.	26
Figure 23. Photographs of test bridge looking northeast.	33
Figure 24. Plan view of bridge superstructure.	34
Figure 25. Cross section of bridge looking in direction of traffic.	34
Figure 26. Negative and positive moment region cross section of a girder.	35
Figure 27. Underside view of diaphragm and girders.	36
Figure 28. Diaphragm/girder connection in negative moment region.	36
Figure 29. Typical web gap in negative moment region.	37
Figure 30. Exaggerated illustration of diaphragm double bending.	38
Figure 31. Web gap double bending due to diaphragm rotation.	38
Figure 32. Confirmed crack and drilled hole retrofit locations.	39
Figure 33. Typical drilled hole retrofit in web with continued cracking.	40
Figure 34. Plan view of gage placement.	40
Figure 35. Web gap gradient instrumentation.	41
Figure 36. Diaphragm strain instrumentation looking northeast and southeast.	42
Figure 37. Out-of-plane displacement instrumentation.	43
Figure 38. Test truck configurations.	44
Figure 39. Middle row tight diaphragm bolt condition.	44
Figure 40. Test truck placement on bridge in lanes.	45
Figure 41. G1 gradient gage strain plots.	47
Figure 42. G2 gradient gage strain plots.	48

Figure 43. D3 bending strain plots.	49
Figure 44. G1 and G2 out-of-plane displacement plots.	51
Figure 45. Photograph of bridge looking northeast.....	59
Figure 46. Plan view illustration of bridge superstructure.	59
Figure 47. Profile illustration of exterior girder with plates labeled.	60
Figure 48. Illustration of bridge cross section with stiffeners.	61
Figure 49. Diaphragm connection with web gap at stiffener clip.	61
Figure 50. Photograph of typical web gap.	62
Figure 51. Web gap bending from diaphragm rotation.	63
Figure 52. Instrumentation locations on superstructure.	63
Figure 53. Photograph of DAS enclosure on Pier 2.....	64
Figure 54. Web gap gradient gage location.....	65
Figure 55. Web gap transducer placement.	66
Figure 56. Diaphragm gage location looking north and east.	67
Figure 57. Illustration of G1 to G3 with diaphragm bolt loosening indicated.	69
Figure 58. Typical load truck configuration.....	70
Figure 59. G1 gradient strain plots.....	72
Figure 60. G2 gradient strain plots.....	73
Figure 61. D4 strain plots.....	74
Figure 62. Web Gap out-of-plane displacement plots.....	75
Figure 63. Longitudinal girder strain plots.....	76
Figure 64. Maximum G1 web gap strains and G2 longitudinal strains for individual truck loadings.	77

Chapter 1. General Introduction

Introduction

The Iowa Department of Transportation (Iowa DOT) has struggled with the problem of fatigue in steel girder bridges for many years. Many of Iowa's 908 steel girder bridges have been in service for more than 30 years and signs of age are beginning to appear. 63 of those bridges are considered by the Iowa DOT to be fracture critical. Approximately 55 percent of the fracture critical bridges have been developing fatigue cracks in the girder webs at connections with the diaphragms, especially in interstate bridges. Engineers are most concerned about bridges with large average daily traffic loads, such as interstates, because of the large loads and frequency of load cycles. In the 1980's the Iowa DOT began installing a drilled hole retrofit at the terminus of the fatigue cracks in an attempt to slow the propagation of the cracking by changing the stress concentration at the crack tips. This retrofit has not always been successful in controlling fatigue cracking. The failure could be the result of two scenarios. The hole may not have been drilled at the actual crack terminus due to difficulty in visually locating this point. Also the stress cycles created in the web may be too great to be controlled by the drilled hole retrofit. The result for both is continued crack growth.

Regardless of the cause of continued cracking in steel girder bridges, the Iowa DOT sanctioned research on a different retrofit to replace the drilling. In the 1990's research was conducted at Iowa State University on a new retrofit based on reducing the cause of the fatigue cracking in the web, rather than controlling the symptom by drilling. This retrofit was based on an understanding of the response of the bridge superstructure to traffic loading. Researchers concluded that cracking in the webs near the diaphragms is primarily a result of forces transferred to the girders by the diaphragms. Differential deflection of the girders with varying traffic loads creates a resisting force in the diaphragms because of the rigid connection with the girders. This force acts directly on the girder webs and causes out-of-plane displacement. Over time, the out-of-plane displacement results in fatigue cracking, especially in bridges with greater and heavier traffic loading.

Given this information, the new retrofit consisted of loosening the bolts at diaphragm/girder connections to relieve the force generated by the diaphragms and

differential deflection of the girders. Loosening the bolts in the diaphragm/girder connection allows the diaphragms to rotate with the differential deflection instead of bending and placing force on the web.

Testing of the retrofit was carried out through short-term field testing of K-type and X-type diaphragm bridges [1,2]. Test bridges were instrumented with strain gages and displacement gages. Load tests were completed on the bridge before and after the bolts were loosened in a sample diaphragm area. Following testing the bolts were returned to the tight condition.

The results from these tests showed that the bolt loosening retrofit reduced strain and displacement in the gap a considerable amount, however several questions were raised about the implementation of this retrofit on in-service bridges. These include how effective the retrofit is on other types of diaphragm bridges, what the long term affects of the retrofit on the superstructure are, and how the stability of the girders is affected by loosening the diaphragms. These questions led to the current research at Iowa State University involving the bolt loosening retrofit.

Three reports are presented in this thesis that describe the resulting research, focusing on determining the viability of implementing bolt loosening as a practically applicable retrofit for web gap fatigue cracking. These reports discuss the changes in bridge response before and after the retrofit was installed, highlighting the cause and effect of the retrofit on strain and displacement of the girder webs.

Field-testing was performed on an I-beam diaphragm bridge and a channel diaphragm bridge to study the effect of the retrofit on other types of diaphragm bridges. Long-term field-testing was completed on an X-type diaphragm bridge, which was part of the 1990's research to study the effect of the retrofit over time. In addition to the retrofit data, new methods of continuous remote monitoring were developed as a result of the long-term research. These new methods will prove to be important in Iowa's future endeavors into health monitoring of bridges.

Stability of the bridges was not directly addressed in these reports. American Association of State Highway and Transportation Officials (AASHTO) design specifications were consulted regarding girder stability on the bridges and were found to be sufficiently

stable without the diaphragms. However, further research should be performed on this subject. The data collected for the reports will be used by other researchers at Iowa State University in the future to prepare in-depth finite element models of the bridges which will be used to further support the effectiveness and safety of this retrofit.

Steel Girder Bridge Literature Review

A literature review of past research involving steel girder bridges was completed prior to field-testing. This provided insight into the cause and location of fatigue cracking investigated by other researchers, as well as retrofit methods in use. Bridge health monitoring and remote monitoring was also reviewed to prepare for the long-term testing.

Khalil and Wipf et al. performed the initial research on the bolt loosening retrofit at Iowa State University in 1998 [1,2]. The investigation was based on loosening the bolts in sample bridges across the state of Iowa. Bridges with K-type and X-type diaphragms, or cross frames, were used in load testing of the retrofit. Field test data were collected with trucks of known weights before and after a portion of the diaphragms were released. Data from these tests showed a reduction in the strain in the web gap fatigue area following implementation of the retrofit. Data from these tests were also used to calibrate finite element models (FEM) created for the bridges. These models were used to study the global effects of cracking in the webs on the bridge. The results of this research demonstrated that the retrofit reduced strain and displacement in the fatigue prone exterior web gaps by at least 48 percent. The bolt loosening retrofit was found to be an effective method of reducing the out-of-plane displacement and strain in the web gap, thus reducing or eliminating fatigue cracking in web gaps.

Fisher et al. [3-8] developed the retrofit currently in use by the Iowa DOT. Fisher's work on steel bridge fatigue addresses many typical failure locations, including the web gap due to out-of-plane deformation. Fisher, in conjunction with Keating, suggests that holes approximately 1 in. in diameter drilled at the terminus of each fatigue crack will control further cracking. In some cases this retrofit is sufficient to stop cracking, as long as the hole is properly drilled at the crack terminus and the web is provided enough flexibility following cracking to relieve strain in the web gap. If the web does not have enough movement other

methods are suggested for permanent repair. These can range from a bolted stiffener/top flange connection to a removal of the diaphragms in cases where AASHTO permits.

Cousins and Stallings et al. [9-14] have conducted considerable research in the area of diaphragm removal in cases involving fatigue in the web gaps. New requirements in the AASHTO bridge design manual allow for more freedom in lateral bracing, which has permitted this type of research. The primary scope of the research focused on load distribution factors. Tests were completed to determine the magnitude of load distribution performed by the diaphragms. Results revealed that the girder of maximum strain during load tests with the diaphragms in place increased 5 to 15 percent when the diaphragms were removed. Cousins and Stallings suggested that this was an insignificant amount when compared to conservative bridge rating calculations.

Azizimini et al. [15,16] completed calculations involving stability of multiple girder bridges with the diaphragms removed. Removal of the diaphragms in the negative moment region removes lateral torsional buckling support of the compression flange. The positive moment region has continuous support from the integral concrete deck. Azizimini's work determined the strength of the girders without the lateral bracing using the AASHTO design manual. Bridges with 3 spans of between 100 and 200 ft with no skew were studied. Calculations showed that the bridges under consideration had sufficient stability in the negative moment region so that compression flange bracing could be removed. Azizimini's research focused on common dimension multiple girder bridges. The results suggest that calculations on other similar bridges will verify that the diaphragms in the negative moment region are not necessarily needed for stability of the structure.

Miki et al. [17] and Zwerneman et al. [18], as well as Stallings, have studied fatigue cracking in locations outside the web gaps due to forces in the diaphragms. Cracking can occur in the stiffener plate, the diaphragm, connector plates, and welds. The location of the cracks discussed in this research outline other fatigue problems that can develop relative to diaphragm connections. Miki's work evaluates stiffeners that are welded to the top flange, which typically protects the web gap from fatigue damage. Numerous other crack locations have developed in the stiffener plate in response to this welded connection.

Health Monitoring Literature Review

Chajes et al. [19,20] completed research on bridge condition assessment. Data was collected from bridges under normal traffic loading to develop an accurate strain history. This information can be used to develop a predicted fatigue life of the structure. To collect this data a bridge monitoring system was installed on site. Instrument Sensors Technologies produced the data acquisition system. Intelleducer strain transducers from Bridge Diagnostics, Inc. were used to instrument the bridge. A NEMA 4 enclosure was installed at the bridge to protect the system from weather and vandalism. The battery power source was ideal for use in remote locations, and the data record trigger allowed the system to monitor inputs and record a burst of data when the selected trigger channel exceeded a threshold.

Aktan et al. [21] also performed research featuring a remote monitoring system. Research was based on the structural identification of a truss bridge; however, the data acquisition method used is applicable in many situations. The system was installed at the bridge site in a powered environmental enclosure and continuously monitored the bridge. The bridge was instrumented with anemometers, accelerometers, strain gages, and inclinometers. Small portions of data were acquired at different times of the day, and as data was collected from instrumentation, a video camera collected visual data to help in interpreting results. This system was connected to a laboratory by a modem. Future plans feature installing a high-speed internet connection. The remote location of the system with telephone connection to the laboratory is a great benefit of this system.

Chapter 2. Bolt Loosening Retrofit for Fatigue Cracking in Steel Girder Bridges with I-beam Diaphragms

A paper to be submitted to the Journal of Bridge Engineering

David Tarries, Terry J. Wipf, Lowell Greimann

Abstract

Many of Iowa's multiple steel girder bridges have shown signs of fatigue cracking due to out-of-plane deflection of the web in the region of the diaphragm connections. This fatigue prone web gap area is located in the negative moment regions where the diaphragm stiffener is not attached to the top flange. The Iowa Department of Transportation (Iowa DOT) has attempted to stop fatigue crack propagation but with limited success. For this reason the Iowa DOT has requested research on a new field retrofit to loosen the bolts in the connection between the diaphragm and the girders. The intent of this research is to show that loosening the bolts at the diaphragm/girder connection in steel girder bridges with I-beam diaphragms is effective in reducing strain in the web gap.

Select web gaps in the negative moment region on an interstate bridge were instrumented with strain gages and deflection transducers to measure out-of-plane displacement. Field tests, using loaded trucks of known weight and configuration, were conducted on the bridge before and after implementing the bolt loosening retrofit.

Results indicate that loosening the diaphragm bolts reduces out-of-plane deflection and strain in the web gap. The reduction in strain correlates to less fatigue in the web gaps and an increase of in-service life of the bridge.

Introduction

Multiple steel girder bridges are common in many portions of the United States. Many states have adopted the steel girder and reinforced concrete deck design as a standard bridge style. Over the past few decades the Iowa DOT and other state DOT's have noted a common fatigue problem among multiple steel girder bridges subjected to heavy traffic volumes; fatigue cracking has been occurring in the girder webs of older bridges at

diaphragm connections. Differential deflection between girders is the main catalyst for this fatigue. As the girders deflect, forces are transferred through the diaphragms to the girder webs. Data shows that the web gap (the area between the web stiffener weld and the top flange fillet) is susceptible to fatigue from these forces. This susceptibility is the focus of this investigation.

Engineers have proposed many solutions for this problem, ranging from stiffener bracing to local web removal. A new retrofit to prevent this cracking has been developed by the Iowa DOT [1,2] that involves loosening the bolts in the diaphragm/girder connections. The diaphragms in multiple girder bridges are primarily intended to transfer wind loads and distribute live load as well as bracing the compression flange of the girders. These are functions that the deck, when hardened, is capable of performing in most cases. Concerns involving adjustment or removal of diaphragms stem from proper bracing of the compression flange in the negative moment region and sufficient distribution of load between girders. Other researchers have demonstrated that these concerns are not always a determining factor in diaphragm placement. Diaphragms, in many cases, can be removed with negligible affects on the bridges loading response. The bolt loosening retrofit allows the diaphragms to remain in position to apply lateral support if required. This allows differential deflection between girders to rotate the diaphragms instead of building up forces that cause fatigue. The objective of this report is to discuss the application of the bolt loosening retrofit to multiple girder bridges with I-beam diaphragms and to document strain and displacement reductions in the web gaps. This report presents supporting data that this method is an effective retrofit for bridges experiencing fatigue in the web gap.

Previous Research

Khalil et al [1,2] researched a bolt loosening retrofit on multiple steel girder bridges with K-type and X-type diaphragms. The study concluded that the bolts in diaphragm/girder connections could be loosened to reduce strain and deflection in the web gaps. The X-type diaphragms exhibited more effective results than the K-type diaphragms when the retrofit was implemented on a number of test bridges in Iowa. Data revealed that the strain and displacement typically reduced by a minimum of 48 percent in exterior girders.

Many researchers have studied fatigue in web gaps and tested retrofits. Stallings and Cousins et al. [3,4,5,6] studied the effects of removing diaphragms completely from multiple girder steel bridges. Their research focused on load distribution between girders through the diaphragms and the importance of the diaphragms in this role. They found that stress in the maximum stress girder increased from 5 to 17 percent when the diaphragms were removed. Their work proposes that removing the diaphragms has minimal impact on the distribution of load between girders and has little affect on design parameters.

Azizinamini [7] studied the effects of removing diaphragms in accordance with the AASHTO Bridge Design Specifications. Azizinamini calculated the lateral torsional buckling stability for multiple girder steel bridges following removal of the diaphragms. Calculations supported safe removal of diaphragms in the particular multiple steel girder bridges documented. Azizinamini's bridges were similar to those found in Iowa and suggest that similar calculations could support removal of diaphragms there as well.

Fisher et al. [8,9] has done extensive research on steel bridges. Much of Fisher's work has focused on the source of cracking in steel bridge members and techniques for repairing/retrofitting known problems. Fisher states that out-of-plane deflection of the web gap due to differential deflection of the girders is a major contributor to web gap fatigue. Bridges with a skew tend to have greater girder differential deflection and therefore more fatigue cracking. The work has led to the development of a retrofit for use on cracks that run perpendicular to the main stress in the girder. Retrofit consists of drilling holes at the terminus of these cracks to limit their propagation and, in some cases, to stop cracking altogether. The Iowa DOT has been utilizing this technique to repair its damaged web gaps for the past 20 years.

Bridge Description

Bridge 5075.5R080, shown in Fig. 1, is a two lane, three span, multiple steel girder bridge crossing the North Skunk River near Kellogg, Iowa. It was built in 1960 and supports eastbound traffic on Interstate 80 in central Iowa. The bridge cross section, with diaphragms, is shown in Fig. 2. The original structure was built with four welded A36 steel plate girders, but in 1978 a fifth plate girder (G5) was added to widen the driving lane shoulder. I-shaped diaphragms support all the girders laterally at a spacing of approximately 20 ft. The bridge

has multiple examples of web gap fatigue cracking near diaphragm connections in the negative moment region. The webs with cracks have had holes drilled in the web following crack discovery. Cracking occurs in the new girder as well as the original girders, especially in the exterior girders. The high occurrence of fatigue cracking in this bridge makes it a critical bridge for fatigue and a prime specimen for retrofit testing.

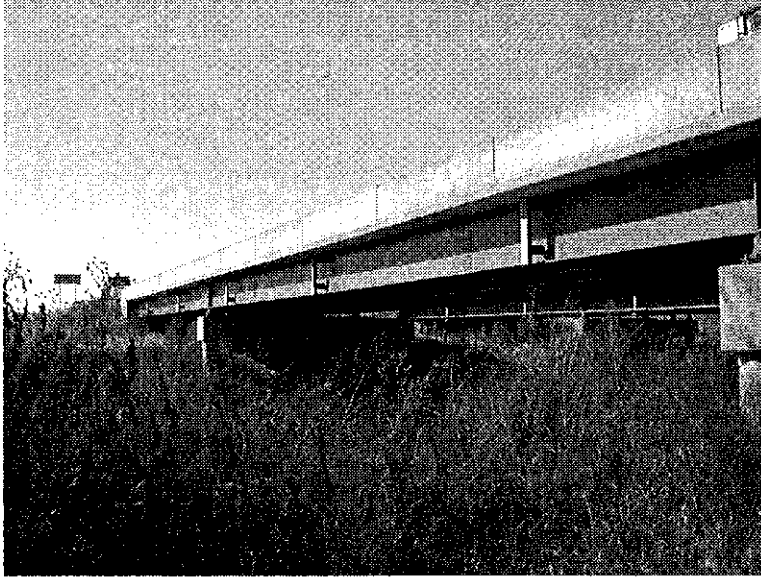


Figure 1. Photograph of test bridge looking northwest.

Figure 2 shows the two 12 ft traffic lanes centered between the four original girders (G1-G4). Figure 3 reveals a plan view of the bridge superstructure, which has a 10-deg skew with the substructure. The western span, Span 1, is 82 ft-6 in., the center span, Span 2, is 105 ft, and the eastern span, Span 3, is 80 ft-6 in.. The five welded plate girders support an 8-in. concrete deck integral with the top flange.

Girders G1 to G4 are spaced at 9 ft-8 in. and girder G5 is spaced at 6 ft-3 in.. As depicted in Fig. 4, the original girders have PL46 \times 3/8 webs with flanges between PL10 \times 1 1/4 to PL16 \times 1 3/4. The interior and exterior girders have different cross sections with similar plates sections. The new girder has PL44 \times 3/8 webs with flanges between PL10 \times 1 3/4 to PL16 \times 1 1/2. Splices in the girders are located 18 ft on either side of the piers. Each girder has shear angles to form a composite connection between the steel girders and reinforced concrete deck.

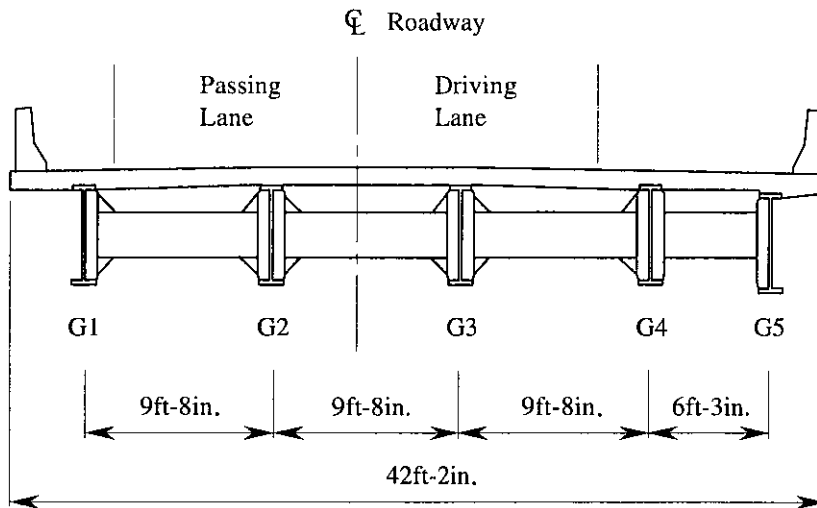


Figure 2. Bridge cross section looking toward direction of traffic.

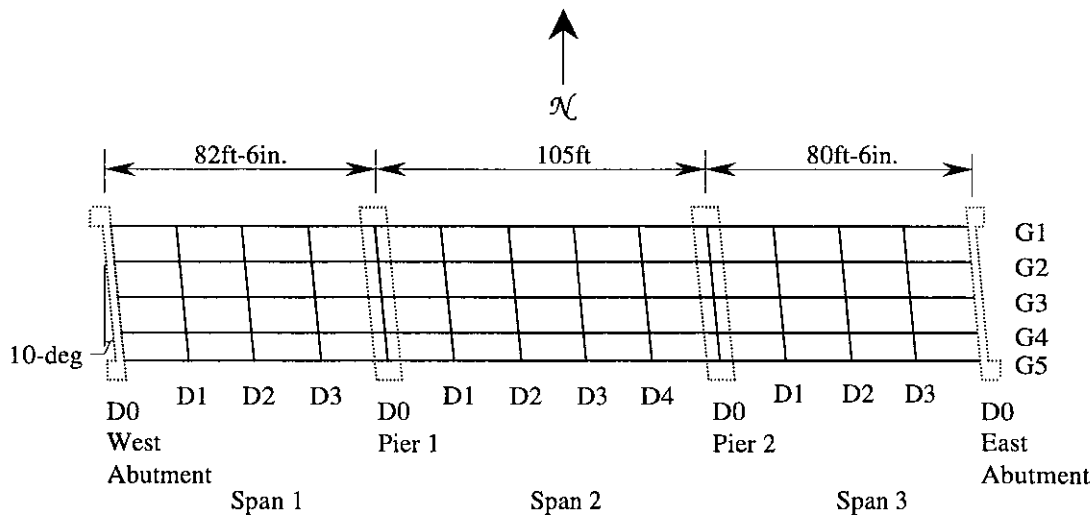


Figure 3. Plan view of bridge superstructure.

Figure 5 shows a photograph of typical diaphragms and girders on the bridge. The diaphragms are rolled W18 \times 50 sections in the spans, W21 \times 68 at the abutments, and W24 \times 76 at the piers. The diaphragms are spaced at 21 ft in the center span and 20 ft-7 in. in the end spans. They are bolted to vertical stiffeners as illustrated in Fig. 6. The vertical stiffeners are welded to the web and the compression flange of the girder. In the negative moment region above the piers the top flange is in compression and is not welded to the

stiffeners. Figure 7 depicts a typical web gap in a negative moment region. A web gap of about 1 in. in the vertical direction exists between the top of the stiffener weld and the bottom of the girder top flange where the stiffener is clipped. As noted previously, fatigue cracks have been found to occur in this region.

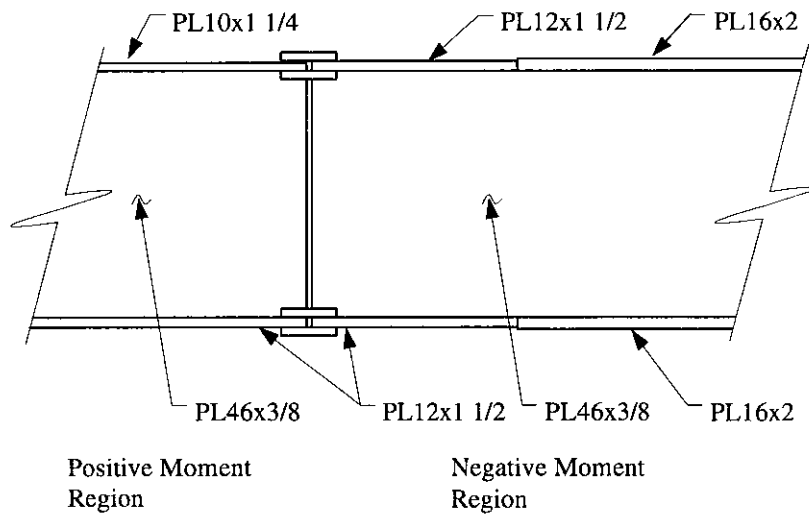


Figure 4. Profile illustration of original interior girder.

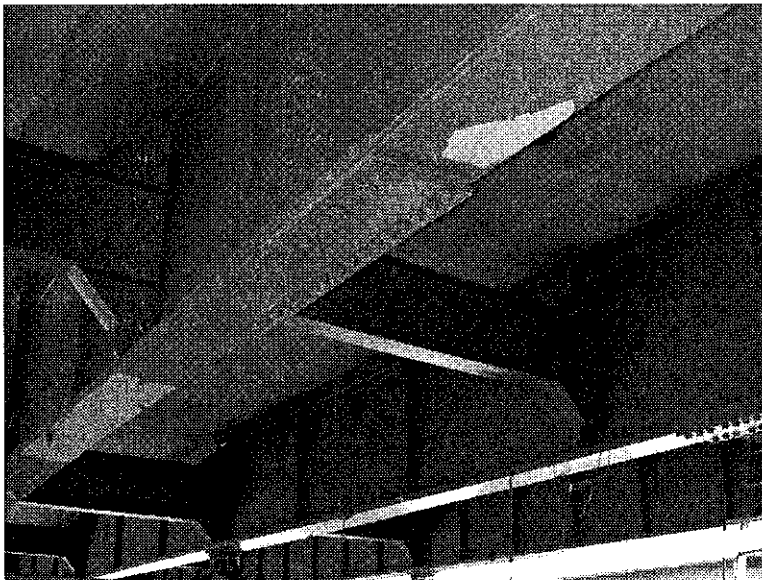


Figure 5. Photograph of underside of the bridge looking northwest.

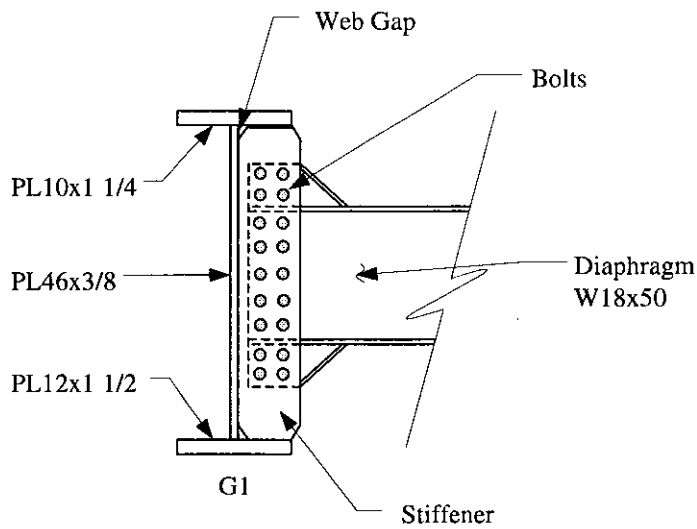


Figure 6. Diagram of a typical diaphragm/girder connection in the negative moment region.

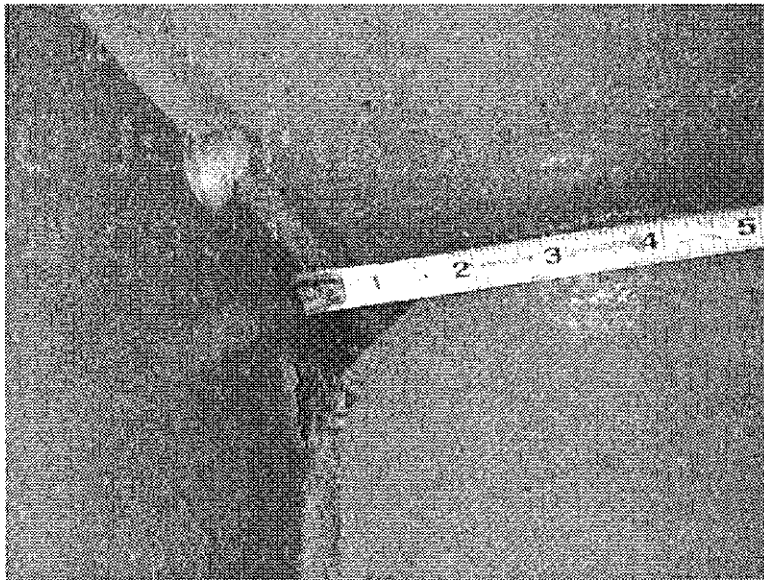


Figure 7. Photograph of typical web gap.

Bridge Behavior and Condition

Differential deflection of the girders causes bending of the diaphragms which is then transferred to the girder webs. This diaphragm action is shown in Fig. 8. The girder webs do not effectively resist this type of behavior, and out-of-plane deflection results in the web gap as illustrated in Fig. 9. Each vehicle crossing the bridge creates a load cycle on the girder

webs. Over time, fatigue cracks may develop in the web gaps. Due to the heavier loads and the greater number of cycles inherent in a large volume roadway, fatigue is more prevalent in interstate bridges.

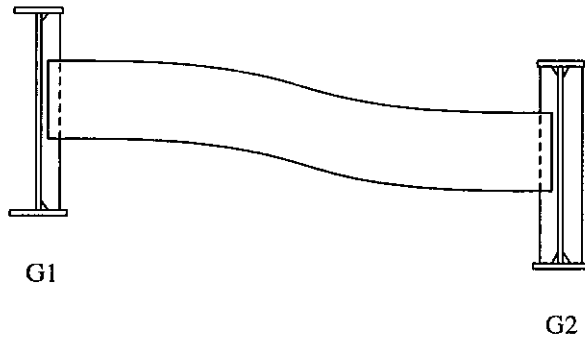


Figure 8. Exaggerated illustration of diaphragm bending due to differential deflection.

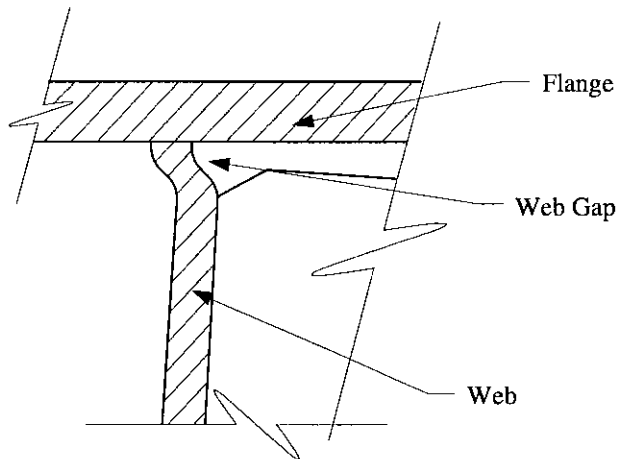


Figure 9. Depiction of web gap double bending.

Fatigue cracks have developed at many of the diaphragm/girder connections in the negative moment region on this bridge. A high concentration of the fatigue cracks appeared in the exterior girders and near the piers of all girders as illustrated in Fig. 10. The original exterior girder on the driving lane shoulder showed fatigue cracking similar to the new exterior girder. The Iowa DOT has been controlling fatigue cracking in this bridge by drilling holes through the web at the terminus of each crack as shown in Fig. 11. However,

crack propagation past the drilled holes, due to high strain or incorrect installation of holes, has demonstrated this method is sometimes ineffective.

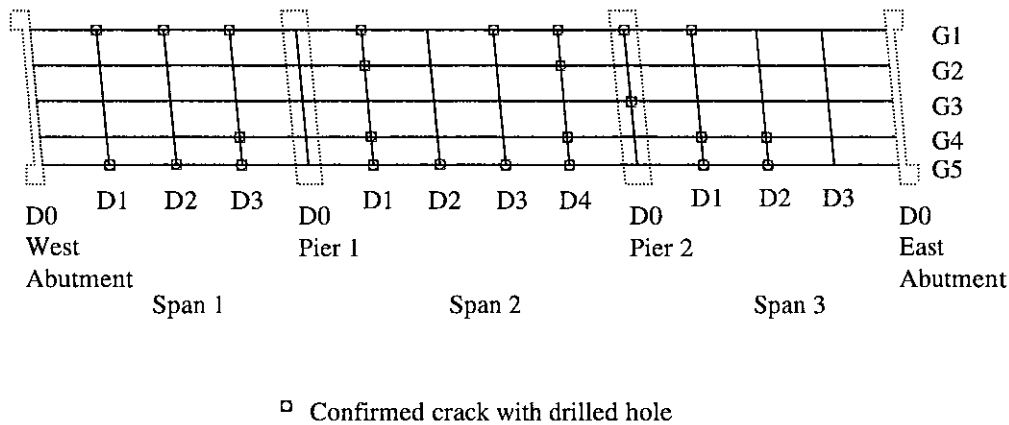


Figure 10. Locations of confirmed cracks and drilled hole retrofits.

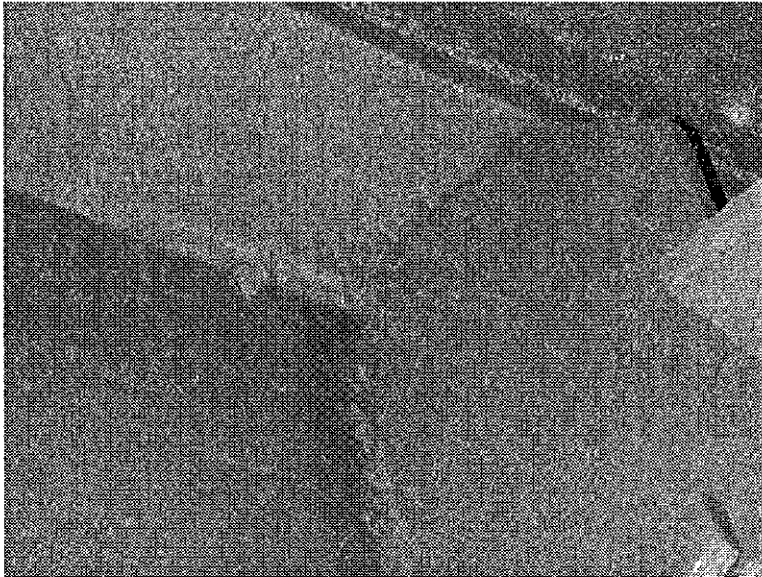


Figure 11. Photograph of typical drilled hole retrofit in a web.

Since out-of-plane displacement of the web is caused by resistance to rotation in the diaphragms relative to the girders, the rigidity at the diaphragm connection directly correlates to the level of out-of-plane displacement. A reduction in the rigidity of the connection would, in theory, allow rotation of the diaphragm and reduce bending in the web. Loosening

the bolted connection between the diaphragms and the girders would reduce this rigidity by changing the bolted rigid connection, which transfers moment to the web gap, to more of a pinned connection, which does not.

Instrumentation

A location between G1 and G2 in the negative moment region of Span 3 was selected for testing. Gages were set up at D1 in Span 3 as seen in Fig. 12. The location had fatigue damage in the G1 web gap but none in the adjacent G2 web gap. The retrofit holes in the web gap at damaged locations made mounting strain gages difficult and the resulting data less accurate, however, the location had the least damage of similar negative moment locations.

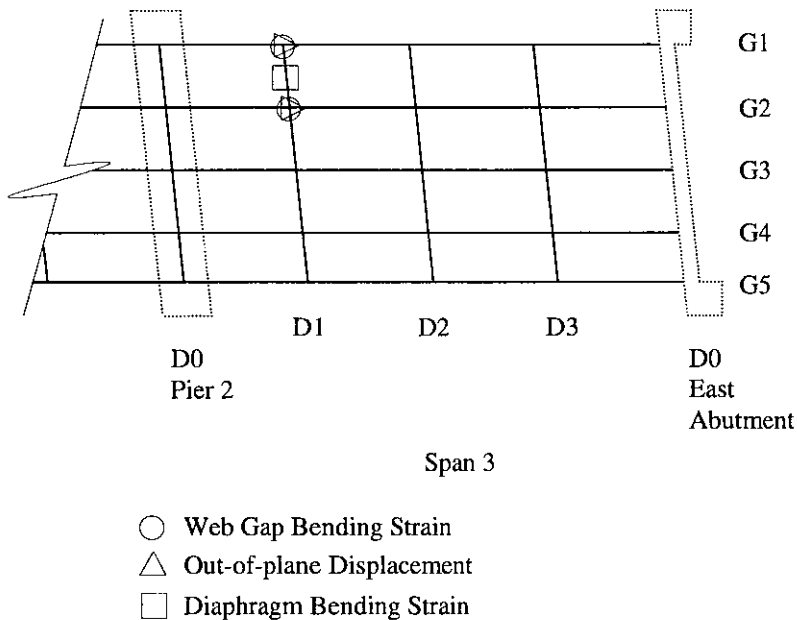
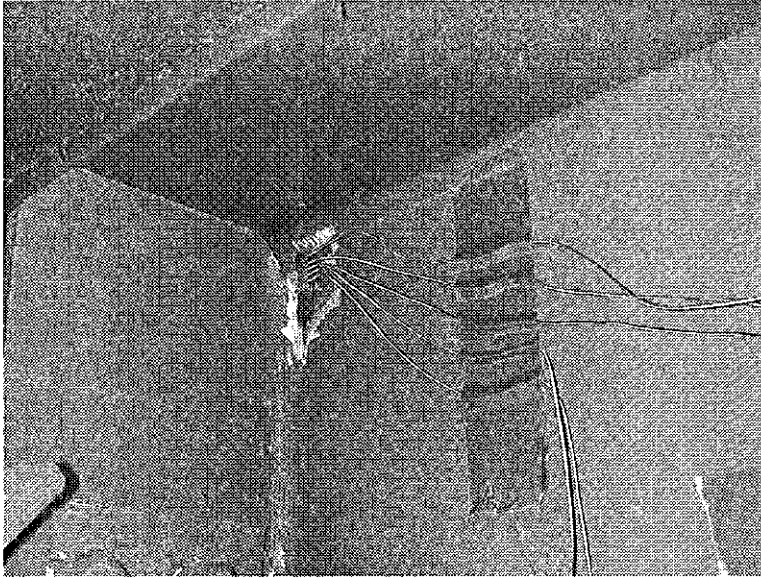


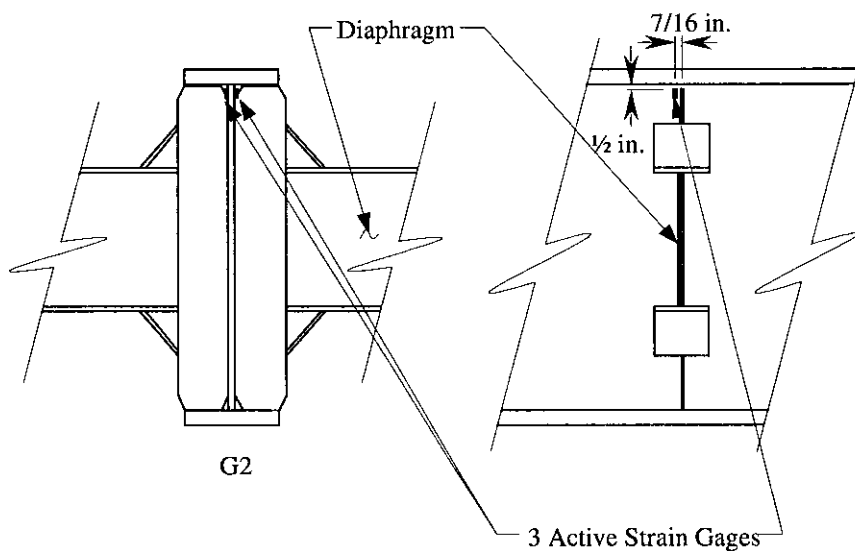
Figure 12. Plan view of gage placement.

Bondable 120-Ohm gradient strain gages were used to measure web gap bending strain to show the strain distribution in the web gap, which is important in determining the effectiveness of the diaphragm connection retrofit. The gradient gages consisted of five small foil backed strain gages factory assembled in a very small unit. They were mounted in, or as close to, the web gap as possible as seen in Fig. 13.

The web gap on this bridge was approximately 1 in. in depth. This made it difficult to place the gradient gages directly in the gap. In this investigation only the top three gages of the gradient were used for data interpretation because the other gages were too far from the web gap to produce reliable data. It is also important to note that the G1 web gap has a drilled retrofit, which forced the gradient gage to be mounted outside the web gap.



a. Close up of a typical gradient gage.



b. G2 gradient gage illustration looking east and south (typ.).

Figure 13. Web gap gradient instrumentation.

Strain gages were also used to measure diaphragm bending strain to determine the change in force transfer due to implementation of the retrofit. Gages were placed at the mid and quarter points of one section of D1 on the top and bottom flanges as shown in Fig. 14. The middle gages were 73 in. from the G1 centerline. The outer gages were 32 in. from the centerline of the nearest girder.

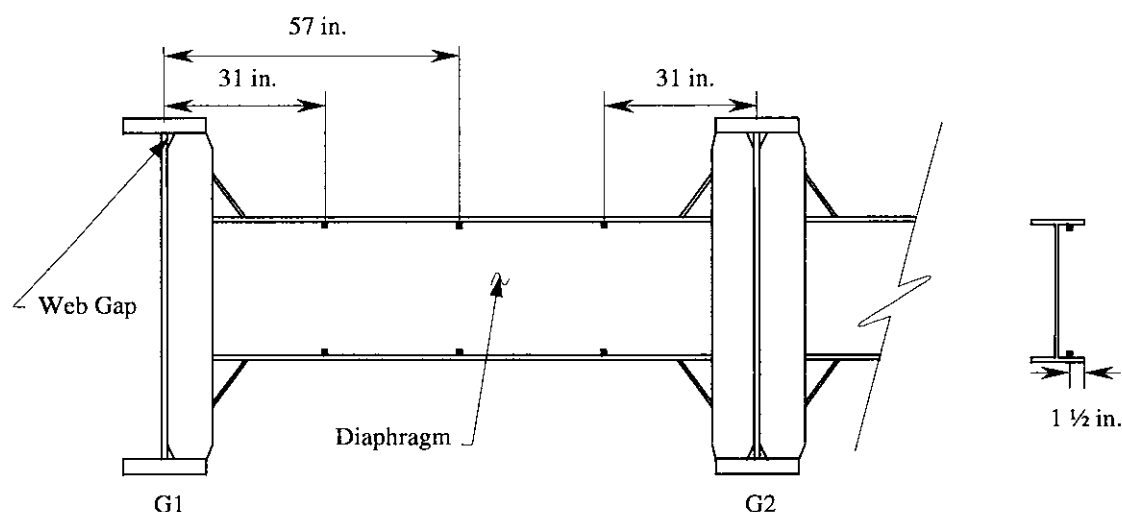
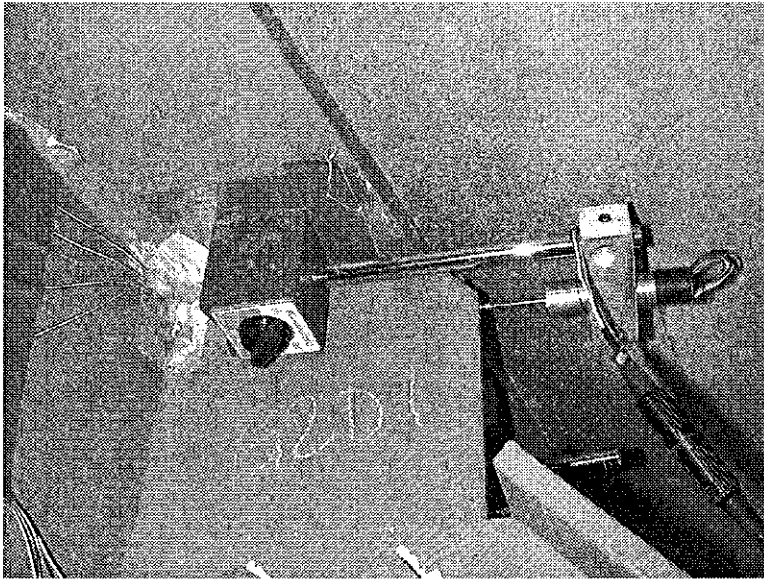


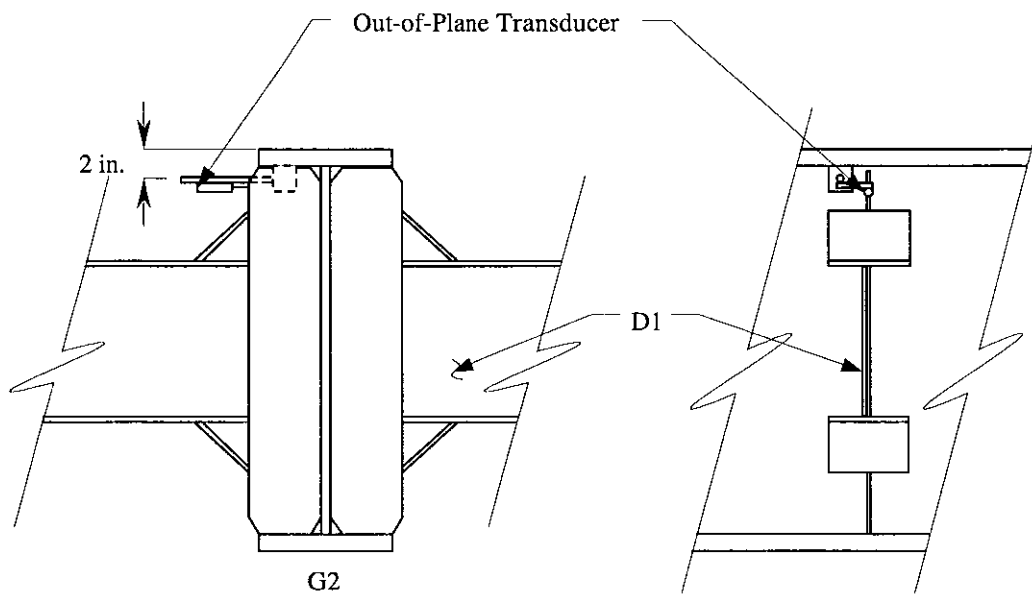
Figure 14: D1 strain instrumentation looking east and south.

Direct Current Displacement Transducers (DCDT's) were used to measure displacement of the web gaps. They were attached by magnetic stands to the girder webs and flanges at the connections with D1 as shown in Fig. 15. G1 and G2 each had a DCDT for out-of-plane displacement measurement. The gage measured out-of-plane displacement of the web by measuring the horizontal displacement of the web stiffener relative to the top flange.

Data from all gages were collected using a data acquisition system (DAS) at a sampling rate of 30 hertz. A total of 31 channels were used. Data were taken as the trucks approached the bridge and continued until both trucks had completely crossed the structure. The data collected from the DAS was imported into a spreadsheet program for analysis. The data from every test was plotted with initial offset removed and noise filtered to facilitate analysis.



a. G2 out-of-plane displacement transducer looking west.



b. G2 transducer illustration looking east and south (typ.).

Figure 15. Out-of-plane displacement instrumentation.

Field Test Description

Information on the standard Iowa DOT 3-axle dump trucks used to load test the bridge is shown in Fig. 16. The average width of a load truck was 6 ft between the rear duals and the length was approximately 18 ft between the front and rear axles. The trucks were loaded with sand to near 50,000 lbs. Truck 1 weighed 49,300 lbs and Truck 2 weighed 49,120 lbs.

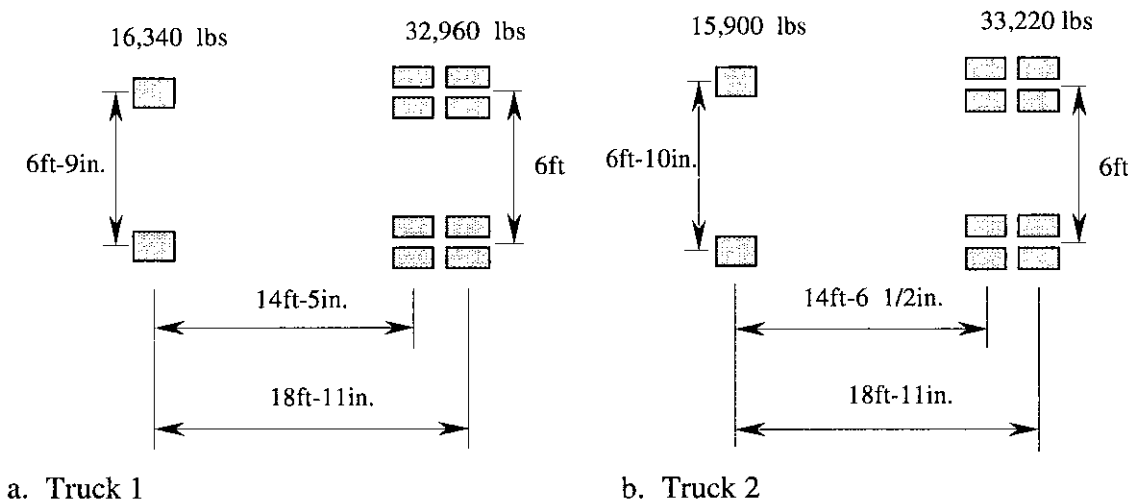


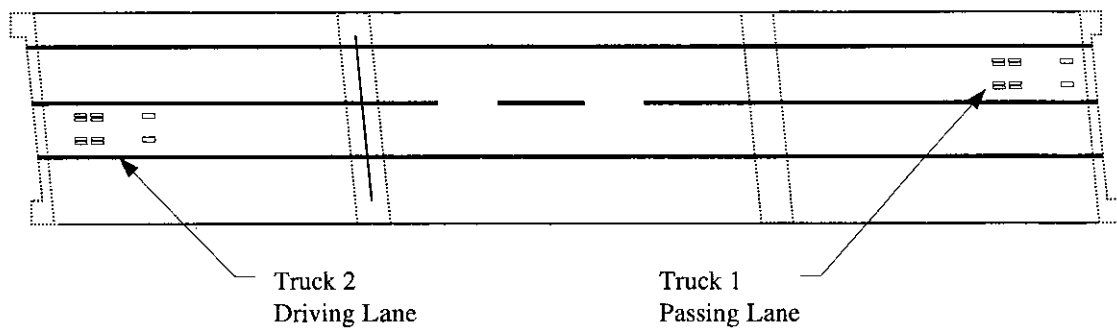
Figure 16. Test truck configuration.

Since the bridge is on an interstate with heavy, high-speed traffic, static tests were determined to be unsafe. The test trucks crossed the bridge at speeds of approximately 60 mph. The test vehicles were separated from ambient traffic by a slow pace vehicle, which held back traffic. This allowed for clean data acquisition during the test with only the load trucks on the bridge.

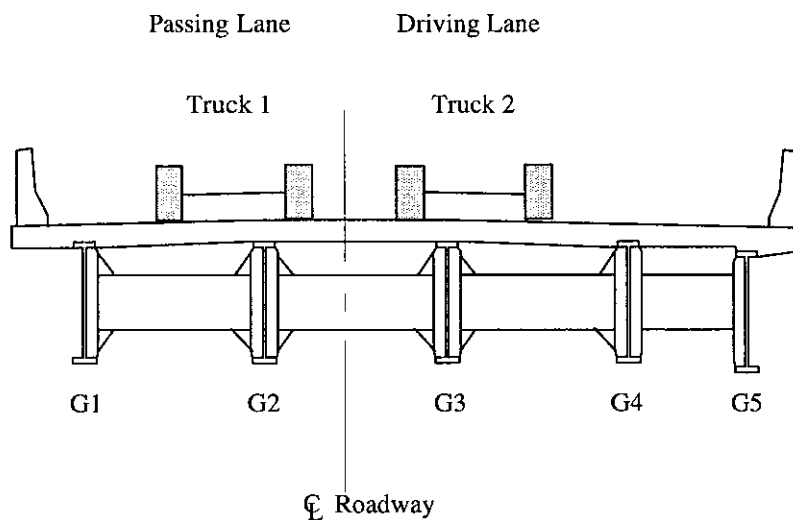
The data presented in this paper represents driving lane loading and passing lane loading, reflecting the typical loading pattern on the bridge. Two trucks crossed the bridge in staggered positions separated by approximately five vehicle lengths. Truck 1 traveled the passing lane and Truck 2 traveled the driving lane, with Truck 1 in the lead as illustrated by Fig. 17. The distance between test vehicles allowed individual data to be acquired for each lane, while running one test pass and minimizing ambient traffic delays. Tests were run with the diaphragm/girder connection bolts in three different bolt conditions: all bolts tight,

bottom row bolts tight, and all bolts loose. The bottom row tight condition is illustrated in Fig. 18. Bolts were loosened in the instrumented diaphragm as well as the adjacent diaphragm to prevent differential displacement between G2 and G3 from affecting the data.

When the bolts were loosened, it was noted that one or two bolts from each side experienced binding. The bound bolts were not tight, but were holding the weight of the diaphragm. The binding in these bolts did not noticeably hinder movement in the connection.



a. Plan view of superstructure with traffic lanes.



b. Cross section of bridge.

Figure 17. Test truck placement on bridge deck.

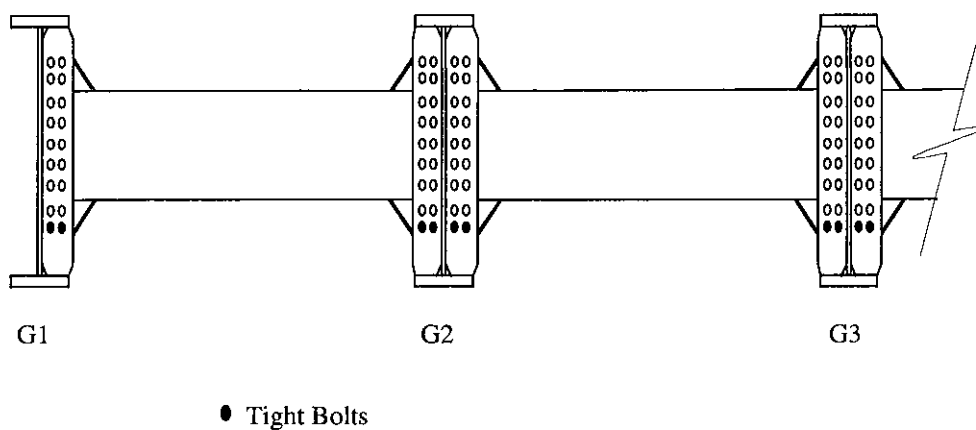
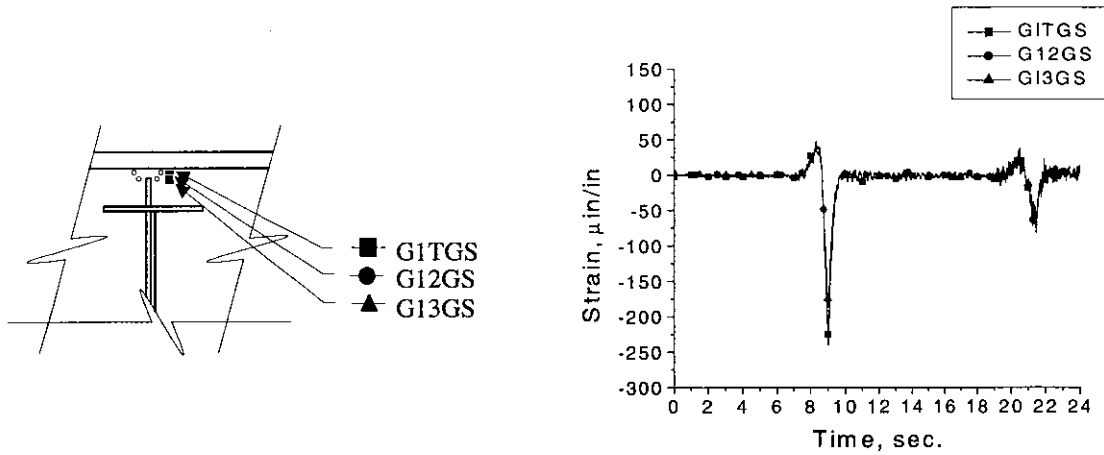


Figure 18. Illustration of bolt loosening condition with bottom row tight.

Experimental Results

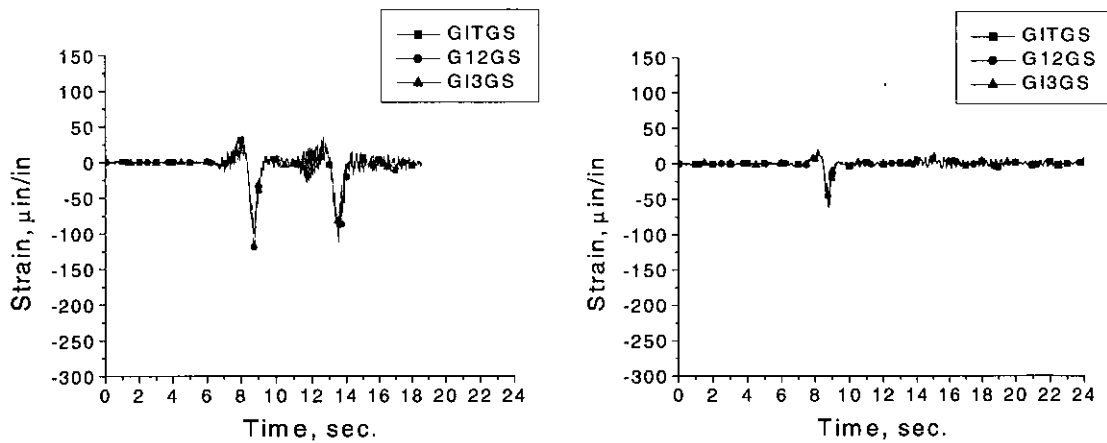
Figure 19 shows the strain gradient in the G1 web gap with the diaphragm/girder connection bolts in the tight, bottom row tight, and loose conditions. The first spike in the data, at approximately 10 sec., represents Truck 1 in the passing lane. The second spike, at approximately 20 sec., represents Truck 2 in the driving lane. The locations of the gages in the web gap near the holes are indicated on the adjoined illustration.

The strain in the G1 web gap is affected primarily by loading in the passing lane, as indicated by the larger strain in the first spike; therefore, the reductions in strain due to this loading are of the greatest interest. Loosening all but the bottom row of bolts reduces the strain in the G1 web gap by nearly 50 percent. Loosening all of the bolts in the connection reduces the strain by approximately 75 percent. This reduction is substantial considering that fatigue cracking is more common in exterior girders. The exterior girders have no diaphragm on the outside of the girder to help limit the deflection in the web gap, which typically results in more frequent cracking.



a. Gradient gage labels.

b. All bolts tight.



c. Bottom row bolts tight.

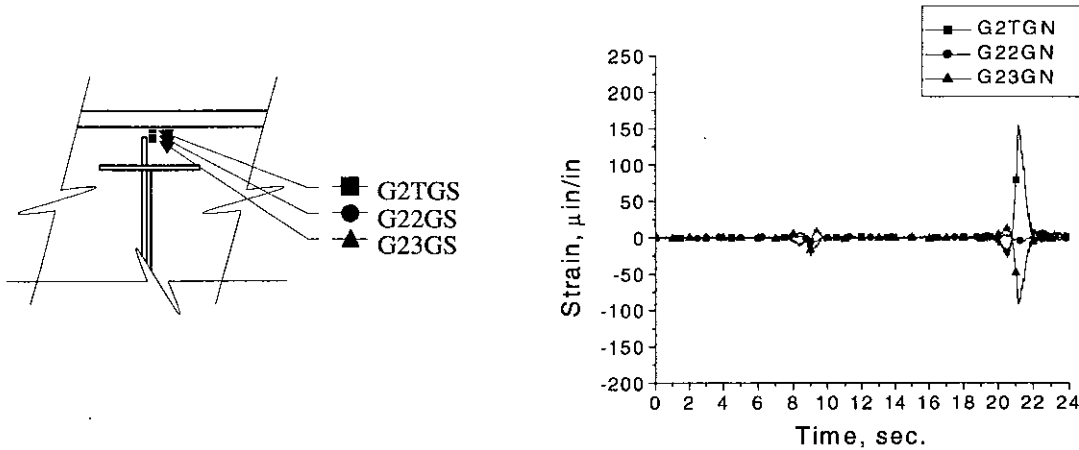
d. All bolts loose.

Figure 19. G1 south gradient strain plots.

Figure 20 shows the strain in the north side of the G2 web gap. The location of the load trucks is the same as the previous test, in the passing lane and the driving lane. The gage positions in the web are also illustrated.

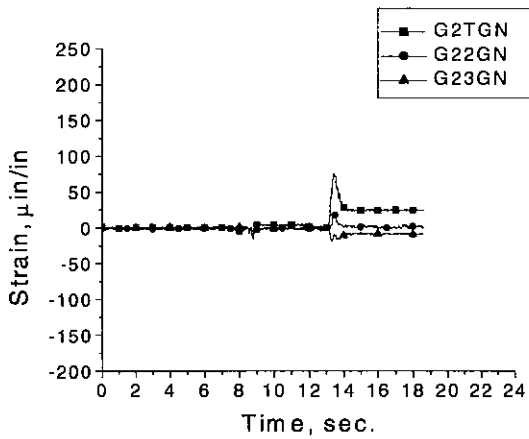
The strain in the G2 web gap is less than that in G1 and affected primarily by loading in the passing lane. The strains on the north and south sides of the webs are approximate negatives of each other with similar magnitudes and opposite signs. For this reason the south side of the web gap was not plotted. This reveals that the gages are in similar vertical

positions on each side of the web gap. Double bending of the web gap is indicated by the difference in value and sign of the strain within the gages in the web gap in the tight and bottom row tight conditions. This bending reaction was illustrated previously in Fig. 9.

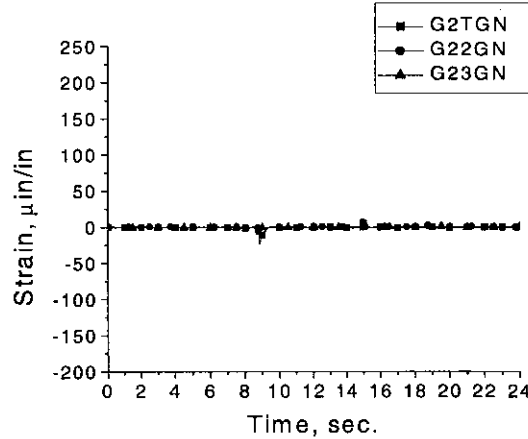


a. Gradient gage labels.

b. All bolts tight.



c. Bottom row bolts tight.



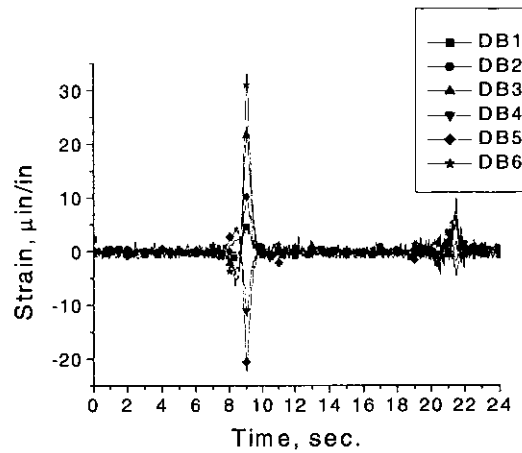
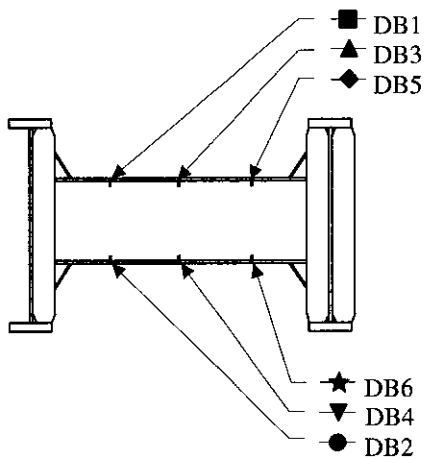
d. All bolts loose.

Figure 20. G2 north gradient strain plots.

The strain in the gap is reduced by 50 percent when all but the bottom row of bolts are loose, but the gages have residual strain following loading in the driving lane. This suggests that forces remain in the gap, resulting from slippage of the bottom row of tight

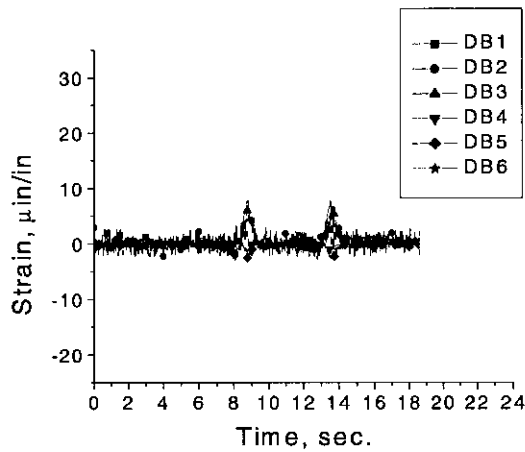
bolts. This is in contrast to no residual strain with all the bolts loose and the strains reduced approximately 90 percent.

Figure 21 shows the strains in D1 between G1 and G2 with the bolts in the tight, bottom tight, and loose conditions. The first spike is due to Truck 1 traveling in the passing lane and the second spike is Truck 2 traveling in the driving lane. An illustration of D1 between G1 and G2 shows the location of the gages on the flanges.

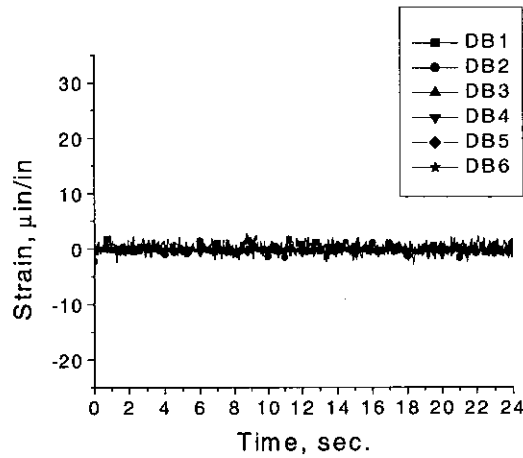


a. Diaphragm gage labels.

b. All bolts tight.



c. Bottom row bolts tight.



d. All bolts loose.

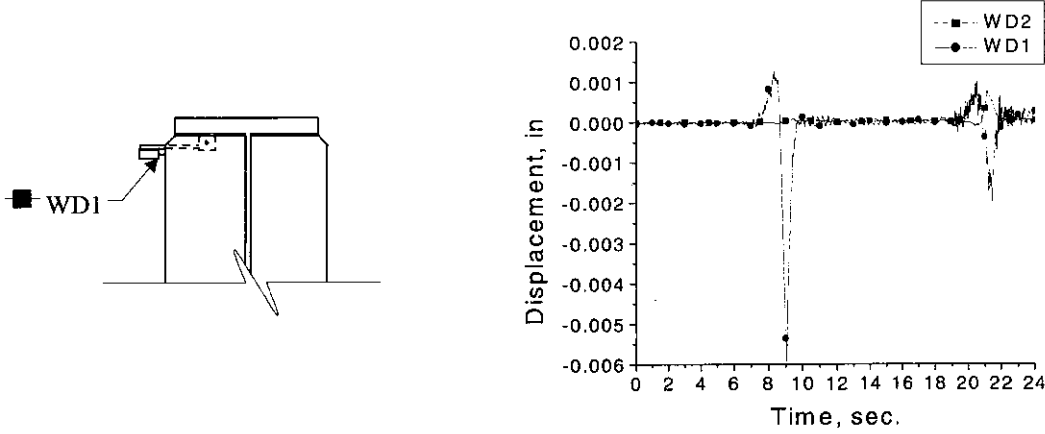
Figure 21. D1 bending strain plots.

The strain in the diaphragm is greater when the loading is in the passing lane than in the driving lane. Greater deflection of G1 relative to G2 when loading is in the passing lane is interpreted as the cause of this reaction. The positive and negative strains in the top and bottom flanges of the diaphragm show that it exhibits double bending between G1 and G2. This response, which was illustrated in Fig. 8., supports that bending forces are transferred through the diaphragms to the girder webs. A correlation can be seen between the strain in D1 and the strain in the G1 web gap. Peak strains in the web gap occur under the same condition as high peak strains in D1. That is, the relative strain magnitudes in the diaphragm under both lane loadings are proportional to those in the G1 web gap in Fig. 19.

The strain in the diaphragm with bottom row tight is reduced nearly 75 percent for loading in the passing lane but is reduced little for driving lane loading (the second peak). However, there is a complete reduction of strain in the diaphragm with all bolts loose. No noticeable change in strain is exhibited in the diaphragm above ambient noise when the bolts are loose. This illustrates that the bolt loosening retrofit effectively releases the force in the diaphragm due to differential deflection.

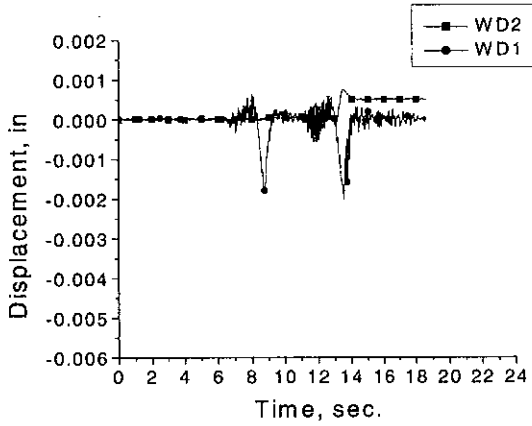
Figure 22 shows the out-of-plane displacement at webs of G1 and G2 with the bolts in the tight, bottom tight, and loose conditions. The data spikes represent the same truck loading as in the web gap figures. A typical illustration depicts the G1 transducer. The G2 transducer is a mirror of G1.

The out-of-plane displacement of the G1 web gap is much greater than the deflection in the G2 web gap when the load is in the passing lane with the bolts tight. The displacement of the G1 web gap is only slightly greater than the G2 web gap when the loading is in the driving lane. These values of displacement can be compared qualitatively to the strains in the web gaps in G1 and G2 as illustrated in Figs. 19, and 20. The bending implied by the strain in the web gaps deflects in the same direction as the recorded displacement of the web stiffener. The magnitude of the out-of-plane displacement also concurs with the web gap strain, which reveals greater deflection and strains in the exterior girder web gap than in the interior girder web gap when the driving lane is loaded.

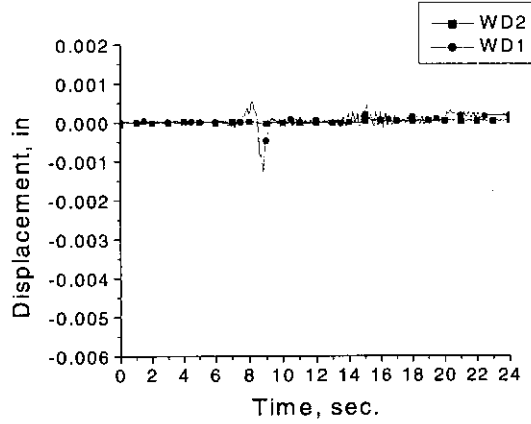


a. Out-of-plane transducer label (typ.).

b. Bottom row bolts tight.



c. All bolts tight.



d. All bolts loose.

Figure 22. G1 and G2 out-of-plane displacement plots.

A reduction of approximately 75 percent occurs in G1 between the tight and bottom tight conditions. Virtually no reduction occurs in the G1 web gap due to driving lane loading. There is also residual deflection in the G2 gap, similar to gradient strain gage results. The effect of the bottom row tight connection on the transfer of forces in the diaphragm was not studied in depth, but the data imply that the connection may be responsible for residual strain in the web gap and diaphragm.

Following bolt loosening the displacement in the G2 web gap is nearly eliminated and the displacement in the G1 web gap is reduced by more than 80 percent, which correlates with the reduction in web gap strains in G1 and G2.

Conclusions

The results of the field tests demonstrate that the retrofit reduces the strain and displacement in the web gap. The plots illustrate that the strain in the diaphragm is also eliminated by the retrofit. The forces in the diaphragm are the catalyst for web gap fatigue cracking and loosening the bolts effectively eliminates those forces.

As suggested by the data plots, partial loosening of the bolts is not nearly as effective at relieving strain and deflection in the web gap and diaphragms as is full loosening of the bolts. The remaining tight bolts in the partially loose condition are capable of transferring force through the girders and continue to displace the web gap out-of-plane.

Removal of the out-of-plane force in the web gap will significantly reduce bending in the web gap. Bending in the web following bolt loosening is uniform along the length of the girder, including the web gap. Bending has occurred in the webs at the top flange connections between the diaphragms since the bridge entered service and cracking has not initiated. Thus, the bolt loosening retrofit increases the fatigue life of the web gap significantly and fatigue cracking is effectively eliminated.

Implementation Issues

The bolt-loosening retrofit provides an inexpensive solution to web gap fatigue cracking and is also effective in preventing cracking in bridges that have not yet developed cracks. The service life of the bridges will increase when the force causing fatigue cracking in the web is removed. Before this retrofit is installed in in-service bridges, a few key points need to be addressed on an individual bridge basis.

Lateral support for the girders and stability of the structure with the diaphragms may be a concern. Bracing for lateral torsional buckling is only important in the negative moment region and the larger girder cross sections in the negative moment region generally provide adequate support over the unbraced length. Calculations were completed for the I-80 bridge based on ASSHTO LRFD design manual requirements that indicate adequate lateral support

if the diaphragms are removed. The stability results will differ for each bridge so individual checks need to be performed for each bridge retrofitted to ensure stability.

Lateral load distribution caused by diaphragms must also be addressed. The change in lateral load distribution of the bridge was not thoroughly tested in this research, but other researchers have found that most bridges are conservatively designed for lateral load distribution and show little change in lateral load distribution with the diaphragms removed. The bolt loosening retrofit relieves the force in the diaphragms and is equivalent to diaphragm removal in terms of lateral load distribution.

A system must be devised to ensure that the loosened bolts remain in place so the diaphragms are not at risk of falling due to nut loosening under vibrations of traffic loading. The method of connection was not researched, but a lock nut or double nut technique may be a solution. Any solution implemented should be periodically inspected to insure that it is functioning properly, and the bolts are secure but loose.

A bridge may be retrofitted if the particular design meets the listed requirements and any other requirements the engineer determines pertinent in each individual situation. Following installation of the retrofit the bridge must be monitored closely until the engineer is convinced the bridge is stable and the diaphragms are safely secured to the stiffeners in a loose manner.

References

1. T.J. Wipf, and L.F. Greimann, A. Khalil. Preventing Cracking at Diaphragm/Plate Girder Connections in Steel Bridges. Ames, Iowa: Center for Transportation Research and Education, Iowa DOT Project HR-393, Iowa State University, 1998.
2. A. Khalil. "Aspects in Nondestructive Evaluation of Steel Plate Girder Bridges", Dissertation, Iowa State University, Ames, Iowa, 1998.
3. T.E. Cousins, and J.M. Stallings. "Calculation of Steel Diaphragm Behavior", Journal of the Structural Division, Vol. 102, No. ST7, pp. 1411-1430, ASCE, July 1976.
4. J.M. Stallings, and T.E. Cousins, and T.E. Stafford. "Effects of Removing Diaphragms from Steel Girder Bridge", Transportation Research Record, Vol. 1541, pp. 183-188, Washington, D.C.: TRB, National Research Council, 1996.

5. T.E. Cousins, and J.M. Stallings. "Laboratory Tests of Bolted Diaphragm-Girder Connection." Journal of Bridge Engineering, Vol. 3, No. 2, pp. 56-63, ASCE, May 1998.
6. T.E. Cousins, J.M. Stallings, and T.E. Stafford. "Removal of Diaphragms from 3-Span Steel Girder Bridge." Journal of Bridge Engineering, Vol. 4, No. 1, pp. 63-70, ASCE, Feb. 1999.
7. A. Azizimini. "Steel Bridge Design Using AASHTO LRFD Bridge Design Specifications (1999 Interim)." Proceedings of National Bridge Research Organization Short Course, Kansas City: NaBRO, November 1999.
8. J.W. Fisher. Executive Summary: Fatigue Cracking in Steel Bridge Structures. Bethlehem, Pennsylvania: Advanced Technology for Large Structural Systems, Report No. 89-03, Lehigh University, 1989.
9. C.E. Demers, and J.W. Fisher. A Survey of Localized Cracking in Steel Bridges 1981 to 1988. Bethlehem, Pennsylvania: Advanced Technology for Large Structural Systems, Report No. 89-01, Lehigh University, 1989.

Chapter 3. Bolt Loosening Retrofit for Fatigue Cracking in Steel Girder Bridges with Channel Diaphragms

A paper to be submitted to the Journal of Bridge Engineering

David Tarries, Terry J. Wipf, Lowell Greimann

Abstract

Multiple steel girder bridges commonly exhibit fatigue cracking due to out-of-plane displacement of the web near the diaphragm connections. The fatigue prone web gap area is typically located in negative moment regions of the girders where the diaphragm stiffener is not attached to the top flange. In the past, the Iowa Department of Transportation (Iowa DOT) has attempted to stop fatigue crack propagation in these steel girder bridges by drilling holes at the crack tips. This retrofit is often only a temporary solution and a more permanent retrofit is required. A new field retrofit has been developed that involves loosening the bolts in the connection between the diaphragm and the girders. The intent of this research is to demonstrate that loosening the bolts at the diaphragm/girder connection is an efficient solution in preventing web gap fatigue cracking in steel girder bridges with channel diaphragms.

The web gaps in a negative moment region on an interstate bridge were instrumented with strain gages and deflection transducers. Field tests, using loaded trucks of known weight and configuration, were conducted on the bridges with the bolts in both the existing tight condition and after implementing the retrofit to measure the effects of loosening the diaphragm bolts.

Results indicate that loosening the diaphragm bolts reduces out-of-plane displacement and strain in the web gap. Reducing the strain in the web gap allows the bridge to support more cycles of loading before experiencing fatigue, thus increasing the service life of the bridge.

Introduction

Many of Iowa's aging multiple girder bridges are experiencing fatigue cracking. In multiple steel girder bridges cracking is most often associated with webs at diaphragms between the main girders. These bridges consist of multiple steel girders spanning longitudinally in the direction of traffic flow with perpendicular steel diaphragms and a concrete deck. Diaphragms are intended to laterally support the girders as required by the American Association of State Highway and Transportation Officials (AASHTO). They consist of crossing angles in an X-type or K-type pattern, I-beam sections, or channel beam sections connected to web stiffener plates on the girders. Fatigue cracks can form on the diaphragm itself or on the girder webs near diaphragm attachments. In Iowa bridges, cracking in girder webs in negative moment regions is prevalent. The fatigue occurs in the web gap of the girders above diaphragm connections (the web gap is the area between the top flange fillet weld and stiffener weld and is generally only an inch or two in depth).

Many retrofit possibilities have been explored, ranging from stiffening the diaphragm/girder connections to drilling holes in the girder web. A new idea has been developed which is intended to reduce the force causing the fatigue in the web gap. The bolts in the diaphragm/girder connection are loosened, giving diaphragms freedom to rotate with the differential deflection of the girders. The Iowa DOT recently supported research involving loosening the bolts of the diaphragm/girder connection of K-type and X-type diaphragms with positive results [1]. The research presented here features the same bolt loosening retrofit applied to bridges with channel diaphragms. The objective of this study is to install the bolt loosening retrofit to a section of a multiple steel girder bridge with channel diaphragms and document the results reflected in strain gages and displacement transducers in the web gap.

Previous Research

Khalil and Wipf et al. [1,2] performed the initial research on the bolt loosening retrofit for the Iowa DOT. The bridges tested had K-type and X-type diaphragms. The focus of the research was on the web gaps in negative moment regions. Strain and displacement instrumentation was arranged in web gaps adjacent to a test diaphragm, which was loosened during the tests. Load trucks crossed the bridge in the original and retrofitted state. Results

showed a minimum reduction of 48 percent of strains in the exterior negative moment region web gaps with maximum reductions nearing 85 percent. The bolt loosening retrofit proved to be more effective in X-type diaphragm bridges.

Many researchers have published papers on fatigue in steel girder bridges. Fisher et al. [3,4] has studied fatigue cracking in steel bridges in a number of common locations, including the web gap of multiple steel girder bridges. He suggested that a temporary retrofit be implemented as soon as a crack is discovered. A hole ranging from $\frac{3}{4}$ in. to 1 in. in diameter should be drilled at the terminus of each crack. This procedure will change the stress concentration pattern around the end of the crack and is intended to stop crack propagation until a permanent retrofit can be implemented, and in some cases stop crack propagation altogether.

Stallings and Cousins et al. [5,6,7,8] have done research involving removal of the diaphragms to eliminate fatigue cracking caused by diaphragm live load reactions in multiple steel girder bridges. Load tests were performed on three span bridges in which the diaphragms were removed and the lateral load distribution was investigated. An increase in stress in the maximum stress girder from 6 to 15 percent was noted. According to the researchers, this stress increase is acceptable in most cases and will not affect a bridge's load rating. Wind loading and other lateral loads may not require the support of all diaphragms. They have determined that in many cases the diaphragm can be removed from a constructed steel girder bridge. In general the integral concrete deck performs the main function of the diaphragms, distributing lateral load, supporting the girders from lateral loading, and preventing lateral torsional buckling. Using these criteria it was determined that some or all of a bridge's diaphragms could be removed safely on a case-by-case basis. Each bridge needs to be evaluated for lateral load and lateral support before diaphragms are removed.

Azizinamini et al. [9] has also evaluated the possibility of removing diaphragms from multiple steel girder bridges. Theoretical calculations were carried out using the AASHTO Bridge Design Specifications to determine the effect of diaphragm removal on lateral torsional buckling. On the bridges Azizinamini tested, the calculations determined that removal of the diaphragms would not affect lateral torsional stability. Lab tests were performed on a constructed portion of a steel girder bridge to test lateral load distribution.

Diaphragms were found to affect load distribution a small amount, but not a significant amount. Azizainamini concluded that diaphragms could be removed in some conditions at the discretion of the bridge owner.

Bridge Description

Bridge 2700.0R035 is a multiple steel girder bridge constructed in 1969 of A36 steel. It carries northbound traffic of Interstate 35 across U.S. Highway 69 on the border of Iowa and Missouri at Iowa milepost 0 as pictured in Fig. 23. It is a three span structure with five steel girders supporting an 8-in. concrete deck. The piers are angled 40-degrees to the girder longitudinal axis and are numbered 1 and 2 from South to North. The girders and diaphragms are designated G1 through G4 and D1 through D4 with D0 indicating diaphragms at piers or abutments as shown in Fig. 24. The deck is 43 1/3 ft wide and contains two lanes with shoulders. Shear lugs on the top flanges of the girders create a composite structure between the steel girders and the concrete deck. The centerline of the roadway is 2 ft west of the center girder as illustrated in Fig. 25. The southern and northern spans, Spans 1 and 3 respectively, are 58 ft-6 in. in length. The center span, Span 2, is 75 ft in length.

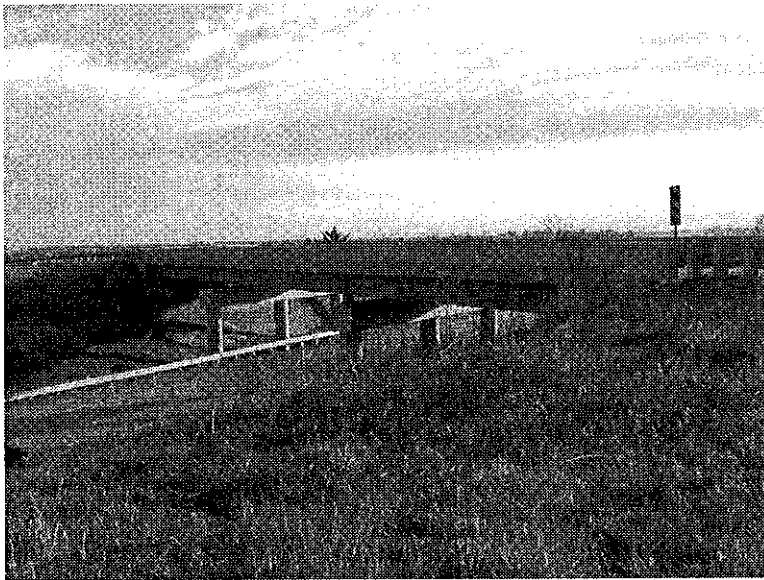


Figure 23. Photographs of test bridge looking northeast.

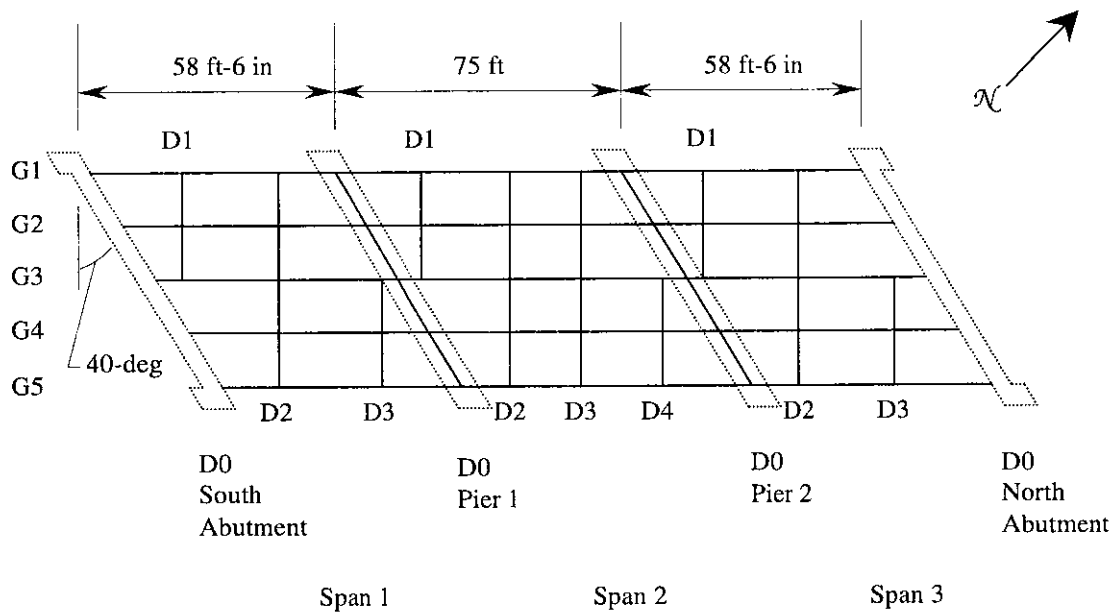


Figure 24. Plan view of bridge superstructure.

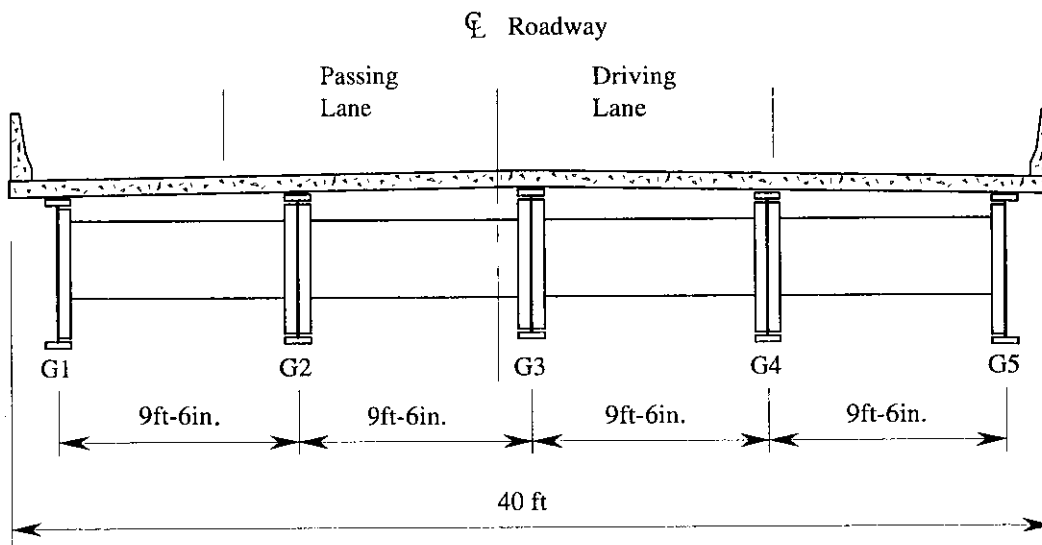


Figure 25. Cross section of bridge looking in direction of traffic.

The girders are spaced at 9 ft-6 in. and have shear angles to ensure an integral connection with the deck concrete. The negative and positive moment regions of the girders have different cross sections along the length of the bridge. The negative moment region has plate girders with PL36 \times 1/2 webs, and PL12 \times 1-3/4 top and bottom flanges. The plate

girders are spliced 17 ft from the piers, at the dead load point of inflection. The positive moment, midspan girders are 36WF135 wide flange rolled sections as illustrated in Fig. 26.

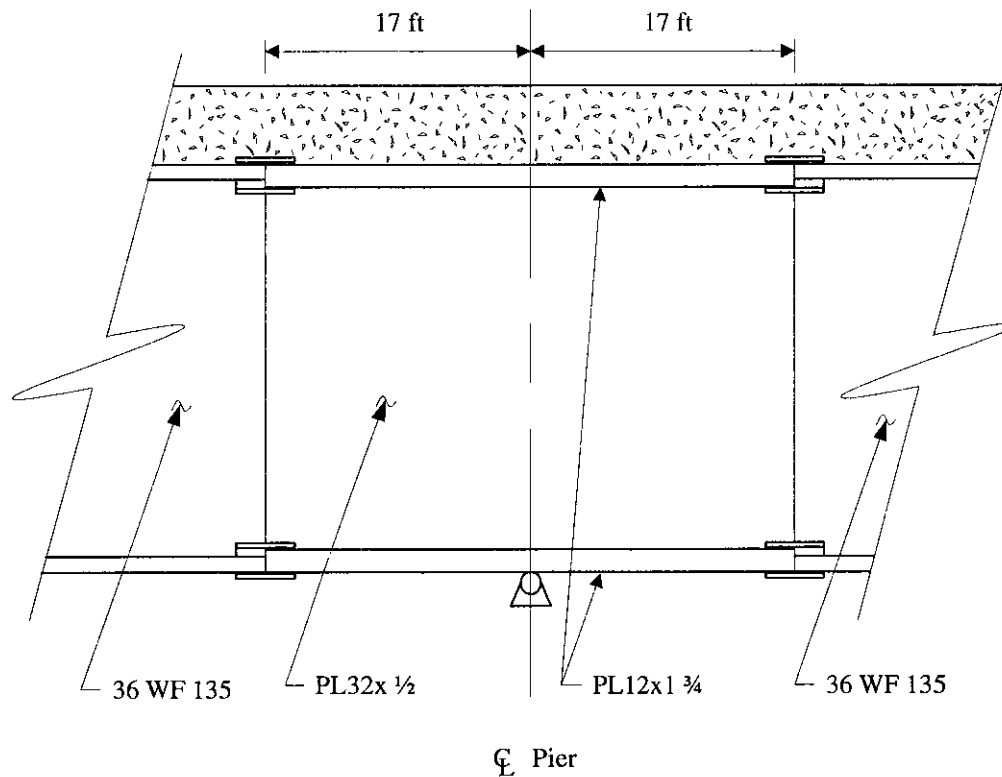


Figure 26. Negative and positive moment region cross section of a girder.

The bridge has channel diaphragms connecting the five girders. The channel diaphragms are rolled 18C42.7 sections. They are bolted to girder web stiffeners at various spacing from 12 ft to 22 ft as shown in Fig. 27. A typical diaphragm/girder connection is illustrated in Fig. 28. The web stiffeners are welded to the web with small gaps at the top and bottom corners of the girder. The web stiffeners are not connected to the top flange of the girders in the negative moment region. The web gap is $\frac{3}{4}$ in. between the stiffener and the top flange as pictured in Figs. 28 and 29. Fatigue cracks in the web gap are typically parallel to the girder flange and are a couple of inches long extending on both sides of the stiffener.

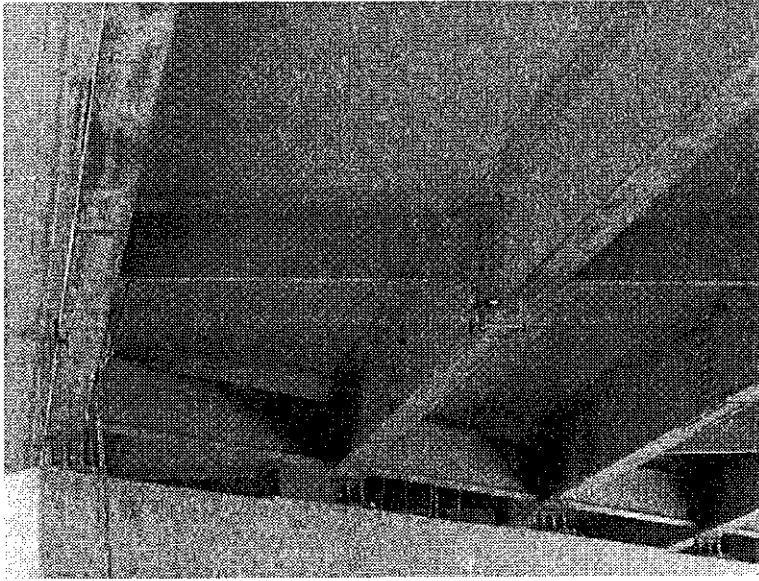


Figure 27. Underside view of diaphragm and girders.

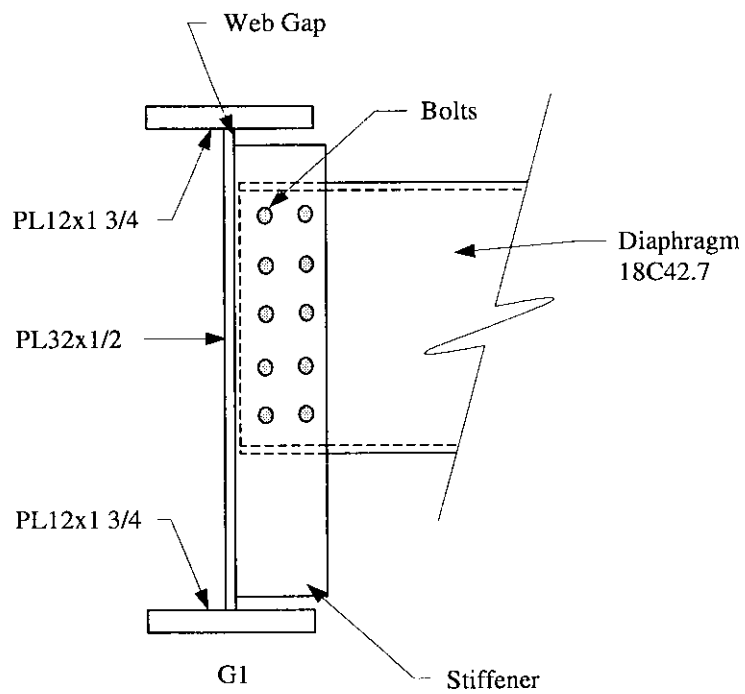


Figure 28. Diaphragm/girder connection in negative moment region.

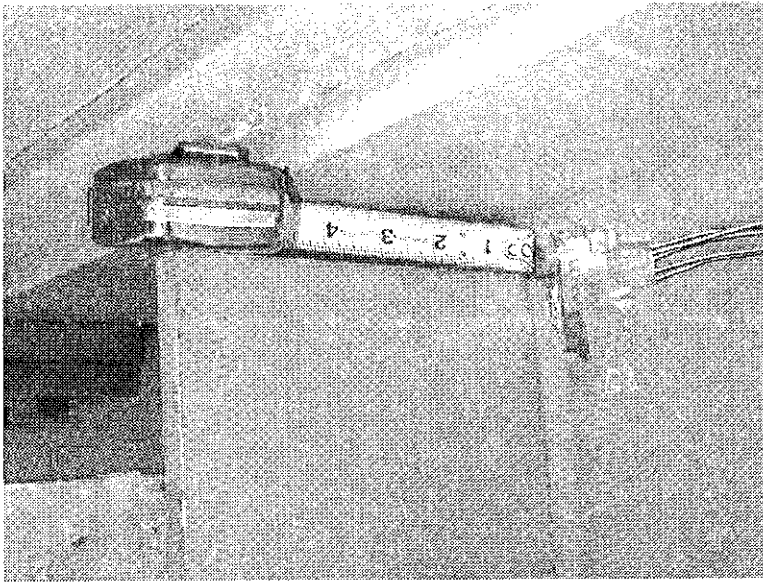


Figure 29. Typical web gap in negative moment region.

Bridge Behavior and Condition

Research proves that the cause of fatigue cracking in diaphragms is differential deflection of the girders. Traffic placement on the deck and stiffness differences between interior and exterior girders results in the independent deflection of each girder. The diaphragms are fixed at each girder and displace with the girders. This creates a bending force in the diaphragms between adjacent girders with different deflections as shown in Fig. 30. The force in the diaphragms creates a force in the girder webs. The webs deflect under the load in the weakest area, the web gap. Traffic crossing the bridge causes the web gaps to deflect out-of-plane.

This reaction is illustrated in Fig. 31 exaggerated to highlight the bending in the web gap. Fatigue cracks are created in the web gap as cycles reach the limit of the steel. For this reason high volume bridges are at a greater risk for fatigue cracking. Retrofitting the diaphragm/girder connection to create a pinned instead of a rigid connection allows the diaphragms to move with the differential deflection without introducing bending into the web gap and causing fatigue.

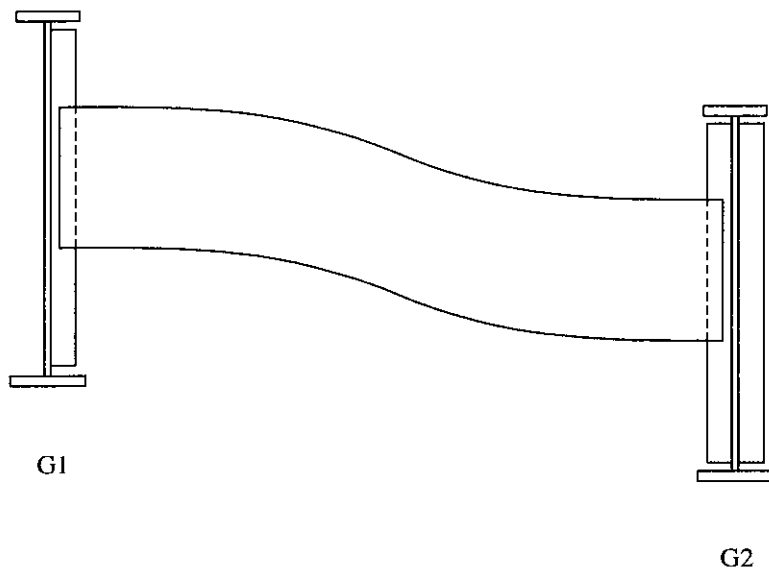


Figure 30. Exaggerated illustration of diaphragm double bending.

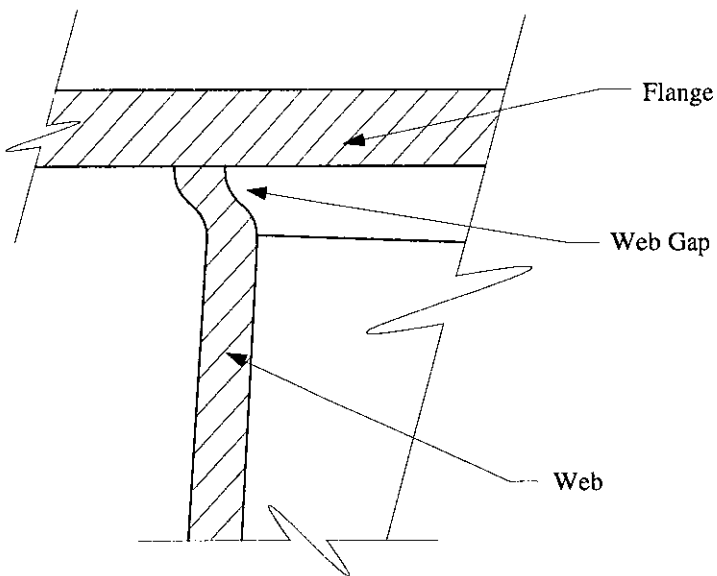


Figure 31. Web gap double bending due to diaphragm rotation.

The 40-degree skew of the piers also plays a role in web gap fatigue. Greater differential deflection is created between girders when axle loads are dispersed between girders at different distances from the support pier. Loading girders at different distances

from the skewed pier creates different bending moments and different deflections. The larger differential deflection can cause greater out-of-plane displacement than would occur in the same bridge with no skew.

Typically the girders in the negative moment regions have a much higher frequency of fatigue cracking due to the composite action of the flange with the concrete deck above the web gap with no stiffener weld on the tension side of the girder. Exterior girders also tend to have a higher frequency of fatigue than interior girders. Bridge 2700.0R035 exhibits these common arrangements of fatigue cracking, as depicted in Fig. 32.

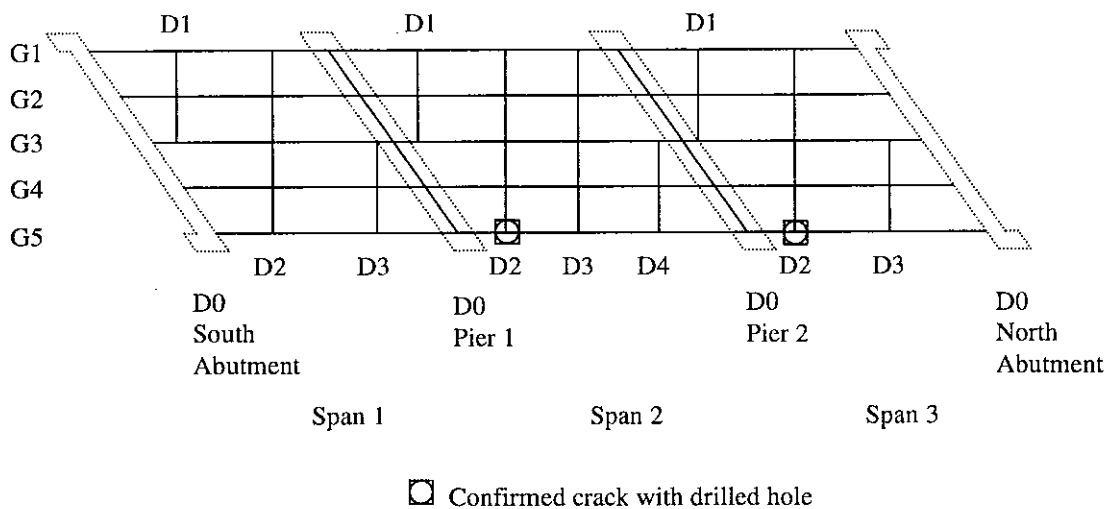


Figure 32. Confirmed crack and drilled hole retrofit locations.

A drilled hole retrofit was implemented on this bridge as standard DOT maintenance procedure on fatigue cracking in web gaps. When a fatigue crack was discovered, the terminus was drilled out with an inch diameter hole to reduce the stress concentration at the tip of the crack. As shown in Fig. 33, this method was not always successful in stopping crack propagation. A new retrofit is needed to provide a more permanent solution to the problem.

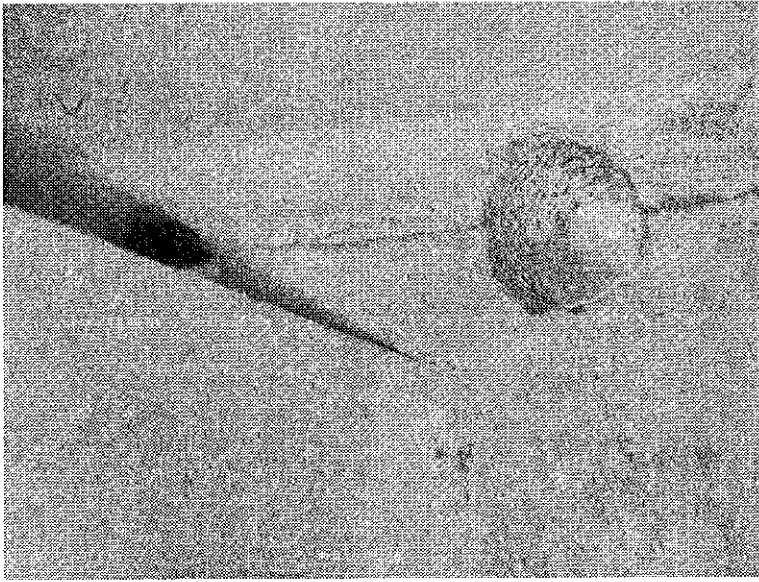


Figure 33. Typical drilled hole retrofit in web with continued cracking.

Instrumentation

A negative moment region on an exterior and interior girder was selected for testing. A location adjacent to Pier 2, with minimum existing fatigue damage was used. A combination of strain gages and displacement transducers were installed to determine the reaction of the bridge. Figure 34 shows the instrumentation installed at D3 in Span 2. The data from these gages was collected by an Optim Electronics Megadac data acquisition system at a sampling rate of 30 hertz.

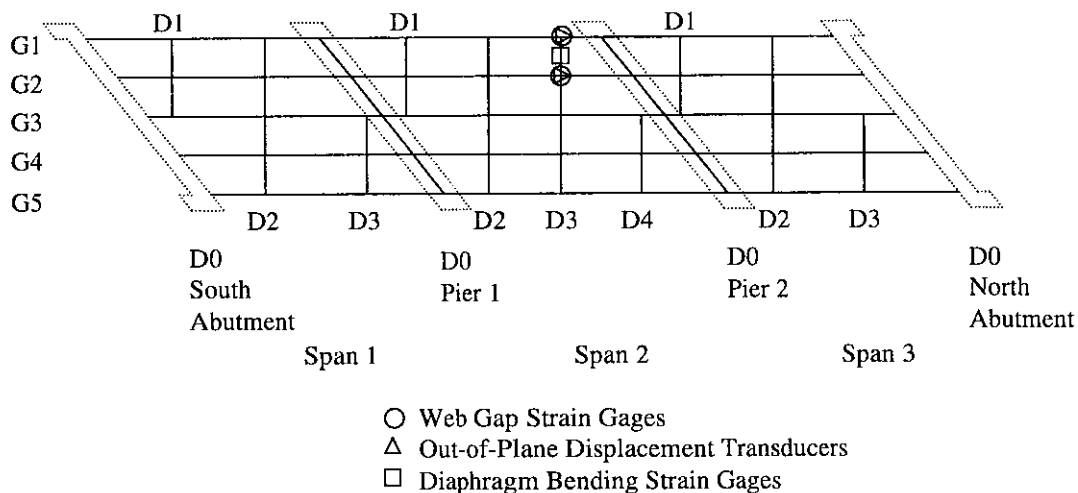
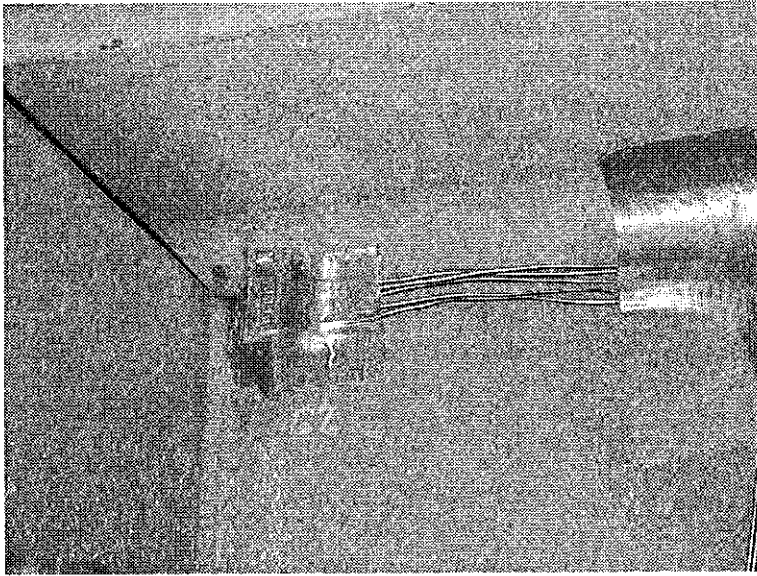
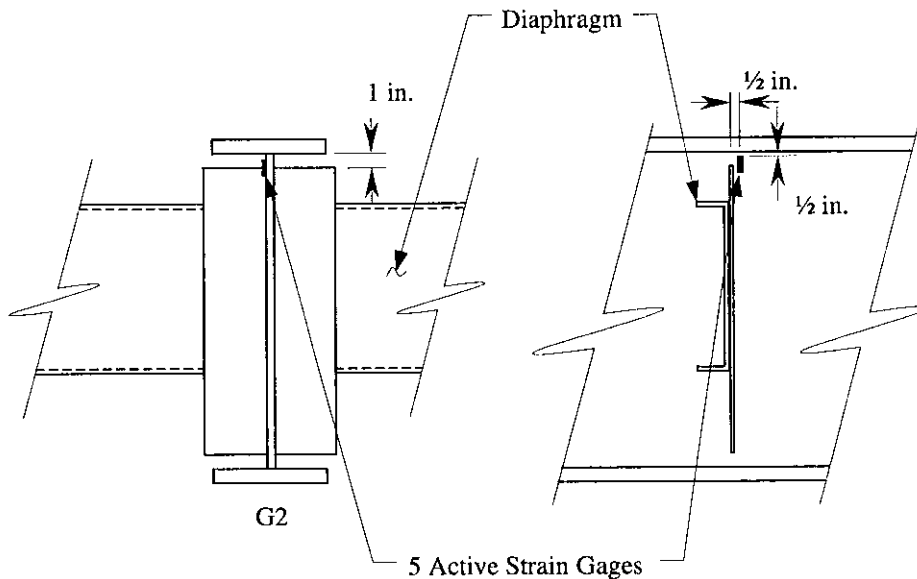


Figure 34. Plan view of gage placement.

Bondable 120-Ohm gradient strain gages were used to measure web gap strain. The gradient gages consisted of five small foil backed strain gages in a factory assembled unit. They were mounted in, or as close to, the web gap as possible as shown in Fig. 35. The gages were oriented to measure web strain in the vertical direction in the web gaps of G1 and G2.



a. Photograph of gradient strain gage in web.



b. G2 gradient gage illustration looking northeast and southeast.

Figure 35. Web gap gradient instrumentation.

120-Ohm foil backed strain gages were used to measure bending strain in the diaphragm. The gages were placed at the mid and quarter points of D3 in Span 2 on the top and bottom flanges of the channel to record the maximum bending strain in each position. The middle strain gages were 56 in. from the centerline of G1, and the quarter gages were 26 in. from the nearest girder centerline as depicted in Fig. 36.

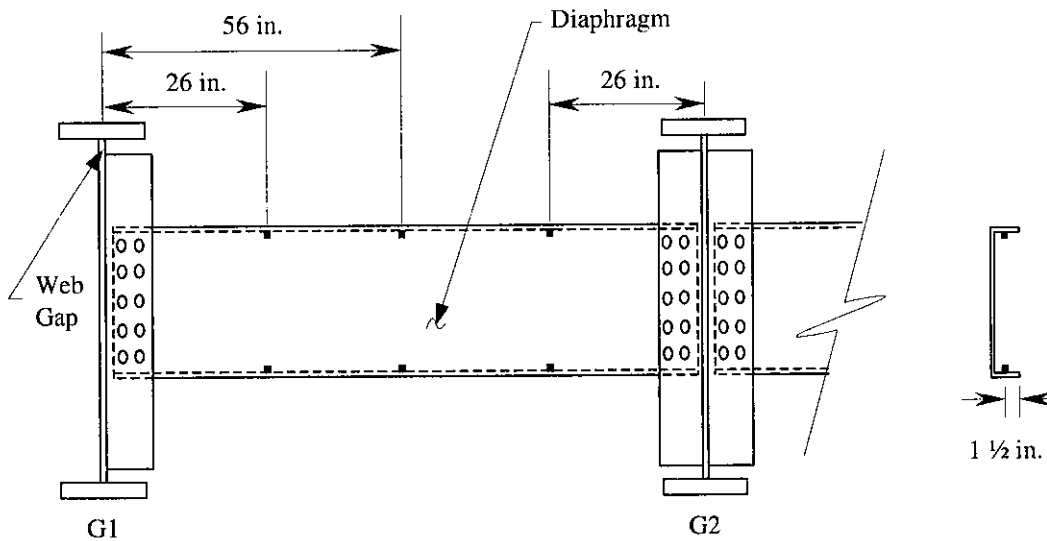
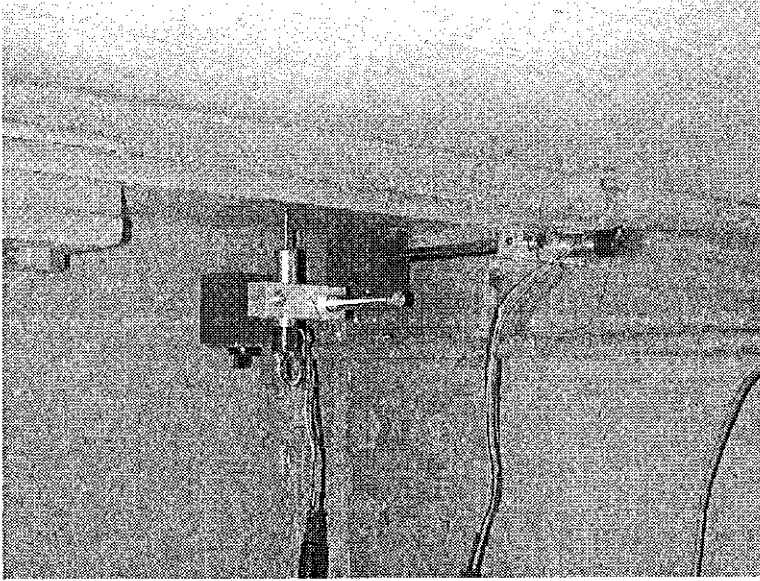
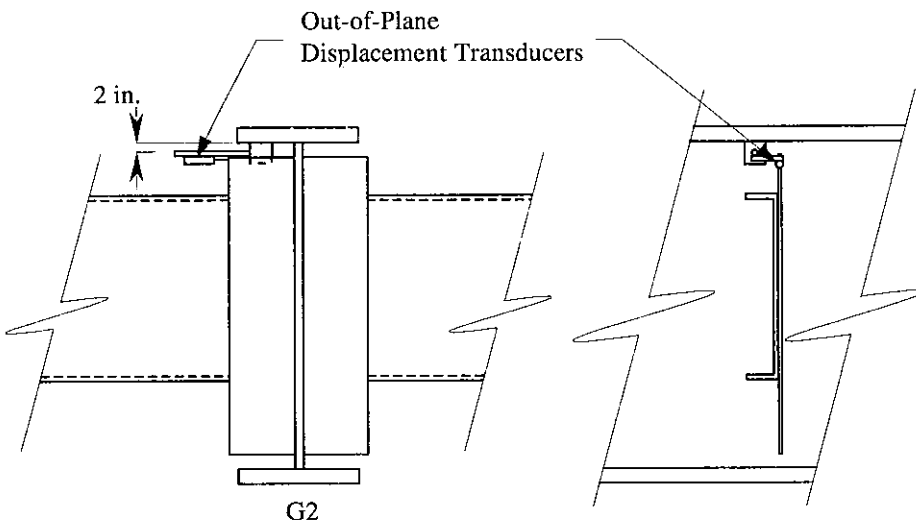


Figure 36. Diaphragm strain instrumentation looking northeast and southeast.

Direct Current Displacement Transducers (DCDT's) were used to measure displacement of the web gaps. Magnets were used to attach the gages to G1 and G2 near the connection with D3. G2 had an out-of-plane transducer measuring the displacement of the stiffener relative to the bottom side of the top flange where the magnet was connected. Figure 37 shows the connection of the transducer on G2. G1 is not pictured and is connected to the girder in an opposite manner. It measured out-of-plane displacement of the web by connecting to the stiffener and measuring the displacement of the top flange. The two gages measured the same type of out-of-plane displacement from different positions on the girder.



a. Photograph of out-of-plane and tipping transducers (not discussed) on G2.



b. Illustration of G2 out-of-plane transducer locations.

Figure 37. Out-of-plane displacement instrumentation

Experimental Approach

Load tests were run on the bridge using Iowa DOT tandem rear axle dump trucks illustrated in Fig. 38. The average width of these trucks was 6 ft between the rear duals and the length is approximately 18 ft from front axle to rear axle. The trucks were loaded with

sand to simulate heavy trucks during testing. Truck 1 weighed 53,340 lbs and Truck 2 weighed 50,080 lbs.

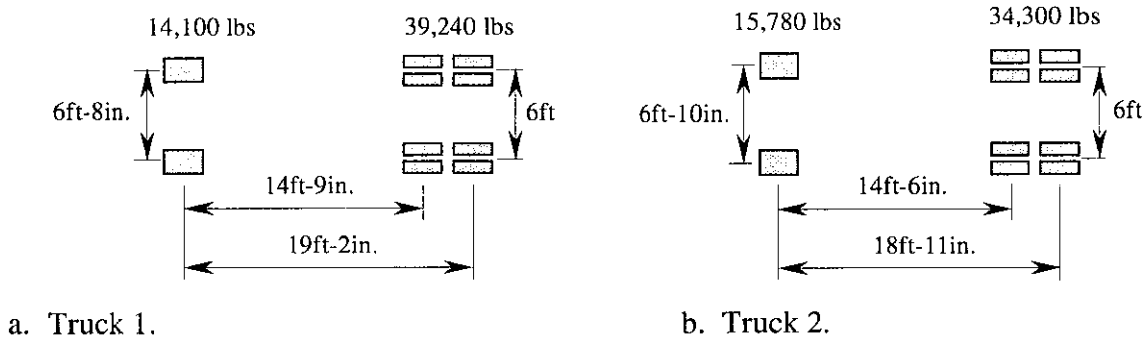


Figure 38. Test truck configurations.

Bolts were loosened on only two diaphragms. The D3 bolts between G1 and G2 were loosened. The adjacent section between G2 and G3 were also loosened to eliminate strain created by differential deflection between G2 and G3. Tests were run with the bolts in the tight, middle row tight, and loose positions. The middle row tight condition is illustrated in Fig. 39. These bolt patterns were tested to see how the web gap strain changed as the diaphragm end condition changed. When all bolts were loosened one or two on each side were held tight in the hole. These bolts were supporting the weight of the girder and did not rotate in place, however the diaphragm was free to rotate.

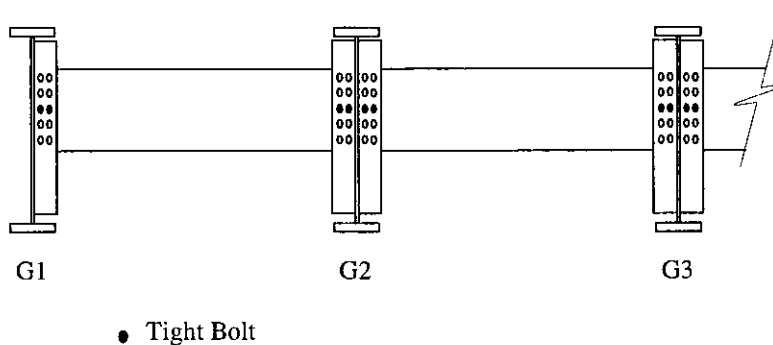
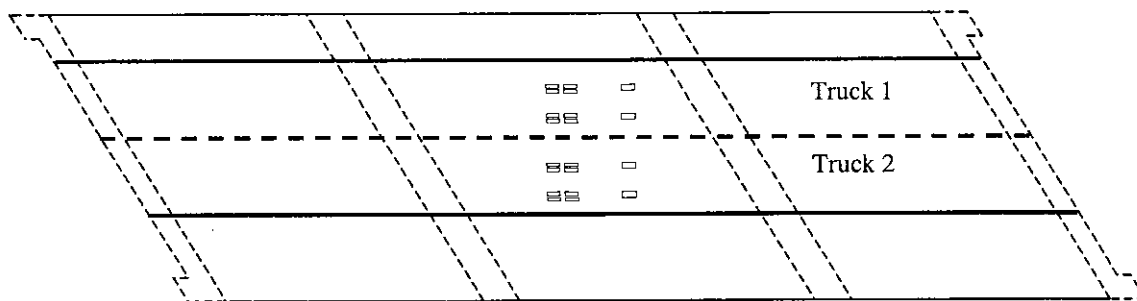
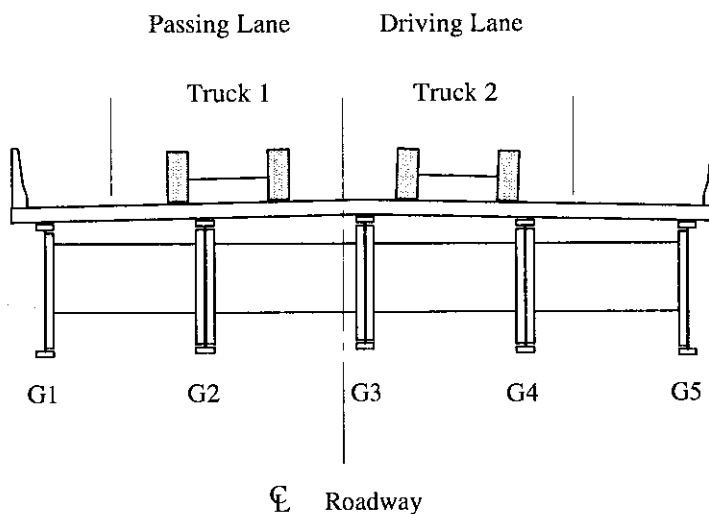


Figure 39. Middle row tight diaphragm bolt condition.

Tests were performed to find which lateral placement caused the largest strains in the instrumented area. Many truck lateral position combinations were tested. A single truck, Truck 1, was driven down the center of the passing lane similar to typical traffic. Tests were also run with the truck straddling G2 and with a wheel path directly on G2. In the end, a two truck side-by-side arrangement was found to be the largest practical loading configuration and is illustrated in Fig. 40. This represented the maximum load occurring when two large vehicles pass each other on the bridge. Truck 1 was in the center of the passing lane, and Truck 2 was in the center of the driving lane.



a. Plan view of trucks in side by side position.



b. Cross section of bridge with trucks

Figure 40. Test truck placement on bridge in lanes.

Due to heavy interstate traffic, load tests were run at near interstate speeds. Static tests were determined to be too dangerous under the traffic load on I-35. The load trucks

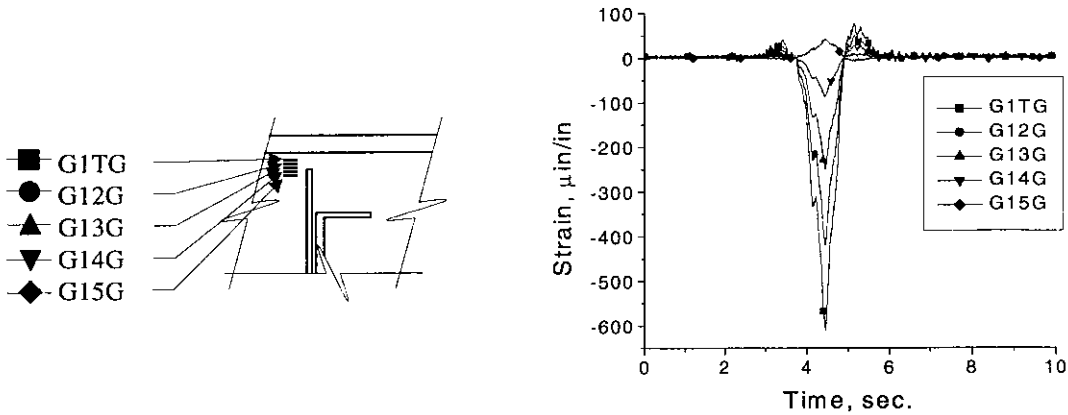
crossed the bridge at approximately 60 mph to maintain the flow of traffic. Running the test at interstate speeds produced results that were similar to the typical response of the bridge under ambient truck loading. A pace vehicle was used to slow down traffic behind the load trucks. This created a gap in traffic during which the test data were retrieved without any interference from ambient vehicles on the bridge. Test data recording was initiated as the load trucks approached the bridge and continued until both had crossed completely over the structure.

Experimental Results

Figure 41 shows the strains in the G1 web gap with the diaphragm connection bolts in the tight condition, middle row tight condition, and loose condition. An illustration of each web gap shows the position of the gages in the gap. The data plots represent the load trucks side by side on the bridge deck with Truck 1 in the passing lane and Truck 2 in the driving lane.

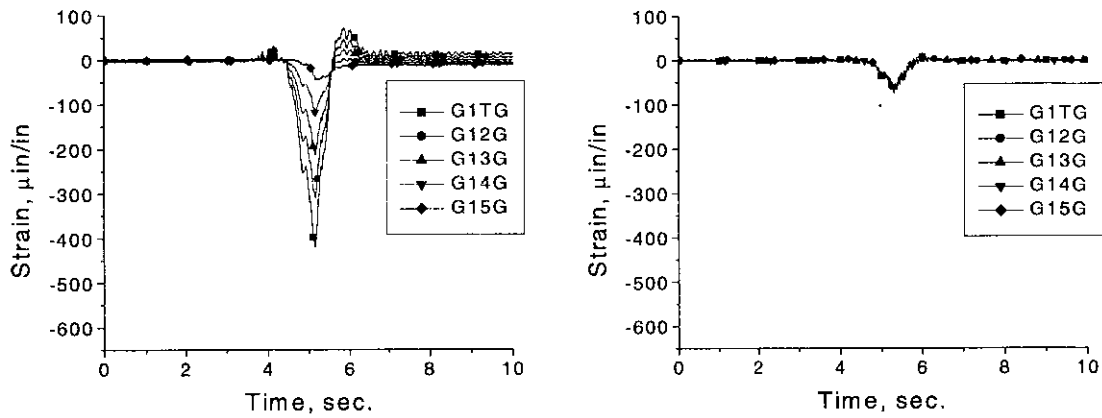
The strain in the G1 web gap when both lanes are loaded is large, about 600 micro strain. The variation in strain and change in sign within the gap indicates double bending of the web. The force in the diaphragm rotates the connection as indicated previously in Fig. 31 caused by greater deflection at G2 than G1. As G2 deflects below G1 the diaphragm rotates and pulls down on the web. The large magnitude of strain in the web gap can be attributed to its location on an exterior girder, girder stiffness, as well as the 40-degree skew of the piers, which increases differential deflection.

Partial loosening of the bolts reduces the strain in the gap by over 30 percent, but double bending is still distinguishable by the strain variations in the gap at peak loading. Loosening all the bolts reduces the strain in the gap by more than 80 percent. All the gages in the gap have approximately the same strain value, suggesting that double bending in the gap has been eliminated. The remaining strain in the web gap suggests a slight uniform bending of the web gap, which is not bending caused by forces in the diaphragms.



a. Gage placement looking southeast.

b. All bolts tight.



c. Middle row bolts tight.

d. All bolts loose.

Figure 41. G1 gradient gage strain plots.

Figure 42 shows the strain in the G2 web gap. The bolt conditions and load placements are the same as in Fig. 41. The positions of the gages in the web gap are indicated in the adjoining illustration.

The strain in G2 web gap with the bolts tight is much smaller than the strain in the exterior web gap. The strain variations in the web gap suggest double bending is occurring at this connection as well. Partial loosening of the bolts is not very effective at reducing the strain in the web. After loosening all but the middle row of bolts the strain is only reduced by approximately 20 percent, and double bending is still present. Full installation of the

retrofit causes a strain reversal in the gap. The overall strain reduces by nearly 40 percent, but the sign is changed. Double bending is also no longer present in the gap when all bolts are loose. This suggests that the web gap is no longer being displaced out-of-plane by the diaphragm.

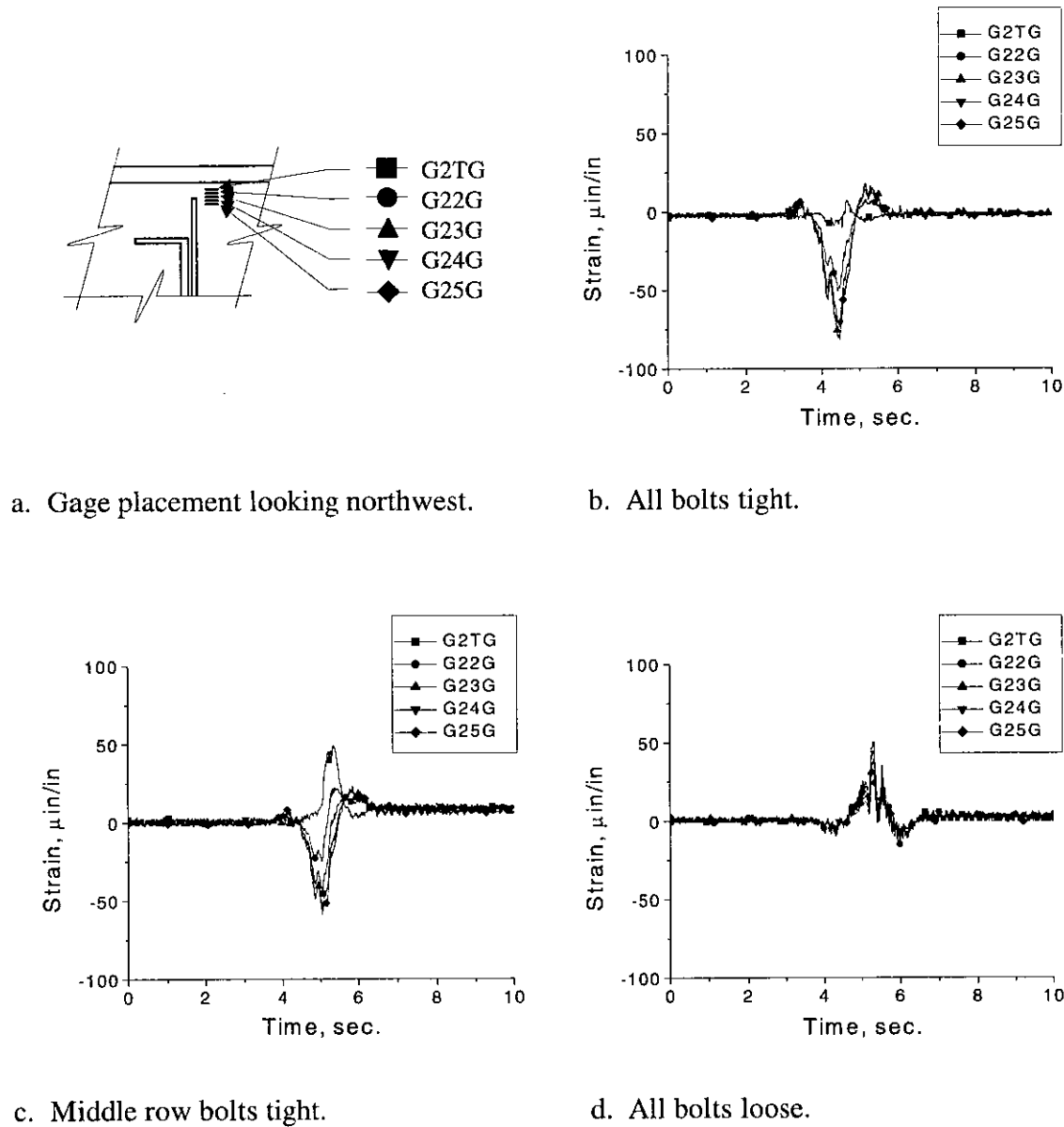
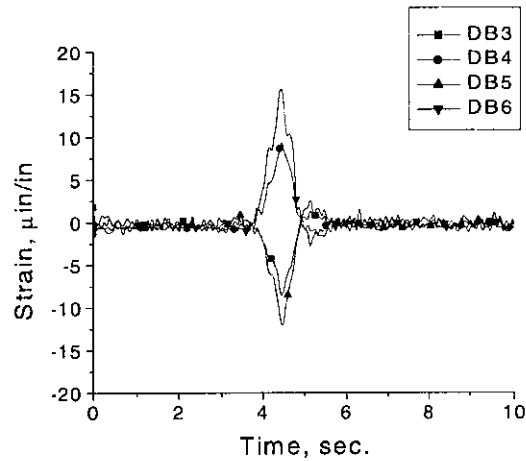
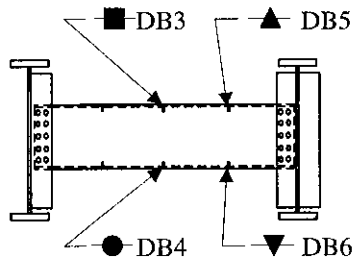


Figure 42. G2 gradient gage strain plots.

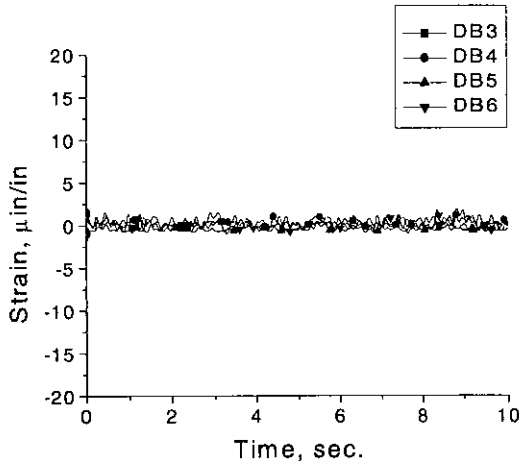
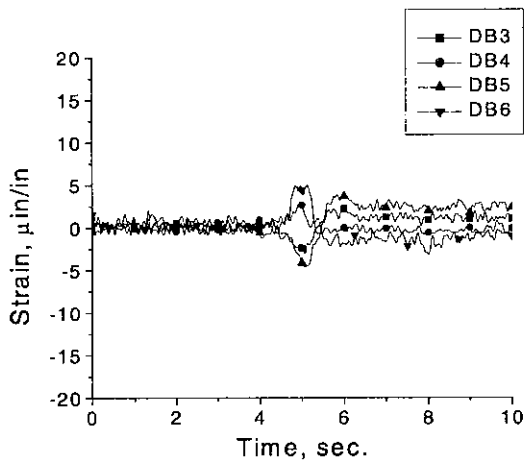
Figure 43 shows the strain in D3 resulting from loading in both lanes with bolts in the tight, middle row tight, and loose position. The trucks are located in the same location as in

previous figures. The positions of the gages on the diaphragm are indicated on the adjoining illustration. Gages DB1 and DB2 were damaged during installation so no data is plotted for the exterior girder side of the diaphragm.



a. Gage placement looking northeast.

b. All bolts tight.



c. Middle row bolts tight.

d. All bolts loose.

Figure 43. D3 bending strain plots.

The data are from gages in the center of the diaphragm and near G2. The top gages are in compression and the bottom gages are in tension, which suggests positive bending of the diaphragm on the interior girder side. Gages DB1 and DB2 were damaged during installation, but, most likely, the strain values near G1, the exterior side, would show

negative bending so that double bending of the diaphragm is occurring, as shown earlier in Fig. 30. The strains in the diaphragm suggest the interior girder deflected more than the exterior girder.

The strain in the diaphragm, with only the middle row of bolts tight, exhibits a near 60 percent strain reduction. This is a larger reduction than the G1 web gap experienced with partial loosening. The strain in the diaphragm exhibits double bending, as with the tight bolt condition, but to a smaller degree due to the reduction of stiffness in the diaphragm/girder connection.

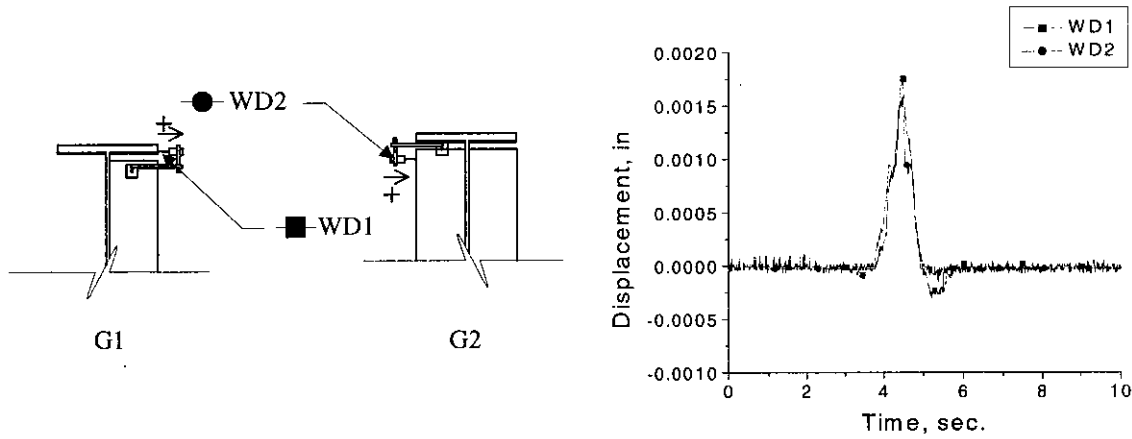
Following loosening of all bolts in the diaphragm connection strain in the diaphragm was reduced 100 percent. This suggests that no measurable force is being transferred between girders in the diaphragm due to differential deflection. Any strains in the web gap with the bolts loose are therefore not a result of diaphragm forces.

Figure 44 shows out-of-plane displacement in G1 and G2 with the bolts tight, middle row tight, and loose. The load trucks are side by side with Truck 1 in the passing lane. The transducer locations are illustrated on the combined diagram. The method of attachment to G1 and G2 are opposite of each other in that the base of WD1 is attached to the stiffener while WD2 is attached to the top flange. The result is similar sign plots for movements at the gaps in the same direction. Typically instrumentation set up in exactly the same method in mirror locations on the right and left side of the girders would have opposite sign for similar movement, but the difference in base connection changes that effect. Movement of the G1 and G2 webs toward the interior of the bridge causes the WD1 to measure greater distance between the right stiffener and the web gap while WD2 measures a greater distance between the flange and the left stiffener as the stiffener moves laterally away from the flange.

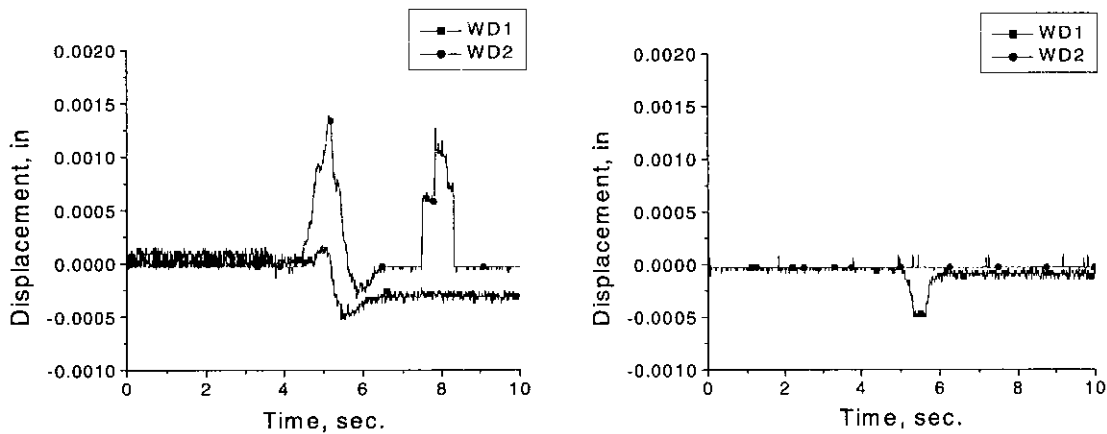
The out-of-plane displacements of the webs of G1 and G2 with the bolts tight are similar in magnitude and direction. The out-of-plane displacements in both web gaps are towards the center of the bridge. The directions of these displacements are reflected in the web gap strains obtained with the bolts tight.

G1 web displacement is changed drastically and reversed displacement direction when the bolts are partially loosened. The maximum displacement reduces by 75 percent. G2 displacement was reduced by less than 25 percent. This non-uniform change is probably

due to the unknown effect of partial bolt loosening. It appears that the exterior girder connection is relieved more than the interior connection when the middle row of bolts is left tight. The friction connection in the G2 diaphragm/girder connection is apparently tight while the G1 connection releases when the bolts are partially loose.



a. Transducer placements looking northeast. b. All bolts tight.



c. Middle row bolts tight. d. All bolts loose.

Figure 44. G1 and G2 out-of-plane displacement plots.

The out-of-plane displacement with all bolts loose shows G1 displacement remains similar to the middle tight condition, and G2 displacement reduced by 100 percent and exhibits no noticeable out-of-plane displacement. This suggests that the partial bolt

loosening was not completely effective, and loosening all bolts results in the greatest reduction of out-of-plane displacements of the web gaps.

Conclusions

The results of the field tests show that the retrofit does reduce strain and displacement in the web gaps of a channel diaphragm bridge. Removing all but one row of bolts created little decrease in strain in the diaphragm and the gap, suggesting that all bolts should be loosened to effectively eliminate diaphragm forces contributing to the strain in the web. Comparing the tight and loose conditions highlights the positive results of the retrofit.

Implementation Issues

Results have shown that implementing the bolt loosening retrofit on multiple steel girder bridges with channel diaphragms is a viable solution to web gap fatigue cracking. However, before this retrofit is installed in in-service bridges, a few key points need to be addressed on an individual bridge basis.

Lateral support for the girders and stability of the structure with the diaphragms loosened is a concern when installing the retrofit. Bracing for lateral torsional buckling is only important in the negative moment region and the larger girders in the negative moment region generally provide adequate support for the unbraced length. ASSHTO design manual calculations indicate adequate lateral support for the I-35 bridge if the diaphragms are completely removed. The retrofit should not jeopardize the integrity of the structure because the diaphragms are still in place to provide lateral support between girders after only a small amount of lateral movement engages the bolts. Each bridge should have individual calculations performed to ensure stability assuming the diaphragms are completely removed.

Lateral load distribution regarding diaphragms must also be addressed. The change in lateral load distribution of the bridge was not thoroughly tested in this research, but other researchers have found that most bridges are conservatively designed for lateral load distribution and show little change in lateral load distribution with the diaphragms removed. Loosening the bolts in the diaphragm/girder connections is equivalent to removing the diaphragms all together when considering lateral load distribution. Both relieve the distribution of force in the diaphragms during loading.

A system must be devised to ensure that the loose bolts remain in place. The bolts must be secured so that they do not inadvertently fall out due to nut vibration under traffic load. The method of connection was not researched, but a lock nut or double nut technique may be a solution. Any solution implemented should be periodically inspected to ensure that it is functioning properly.

Prior to installation of the retrofit each particular bridge must meet the listed requirements and any other requirements determined by the engineer of record. Following installation of the retrofit the bridge must be monitored closely until the engineer is convinced the bridge is stable and the diaphragms are safely secured to the stiffeners.

References

1. T.J. Wipf, and L.F. Greimann, A. Khalil. Preventing Cracking at Diaphragm/Plate Girder Connections in Steel Bridges. Ames, Iowa: Center for Transportation Research and Education, Iowa DOT Project HR-393, Iowa State University, 1998.
2. A. Khalil. "Aspects in Nondestructive Evaluation of Steel Plate Girder Bridges", Dissertation, Iowa State University, Ames, Iowa, 1998.
3. J.W. Fisher, and P.B. Keating. "Distortion-Induced Fatigue Cracking of Bridge Details with Web Gaps." Journal of Constructional Steel Research, Vol. 12, pp. 215-228, ASCE, 1989.
4. J.W. Fisher. Executive Summary: Fatigue Cracking in Steel Bridge Structures. Bethlehem, Pennsylvania: Advanced Technology for Large Structural Systems, Report No. 89-03, Lehigh University, 1989.
5. J.M. Stallings, and T.E. Cousins, and T.E. Stafford. "Effects of Removing Diaphragms from Steel Girder Bridge", Transportation Research Record, Vol. 1541, pp. 183-188, Washington, D.C.: TRB, National Research Council, 1996.
6. J.M. Stallings, and T.E. Cousins. "Fatigue Cracking in Bolted Diaphragm Connections." Proceedings of the 15th Structures Congress 1997 Portland, Vol. 1, pp. 36-40, New York: ASCE, 1997.

7. T.E. Cousins, and J.M. Stallings. "Laboratory Tests of Bolted Diaphragm-Girder Connection." Journal of Bridge Engineering, Vol. 3, No. 2, pp. 56-63, ASCE, May 1998.
8. T.E. Cousins, J.M. Stallings, and T.E. Stafford. "Removal of Diaphragms from 3-Span Steel Girder Bridge." Journal of Bridge Engineering, Vol. 4, No. 1, pp. 63-70, ASCE, Feb. 1999.
9. A. Azizimini, S. Kathol; and M. Beachman. "Effects of Cross Frames on Behavior of Steel Girder Bridges." 4th International Bridge Engineering Conference Proceedings, pp. 117-124, Washington, D.C.: TRB, 1995.

Chapter 4. IA 17 Continuous Remote Monitoring of Bolt Loosening in an X-type Diaphragm Steel Bridge

A paper to be submitted to the Journal of Bridge Engineering

David Tarries, Terry J. Wipf, Lowell Greimann

Abstract

Multiple steel girder bridges frequently experience fatigue cracking due to out-of-plane displacement of the web in the region of the diaphragm connections, especially in the negative moment portions of the girders. The web gaps are located at diaphragm connections where the stiffeners are not attached to the web or top flange near the fillet of the girder. In the past, the Iowa Department of Transportation (Iowa DOT) has drilled holes at the crack tips in an attempt to stop fatigue crack propagation in steel girder bridges. This retrofit was designed as a temporary solution in most cases and a more permanent retrofit for Iowa bridges is required. A new field retrofit has been developed that involves loosening the bolts in the connections between the diaphragms and the girders. Research on the retrofit has been initiated, however, no long-term studies of the effects of bolt loosening have been performed. The intent of this research is to develop a continuous remote monitoring system to investigate the bolt loosening retrofit over a number of months, ensuring that the measured strain and displacement reductions are not affected by time and continuous traffic loading on the bridge. This will provide further evidence that the retrofit is an effective method of preventing web gap fatigue cracking in steel girder bridges.

Web gaps in a negative moment region on an Iowa DOT highway bridge with X-type diaphragms were instrumented with strain gages and deflection transducers. Field tests, using loaded trucks of known weight and configuration, were conducted on the bridges with the bolts in the tight condition and after implementing the retrofit to measure the effects of loosening the diaphragm bolts. Long-term data was also collected by the system that indicated the response of the bridge to ambient truck loading a number of months before and after the retrofit was installed. The system continuously monitored the bridge and saved only significant data useful for analysis. The collected data was retrievable by a modem

connection to the remote system. The features and ruggedness of this system reveal its usefulness in remote bridge monitoring and it will be used as a pilot system for future monitoring projects in Iowa.

Results indicate that loosening the diaphragm bolts reduces strain and out-of-plane displacement in the web gap, and that the reduction is not affected over time by traffic or environmental loading on the bridge. Reducing the strain in the web gap allows the bridge to support more cycles of loading before experiencing fatigue, thus increase the service life of the bridge.

Introduction

Fatigue cracking is a common problem in multiple steel girder bridges with long service lives. The Iowa DOT has been dealing with this problem for years. Fifty-five percent of the Iowa's fatigue critical steel girder bridges exhibit fatigue cracking, fifteen percent of the structures overall. In almost all cases, these cracks occur in the web gaps at diaphragm connections with girders in the negative moment region. The web gap is approximately an inch of girder web not welded to the stiffener between the top flange and web stiffener welds. The stiffener plates in bridges are not welded to the tension flange as required by specifications for steel bridge design, allowing the potential for movement in the web gap. Forces created in the diaphragms by differential deflection of the girders apply force to the web gaps causing them to displace out-of-plane, which can result in fatigue cracking over time.

The Iowa DOT has been implementing a retrofit by drilling holes at the terminus of each crack to change the stress concentrations. The hole drilling method is not always effective either by design or installation, and the Iowa DOT has initiated a study of a new retrofit method. The new retrofit consisted of loosening the bolts that connect the diaphragms to the girders so the rotational freedom created allows the diaphragms movement independent of the girders while still supporting lateral load when needed.

The affects of loosening bolts at diaphragm/girder connections over a long period of time are unknown. The stability of the retrofit directly after installation has been previously studied, but no research has focused on the long-term effects of the retrofit. A test following the stability of the retrofit months after installation is required to ensure the retrofit can be

implemented safely. The objective of this research is to document the results of a long-term monitoring study of the bolt loosening retrofit on a bridge in Iowa to demonstrate that the reaction of the bridge is constant over time with traffic loading. In order to achieve this objective a data acquisition system (DAS) was assembled that monitored the bridge continuously from an on-site location. The system was well suited for long-term studies and could not only distinguish and record important data, but could also be controlled remotely by a modem connection. Real-time displays of the instrumentation on the bridge provided practically instant indications of the condition of the bridge without a site visit. The system was developed not only for this project, but also as a model for future remote bridge monitoring applications. Its adaptability and rugged design make it useful in many monitoring situations.

Previous Research

Khalil and Wipf et al. [1,2] have studied the affects of loosening the bolts of K-type and X-type diaphragms in multiple steel girder bridges. Research for the Iowa DOT included field-testing of the retrofit in select bridges in Iowa. The test bridges were instrumented and load test data was collected prior to bolt loosening. The bolts in a small portion of the bridge, around the instrumentation, were loosened and more load test data was collected. The results of this testing showed that the retrofit was more effective in X-type diaphragm bridges and that a reduction in strain and displacement in the exterior web gap of at least 48 percent occurred following installation.

Fisher et al. [3] has spent many years researching a hole drilling retrofit for fatigue cracking in steel bridges. Holes can be drilled at the terminus of cracks parallel to the primary stress in a member to change the stress concentration at the crack tip. This retrofit was applied to many types of cracking but was specifically applied to cracking in the web gaps of girders. This retrofit will stop the propagation of the crack in situations where the web is cracked enough to allow adequate rotation of the diaphragm during differential deflection. In most cases however, this retrofit is a temporary repair and other action needs to be taken to repair the problem. A bolted connection between the stiffener plate and the top flange is suggested.

Other research has been conducted to determine the effectiveness of removing the diaphragms altogether. Cousins and Stallings et al. [4,5], as well as Azizimini et al. [6] studied this possibility. Cousins and Stallings field-tested bridges with the diaphragms removed to determine the effect this had in lateral load distribution factors. The bridges tested were typical three span multiple girder bridges. The results demonstrated that the girder experiencing maximum strain could be expected to increase by 5 to 15 percent following removal of the diaphragms. They concluded that this value is not significant to affect most bridges as the load ratings are generally conservative enough to handle a 15 percent change. Thus, the bridges tested did not experience a change in service load capacity following removal of the diaphragms. Azizimini studied the diaphragm removal option from the bridge stability standpoint. Calculations using the AASHTO design manual on select three span multiple girder bridges demonstrated that the diaphragms were not required for lateral torsional support. This research suggests that on typical three span bridges the diaphragms may not be required for load distribution or stability.

A number of researchers have collected data on bridges using remote monitoring systems. Chajes et al. [7] and Aktan et al. [8] designed and implemented remote monitoring systems on bridges involved in their studies. Chajes set up a battery-powered system that could be triggered by a monitored channel reaching a threshold. The system conserved data space by collecting only data that exceeded a predetermined trigger value. The battery power of the system also allowed for remote installation without connection to a power source. Aktan's system was connected to external utilities that allowed the system to be powered continuously and contacted from a secure location. A video camera and many gages were installed to monitor the bridge and data was collected at certain times of the day. The data from the remote tests was easily accessible and downloadable to a computer in the laboratory. The system is planned to be upgraded to a high-speed internet connection in the future allowing real-time display of data and pictures and efficient downloads.

Bridge Description

Bridge 4048.2S017, pictured in Fig. 45, was selected for testing because it is an X-type diaphragm multiple girder steel bridge with no existing fatigue cracking in the web gaps. It was also used in previous bolt loosening retrofit research for the Iowa DOT [1,2]. It

is a five-girder bridge built in 1970, and it carries north and south Iowa Highway 17 traffic across the Boone River in central Iowa's Hamilton County. The bridge has three spans with no skew, and an 8-inch concrete deck. The two exterior spans are 97 ft-6 in. and the center span is 125 ft. Figure 46 shows a plan view of the bridge; girders are designated with G and diaphragms are labeled with D. Diaphragms at piers and abutments are numbered 0.

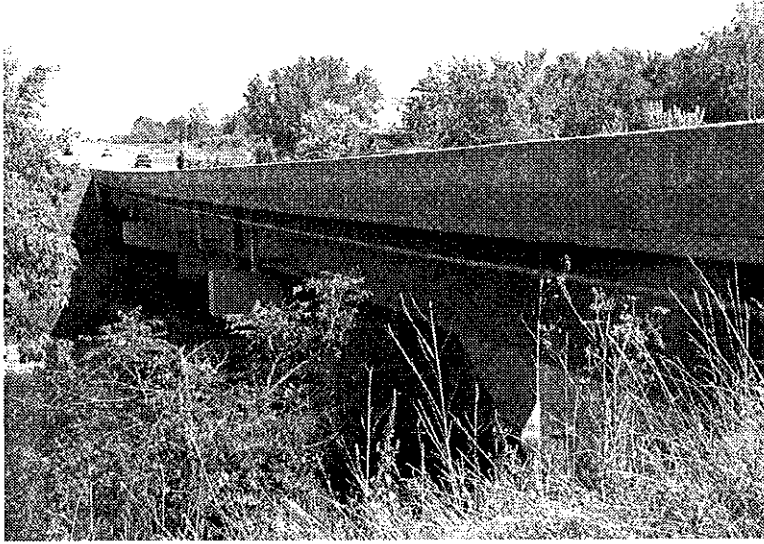


Figure 45. Photograph of bridge looking northeast.

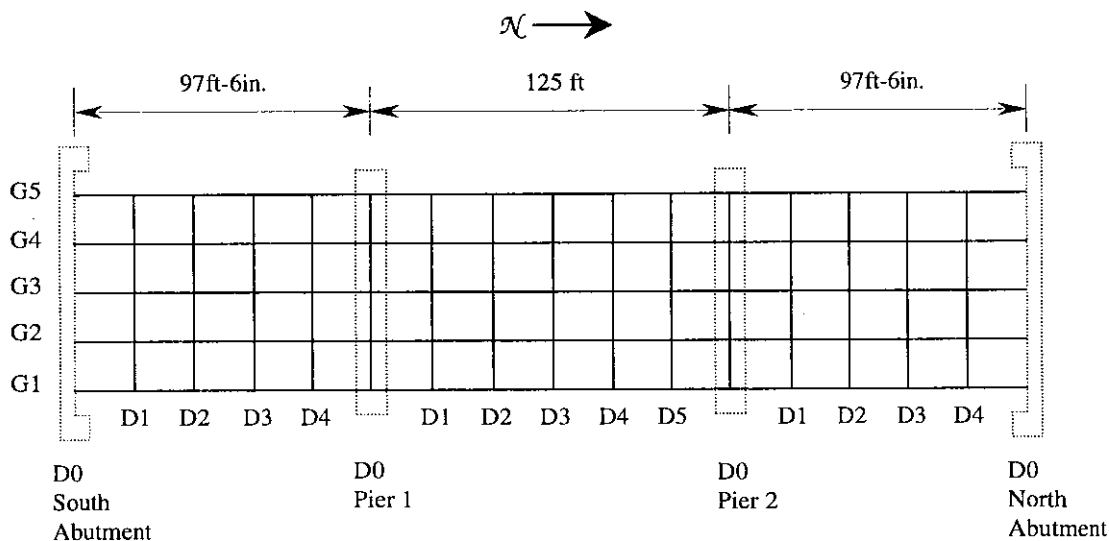


Figure 46. Plan view illustration of bridge superstructure.

The girders in this bridge are spaced at 10 ft on center and are not a uniform cross section throughout the length of the bridge. The negative and positive moment regions of the girders as well as interior and exterior girders have varying cross sections. The negative moment regions have two different sections, and the positive regions have one. The interior girders are slightly larger than the exterior girders. On interior girders the webs are PL59 1/2 \times 3/8. The section 11 ft either side of the pier bearings has PL21 \times 1 1/2 flanges. The rest of the negative moment region, 30 ft either side of the bearing, is has PL15 \times 1 1/2 flanges. The interior girders positive moment sections consist of PL60 3/4 \times 3/8 web with PL15 \times 1 bottom flanges and PL12 \times 3/4 top flanges as shown in Fig. 47. The exterior girders are very similar cross sections except that plates are typically 1/8 in. thinner in dimension.

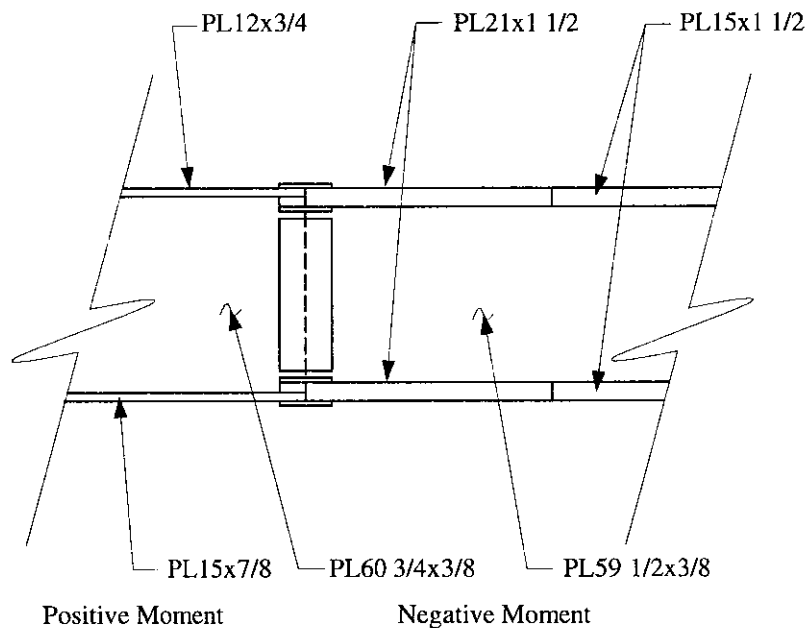


Figure 47. Profile illustration of exterior girder with plates labeled.

The diaphragms in this bridge are an X-type diaphragm made up of angles and a horizontal T section as illustrated in Fig. 48. The exception is that diaphragms at the abutments and piers, D0, are wide flange sections. The diaphragms are spaced 20 ft apart along the length of the bridge. The angles are L4 \times 3 \times 5/16 and the T is an ST5WF10.5 and they are bolted to web stiffeners on the main girders as shown in Fig 49. The connection of the stiffener to the web stops short of the fillet weld of the top flange where clips in the

stiffener do not touch the girder web. The area of the web between the stiffener weld and the top flange is the web gap, which is pictured in Fig. 50.

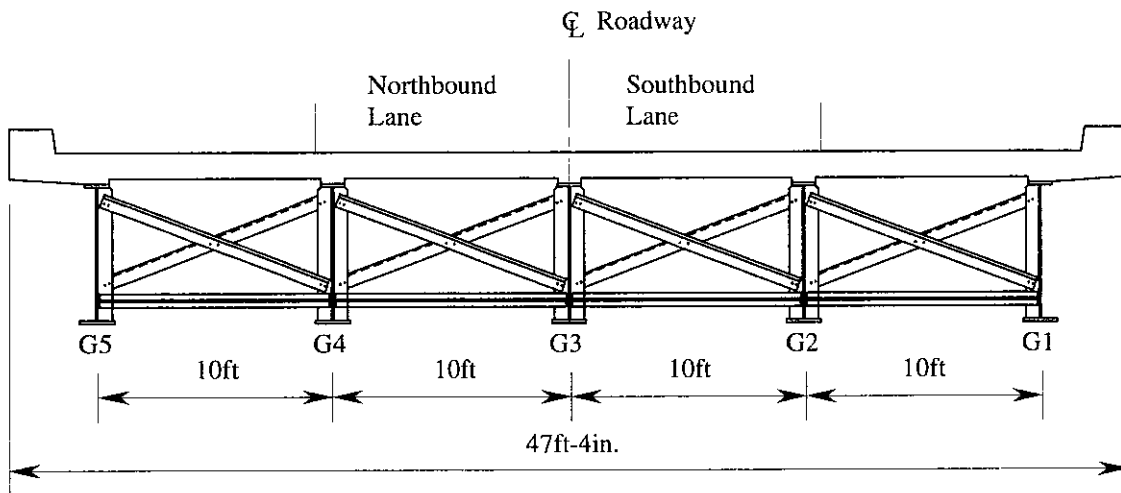


Figure 48. Illustration of bridge cross section with stiffeners.

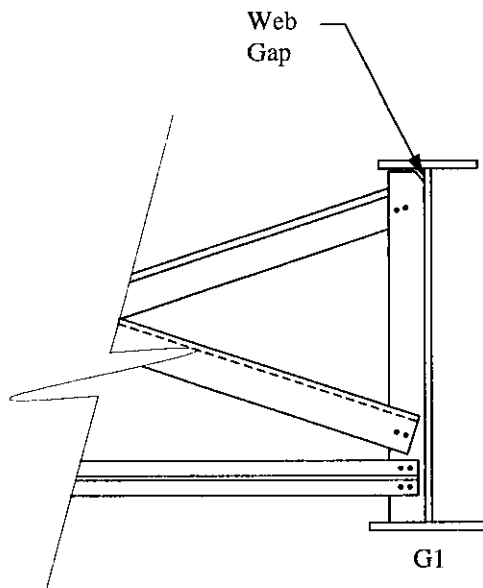


Figure 49. Diaphragm connection with web gap at stiffener clip.

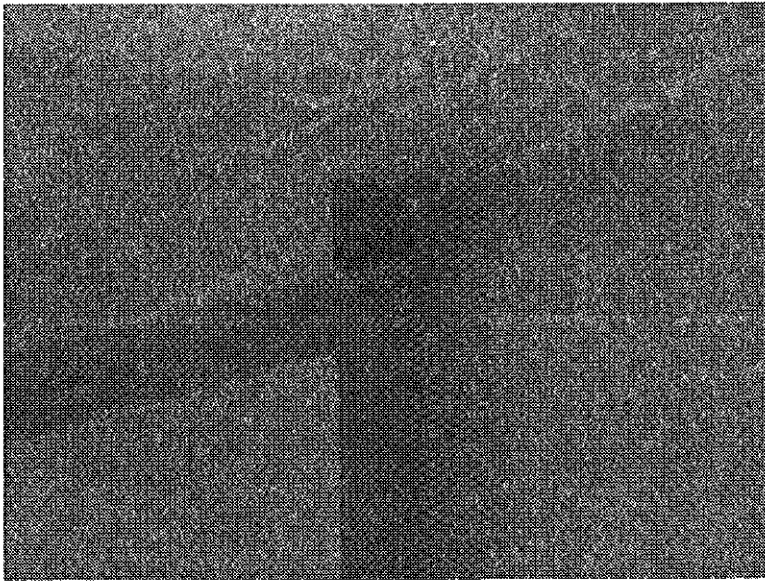


Figure 50. Photograph of typical web gap.

Fatigue cracking among Iowa bridges is typically associated with this web gap region. Traffic crossing the bridge causes the girders to deflect relative to each other. Bending forces are created in the diaphragms between girders, as the diaphragm/girder connection does not allow rotation of the diaphragm to occur. The rotation of the diaphragms causes a force on the girder web, which results in out-of-plane displacement of the web gap, as illustrated in Fig. 51. Repeated cycles of out-of-plane displacement can lead to fatigue cracking. Typically fatigue cracking occurs in the negative moment region web gaps and more commonly in the exterior diaphragm/girder connection due to the stiffness of the integral deck and top flange and the diaphragm force in the exterior girder. The highway 17 bridge was selected because it has no fatigue cracking in the web gaps. Instrumenting web gaps with no cracks and drilled holes provides a better environment for accurate strain readings in the web gap. Strain gages are more easily applied near the web gap in gaps without cracking. It also ensures that the out-of-plane displacement of the web gap is not increased by discontinuity in the web gap.

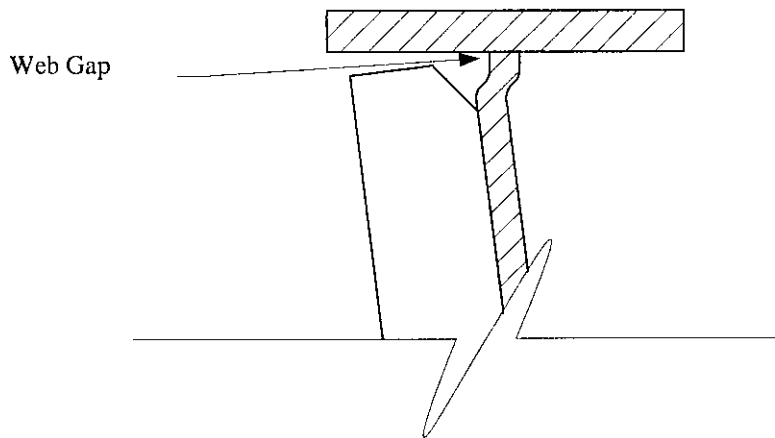


Figure 51. Web gap bending from diaphragm rotation.

Experimental Approach

A negative moment region at an exterior and interior girder was used for instrumentation because this region is most commonly associated with web gap fatigue cracking. A combination of strain gages and displacement transducers were installed to determine the reaction of the bridge to the retrofit. An area below the northbound lane in Span 2 between G1 and G2 was used for the majority of instrumentation as shown Fig. 52.

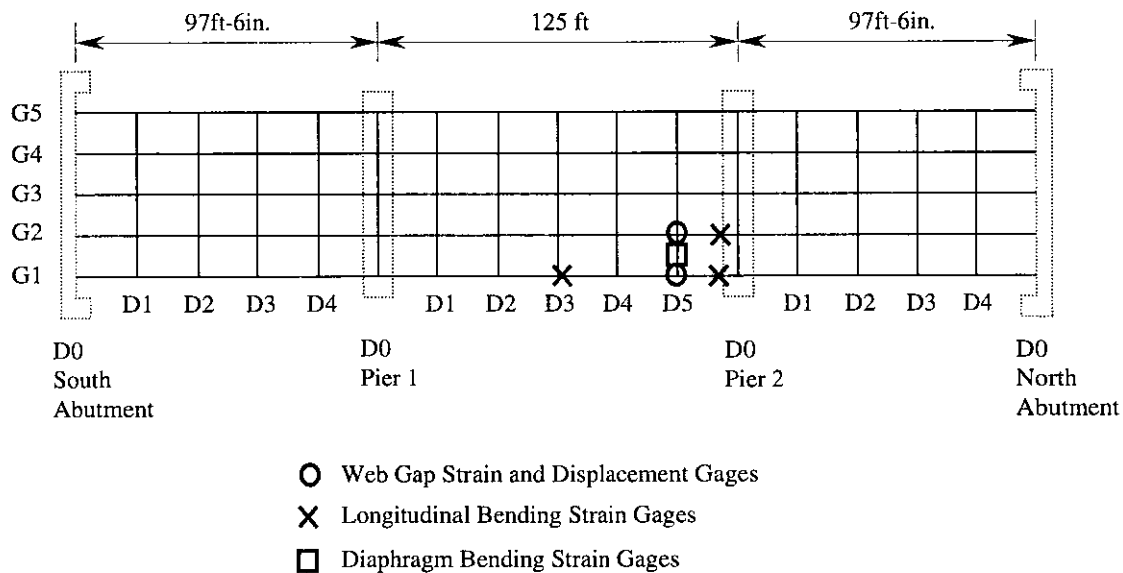


Figure 52. Instrumentation locations on superstructure.

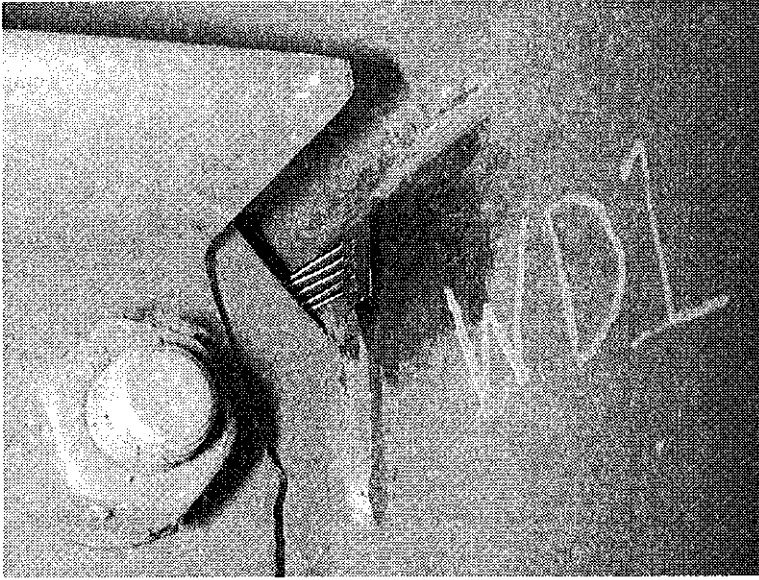
Due the long-term nature of this test, a remote monitoring data acquisition system was used. The system requirements for an on-site application include: capability of stand-alone data collection so that no supervision of the system is required, ability to withstand harsh environment of remote deployment, and ability to be controlled and monitored by modem or radio connection. The system selected after product testing was a Campbell Scientific CR 9000 data acquisition system. It possessed a high scan rate and had a modem connection for upload, download, and real-time viewing of data. Initially a system with 28 channels was purchased, and the instrumentation for the test was designed with that limit. An enclosure for the unit was attached to the top of Pier 2 between G1 and G2 as shown in Fig. 53. The enclosure provided protection for the DAS from the elements and vandalism during the test period. Instrument cables were wired into the box through electrical conduit to limit the environmental access to the DAS electrical systems. Electrical power and telephone utilities were installed at the site and routed to the enclosure to power and control the system. The same instrumentation for both the short-term and long-term tests was used.



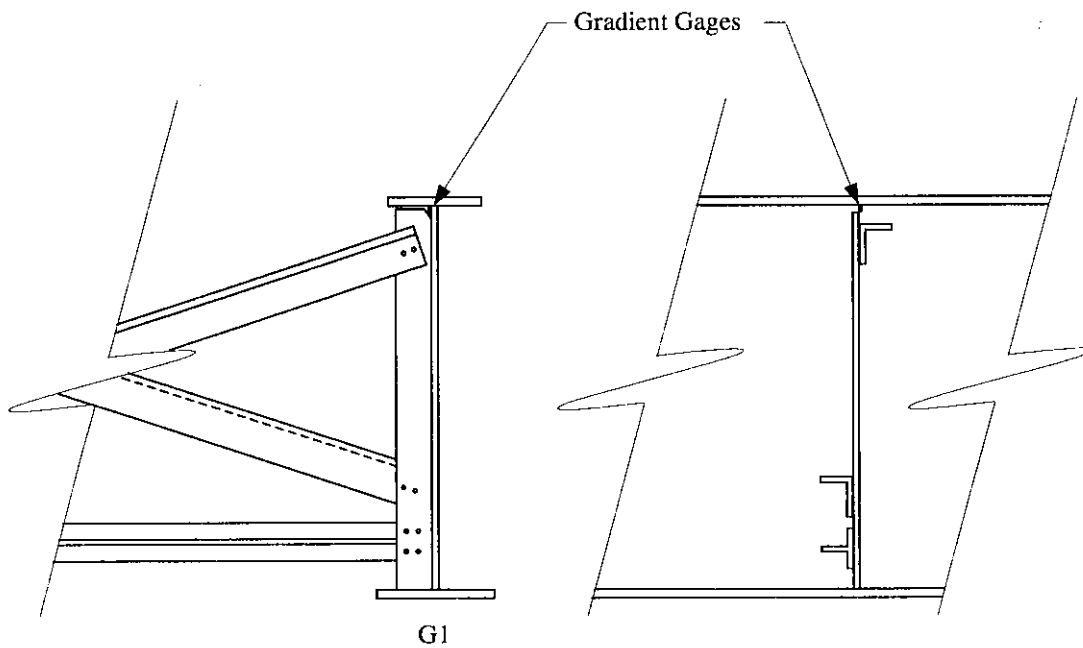
Figure 53. Photograph of DAS enclosure on Pier 2.

Gradient strain gages were used to measure strain in the web gaps. The gradient gages consisted of five foil backed strain gages assembled in one unit. The entire gage was approximately 1 in. by $\frac{1}{2}$ in. as seen in Fig. 54. One gage was placed in the G1 web gap at

D5, and another in the G2 web gap at D5. These gages are not rugged and had to be replaced during the course of the testing as the environment eventually damaged the gages.



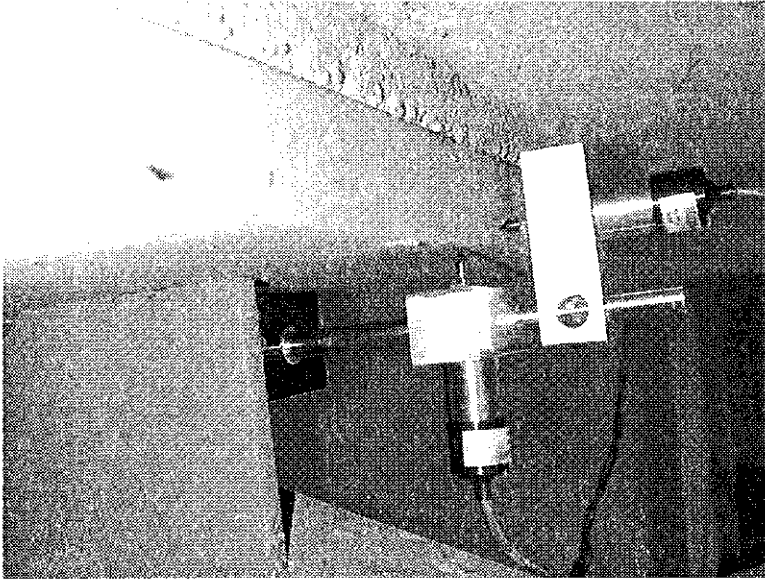
a. Photograph of G1 gradient gage.



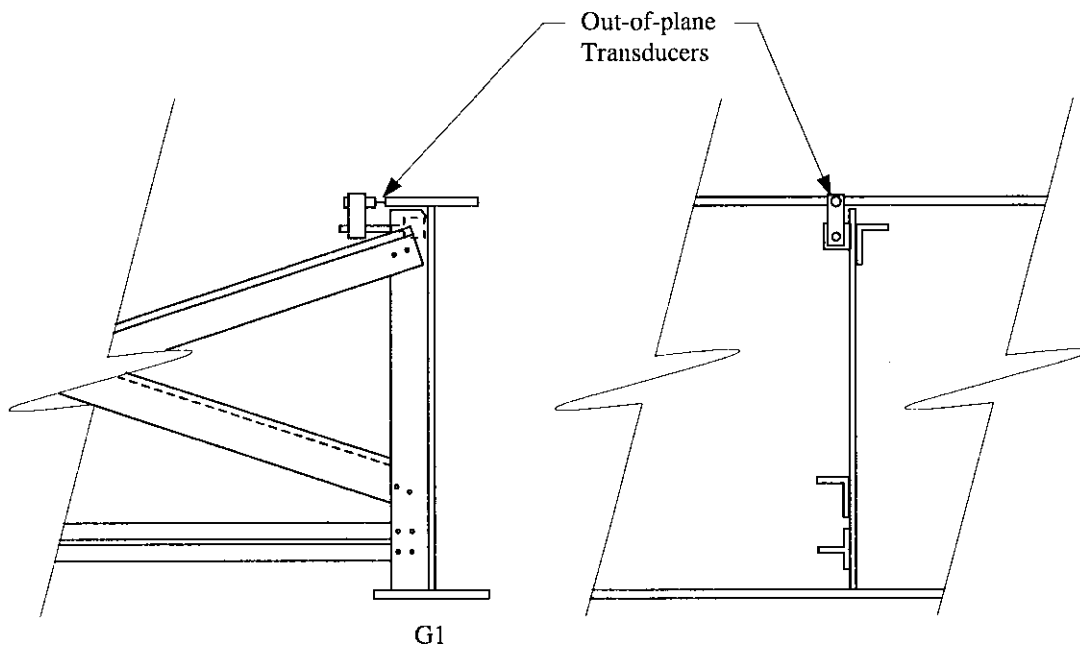
b. G1 web gap gradient gage position looking north and east.

Figure 54. Web gap gradient gage location.

Environmentally shielded direct current displacement transducers (DCDT's) were used to measure out-of-plane displacement in the web gap. The DCDT's had covers to protect movable parts from the environment and to allow them to function properly in dust, condensation, and ice. The transducers can be seen in Fig. 55.



a. Photograph of out-of-plane and tipping transducers.



b. Transducer locations looking north and east.

Figure 55. Web gap transducer placement.

Two DCDT's were mounted on G1 as well as G2. Magnets were used to hold the gages to the bridge and epoxy was used to reinforce the magnetic attachment. One gage measured the out-of-plane displacement of the web between the top of the web stiffener and the vertical face of the top flange. The other measured tipping in the girder flange between the girder web and the edge of the underside flange face, which is not discussed in this report.

Durable 120-Ohm weldable strain gages were used on the diaphragm and girders to measure strain. These gages are manufactured for outdoor use and are sealed from the environment. The welded bond between the bridge and the gage also ensures a long life for the gage because the gage is less likely to delaminate from the bridge or develop electrical shorts over time. Three gages were placed on the diaphragm as shown in Fig. 56. One gage was welded to each member of the diaphragm to monitor the forces transferred between girders. Five gages were welded to the girders near the pier and at mid span. G1 and G2 had a gage mounted on the top and bottom flanges 36 in. from the pier. The fifth gage was placed in the center of Span 2 on G2. It was added after long-term testing had started as a possible alternative control trigger for the DAS.

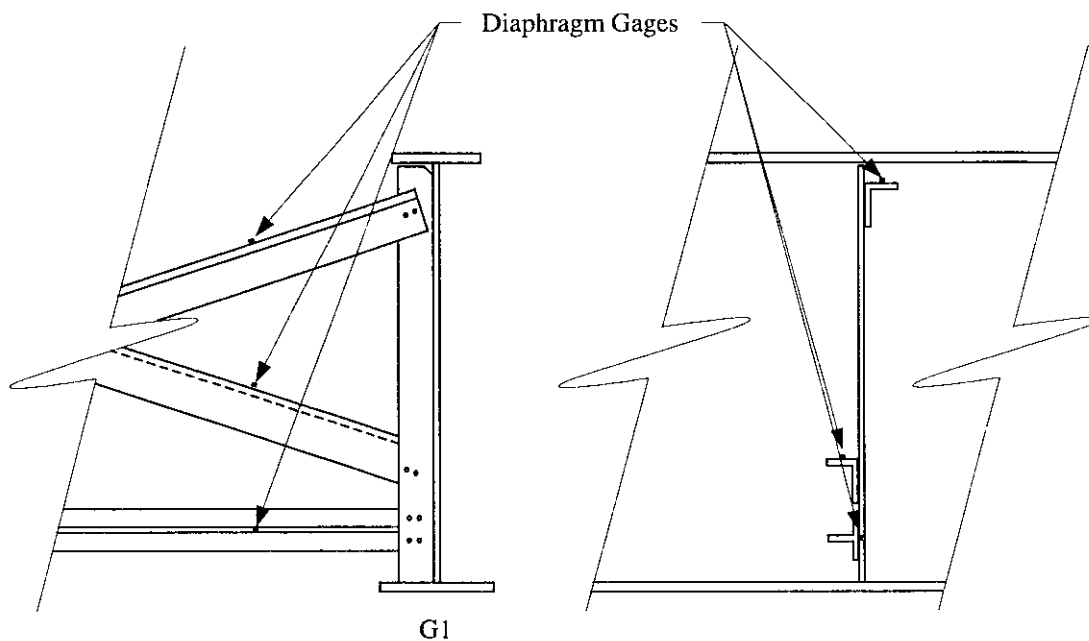


Figure 56. Diaphragm gage location looking north and east.

Test Procedure

Load testing the bridge occurred in several phases before and after the retrofit was installed. An initial load test was performed on September 6, 2000 with the bridge in its original state, without the retrofit installed. An Optim Electronics Megadac DAS was used to collect data from this initial test. The Megadac was used frequently by researchers at Iowa State University and was known to provide accurate measurements. It was important to collect reliable initial data to provide a basis for evaluation of subsequent continuous monitoring data. A standard Iowa DOT dump truck was used for the load testing of the bridge. The truck weighed 49,560 lbs and crossed the bridge at different speeds in the northbound lane. A similar truck, weighing 45,980 lbs, was used to load the southbound lane to document the effect of traffic not directly over the instrumented area.

In March of 2001 the first test model of a continuous monitoring DAS, an IOtech Inc. Logbook 300, was brought on line after months of testing. The DAS constantly monitored the gages on the bridge and stored the information in its short-term memory. When a programmed trigger threshold was reached, the system recorded a predetermined period of data into a data bank. A strain gage on the bottom flange of G2 was used as a trigger to inform the DAS that a truck of substantial size was traveling in the northbound lane. A strain of more than 20 micro strain was equivalent to a truck of approximately 50,000 lbs and caused the system to permanently record 12 sec of data; 6 sec before the trigger event, and 6 sec after. Two weeks of data were obtained using this system, but it was not suitable for the harsh environment in a remote location, and data collection was halted pending installation of a new, more reliable, system.

In September 2001 installation of the Campbell Scientific CR 9000 continuous monitoring DAS was completed and testing with ambient traffic was initiated. The Campbell system was durable enough to withstand the field testing environment and was selected as the DAS for this research. The DAS constantly monitored the gages of the bridge at 100 Hz and stored the information in short-term memory. The G1 gradient gage was used as a trigger to inform the DAS that a truck of appropriate size was traveling in the northbound lane. A strain of more than 200 micro strain, again a truck of approximately 50,000 lbs, caused the system to record 16 sec of data in long-term memory; 8 sec before the trigger event, and 8

sec after. The data saved during a trigger event was averaged to 10 Hz to reduce storage size and to smooth the data for later analysis. This system recorded ambient truck traffic on Highway 17 through December 2001, when the bolt loosening retrofit was installed.

The bolt loosening retrofit was installed on December 18, 2001. Load tests using an Iowa DOT truck of 39,660 lbs at 55 mph were completed before and after the bolts were loosened to verify ambient data collected by the DAS. Data was recorded for 16 sec, as it was with ambient traffic, but the controlled load tests had only the load truck on the bridge during each test. Northbound and southbound test passes were completed. Unfortunately the load test data for the loose bolt condition were lost shortly after testing and only the tight bolt condition data was retrieved for analysis. A second test with a DOT truck, as discussed below, was required to collect loose bolt data.

The retrofit was installed on 2 bays of D5 between G1 and G2, and G2 and G3, as seen in Fig. 57. The bolts connecting the horizontal T section to G1 were not loosened because they were inaccessible, but the member was released on the G2 side. Releasing the diaphragm between G2 and G3 prevented forces induced in the diaphragm between them from affecting the instrumentation on G2. The bolts were loosened just enough to allow free movement of the diaphragm members and the nuts were bound in place by the paint on the end of the bolts. In some cases liquid thread locker was used to further secure the nuts.

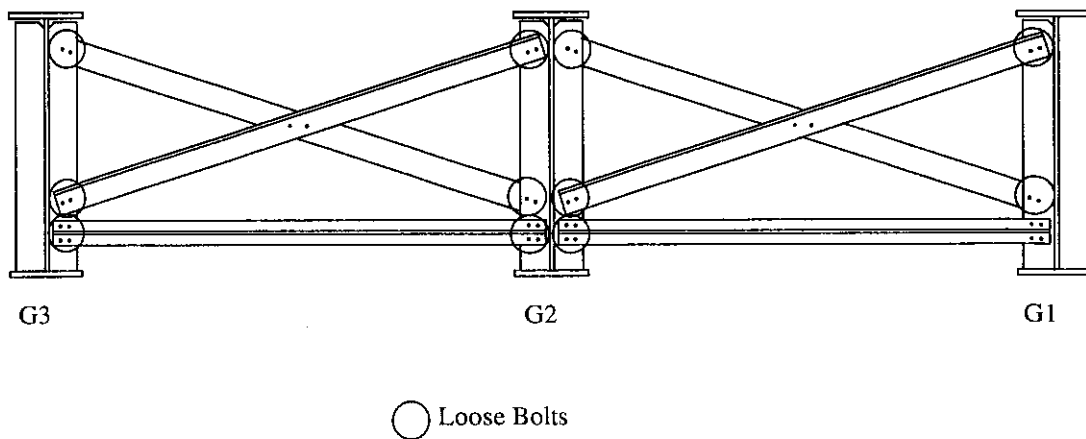


Figure 57. Illustration of G1 to G3 with diaphragm bolt loosening indicated.

Following the load tests, the DAS was returned to continuous monitoring mode. Due to the reduction in web gap strain with the retrofit in place, a strain gage on the bottom flange

of G2, 36 in. from the pier, was used to trigger the DAS. The strain in this gage was not affected by the local loosening of diaphragm bolts in two diaphragm sections and was useful in comparing truck signatures before and after bolt loosening.

Other researchers [4,5] have suggested a change in the lateral load distribution in a bridge that has had the diaphragms removed. The strain in the two girders directly associated with diaphragm loosening in this test show little sign of reduction or increase in loading. The results only reflect a small portion of the bridge with only two diaphragms loosened, but it can be concluded from them with a fair amount of certainty that loosening the diaphragms on this bridge has little affect on its lateral load distribution. Because of this phenomenon trucks of similar weights in similar positions on the bridge create similar longitudinal strain values, regardless of the retrofit state of the bridge.

Due to the loss of loose bolt data with a DOT load truck a second load test was completed on February 5, 2002. A DOT load truck of 49,960 lbs crossed the bridge at 55 mph. The truck was placed in the northbound lane. This data combined with the previous controlled load test data with the bolts tight provides a signature load pattern that is used to interpret ambient loading data for the bridge in the tight and loose conditions. Ambient trucks of similar configurations and loadings exhibit similar strain patterns to the DOT trucks and can be selected for analysis based on that similarity. The typical configuration for a DOT load truck is shown in Fig. 58.

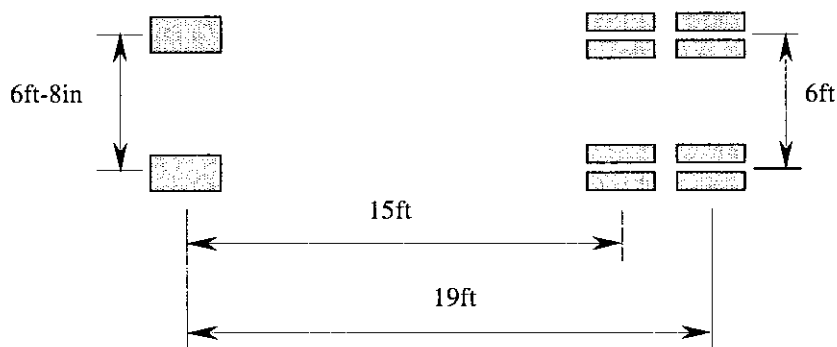


Figure 58. Typical load truck configuration.

Short-Term Experimental Results

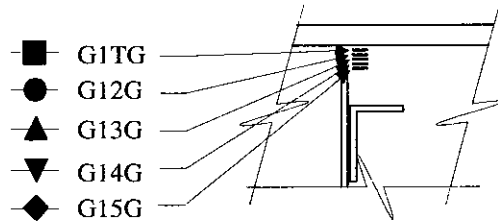
The data used to examine the short-term response of the bridge were the tight bolt data from December 18, 2001 and the loose bolt data from February 2, 2002. It was desirable to use the same truck and weight for comparison of data before and after the installation of the retrofit, but it was not possible due to the loss of loose bolt data so a different truck was used. The Truck T (tight bolts) and the Truck L (loose bolts), as they are designated, had comparable configurations; however, the tight truck weighed 39,660 lbs as previously stated, and the loose truck weighed 49,960 lbs.

Testing of this and other bridges have shown little change in the longitudinal strain in the bottom flange of the girders near the pier before and after installation of the retrofit. Because the longitudinal strain is relatively unchanging between tight and loose bolts it can be used to normalize the data from the lighter Truck T to the heavier Truck L. It is assumed that a linear relationship exists between the data obtained in each test and that the difference in load can be factored out of the results. The importance of the data is not exact values, but the overall reduction of strain in the web gap in the long and short-term. Introduction of normalization to the Truck T data increased strain and displacement values and also increased the resulting reductions from the retrofit. The figures presented show the unnormalized data, however, the reduction percentages were calculated including a normalization factor of approximately 0.2.

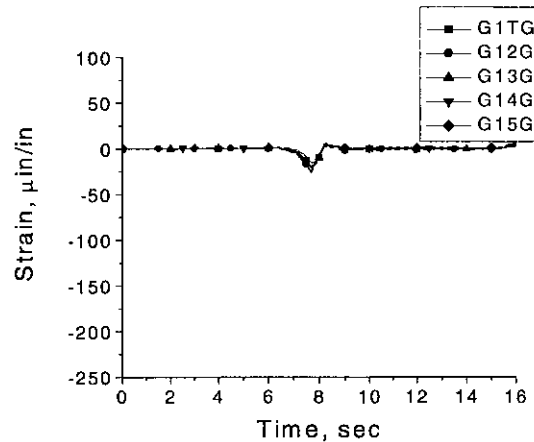
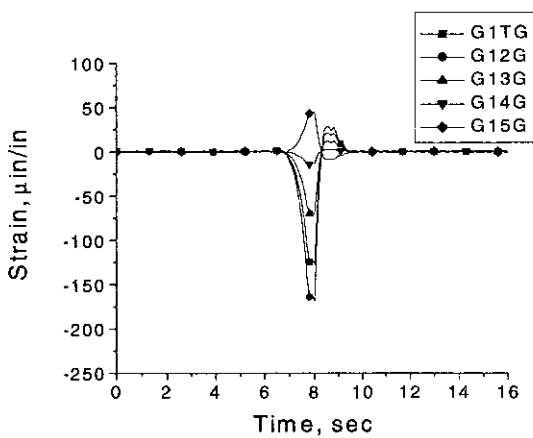
Figure 59 shows the strain in the G1 web gap with the diaphragm/girder connection bolts in the tight and loose conditions. Each plot represents a single load truck in the northbound lane above the instrumentation. The tight data is from Truck T and the loose data is from Truck L. The location of the individual gradient gages is indicated on the adjoining illustration.

The strain in the web gap is reduced by more than 80 percent when the bolts are loose. This value is even larger when the increased weight of the loose truck is taken into consideration. The strain with all bolts tight would be greater with a larger load, and the subsequent reduction would be greater than 80 percent. The strain changes sign within the gap when the bolts are tight, indicating double bending of the web gap, shown previously in Fig. 51. A small amount of strain remains in the web gap following loosening of the bolts,

however, the double bending is removed from the web gap as suggested by the uniform strain throughout the gap. This suggests that the diaphragm is no longer creating the displacement in the web gap.



a. Location of gradient gage looking east at G1.



b. All bolts tight.

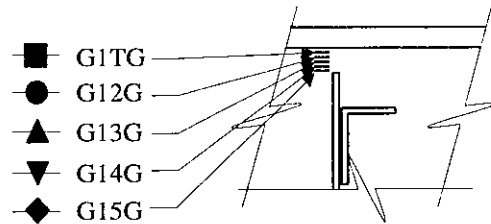
c. All bolts loose.

Figure 59. G1 gradient strain plots.

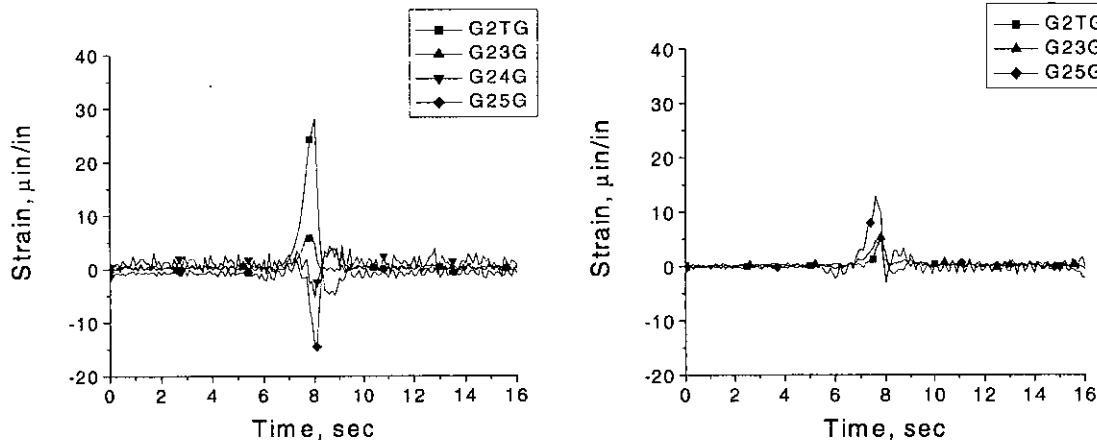
Figure 60 shows the gradient gage strain in the G2 web gap. The gage is located on the east side of G2 as illustrated in the figure. The loading is from Truck T and Truck L as in the previous figure. All gages are not shown in each plot because two of the gages suffered environmental damage between tests. Extended exposure to the elements occasionally damages the gages mounted on the bridge.

The maximum strain in the G2 web gap is in the G2TG location, which was functioning during both tests. The plots show a reduction of strain in the gap at that gage of approximately 50 percent. Double bending is noticeable in the G2 web gap as well as the G1 web gap as illustrated in Fig. 51. Loosening the bolts does not eliminate the double bending

in the G2 web gap. The strain values of each gage are not equal, which indicates uniform bending; however, they are all the same sign and of similar values, suggesting a near uniform bending of the gap.



a. Location of gradient gage looking west at G2.



b. All bolts tight.

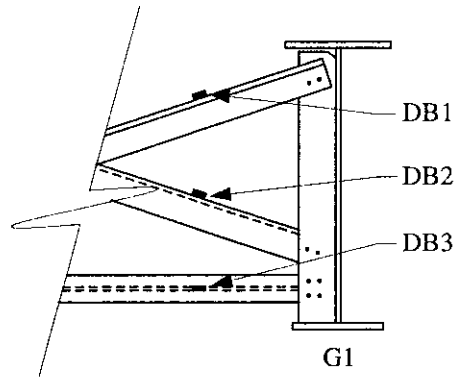
c. All bolts loose.

Figure 60. G2 gradient strain plots.

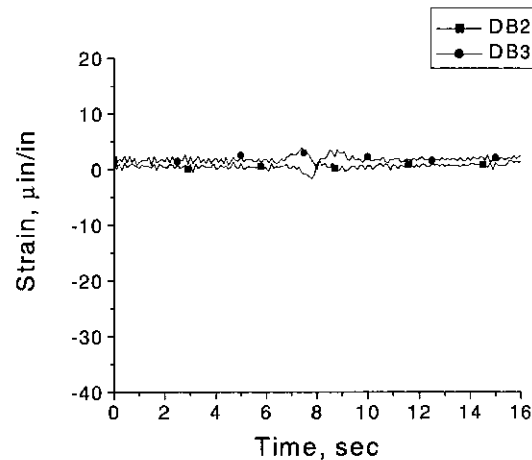
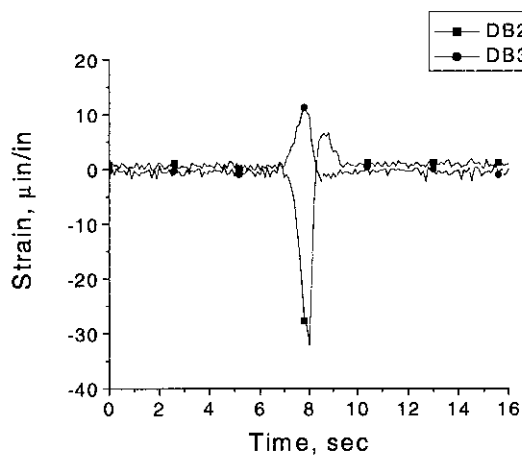
Figure 61 shows the strain in D4 between G1 and G2 before and after the bolt loosening retrofit. The gages were located on the G1 side of the diaphragm as indicated. Gage DB1 was inoperable at the time of the test and is omitted from the plots. The tight and loose truck loadings were different as presented above.

The strain in the diaphragm members was not completely eliminated by the bolt loosening retrofit, but the values are significantly reduced, only slightly less than 100 percent. The remaining strain in the diaphragm may be a result of the tight bolts at G1 on the

bottom T as is also suggested by slight double bending of web gap G2 with the bolts loose, as discussed above.



a. Location of strain gages looking north at D4.



b. All bolts tight.

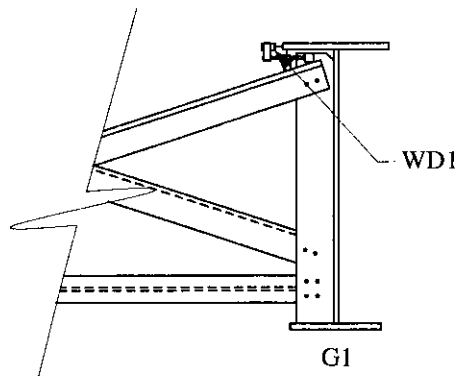
c. All bolts loose.

Figure 61. D4 strain plots.

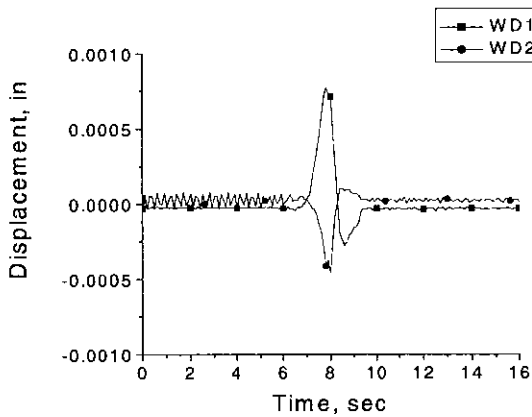
Figure 62 shows the out-of-plane displacement in the G1 and G2 web gaps at D4. The location of WD1 on the web stiffener is illustrated. Transducer WD2 is in a similar location to WD1 except it is mounted on G2 between G1 and G2. Truck T and Truck L are the load for each plot, as above.

Out-of-plane displacement of the web gaps is reduced, but not eliminated by the bolt loosening retrofit. The displacement in the web gaps is reduced by at least 50 percent. The reduction of peak displacement in the web gaps corresponds in a similar manner to the

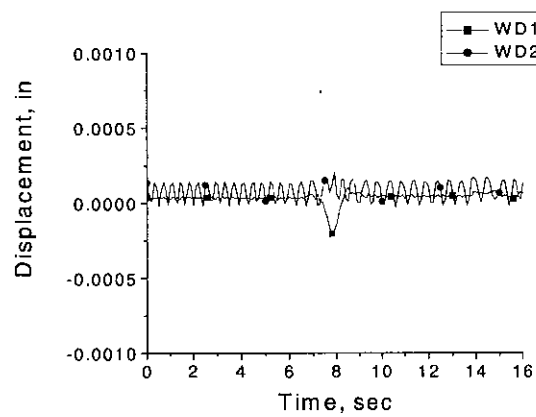
reduction of peak strains in the web gaps, which verifies a relationship between the strain and displacement in the gaps.



a. Location of G1 transducer looking north at D4.



b. All bolts tight.



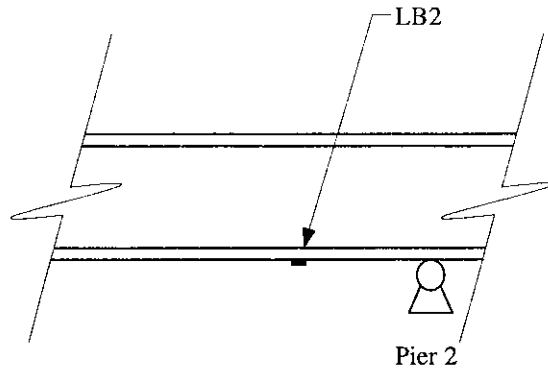
c. All bolts loose.

Figure 62. Web Gap out-of-plane displacement plots.

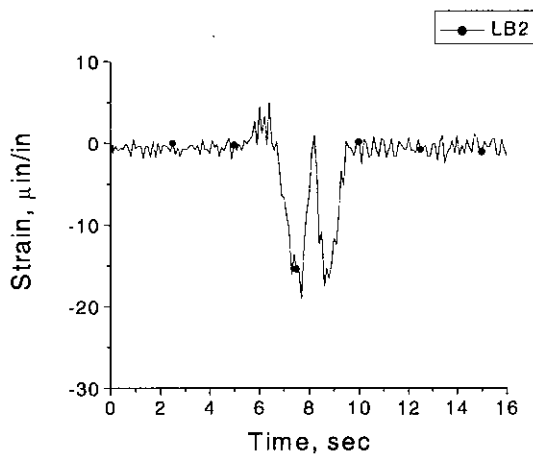
Figure 63 shows the longitudinal strain in the bottom flange of G2 near Pier 2 in the negative moment region. The loading during the plots is the same as previous figures. The gage position is 36 in. from the Pier 2 bearing.

Longitudinal strain in the girders is not affected by the loosening of bolts on such a small scale. Because of this, the longitudinal strain is effective in determining the general truck weight and for triggering the DAS. Fig. 63 reflects this fact by depicting similar strain patterns for each test, before and after loosening bolts. The loose bolt plot indicates an increase in maximum strain of approximately 20 percent, which correlates directly to the 20

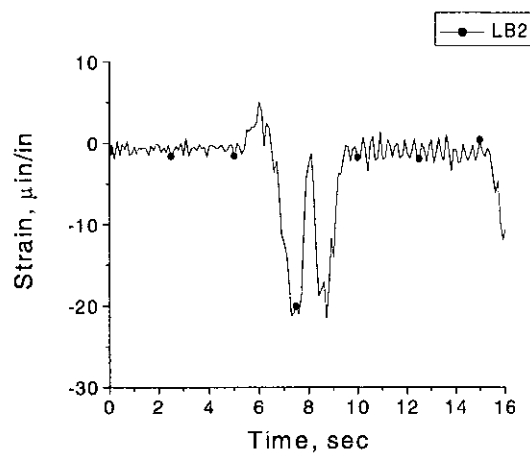
percent increase in load of the tight truck compared to the loose truck. This is the basis of the normalization of data discussed previously.



a. Location of G1 transducer looking north at D4.



b. All bolts tight.



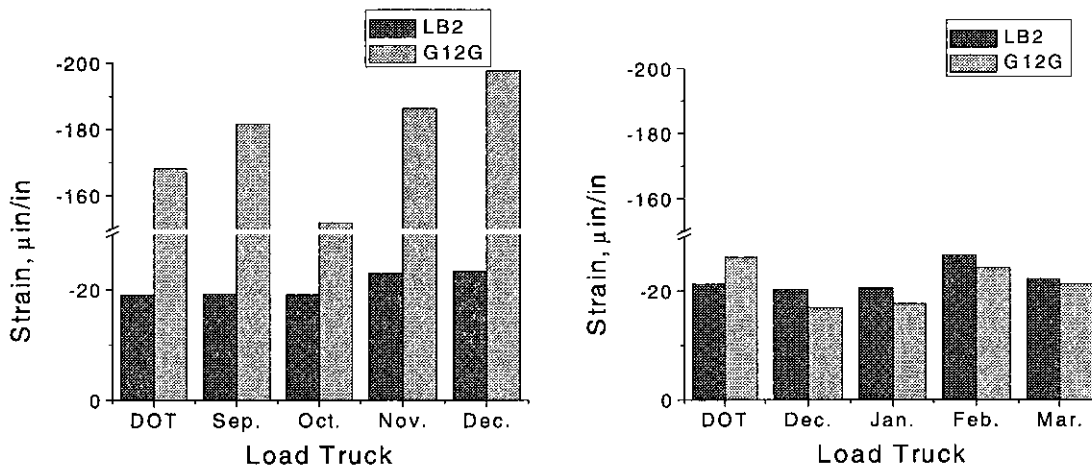
c. All bolts loose.

Figure 63. Longitudinal girder strain plots.

Long-Term Experimental Results

One of the goals of this research was to monitor the effect that the bolt loosening retrofit has on an in-service bridge over a long period of time. Ambient data was collected over eight months - four months of tight data and four months of loose data. Trucks of similar weights were compared throughout testing to investigate any change in strain value with the bolts tight and loose.

The results were compared using the longitudinal strain, depicted in Fig. 63, because of the continuity of values between tight and loose conditions for equal weight trucks. As discussed previously, the change in longitudinal bending strain between tight and loose bolt conditions has proven to be negligible under the same load condition. The DOT load trucks exhibited a longitudinal strain of approximately 20 micro strain in LB2 so that value was used to distinguish trucks of similar weight. Figure 64 shows the maximum strain in the G1 web gap of selected vehicles collected during testing with the bolts tight and loose. One vehicle for each month is presented along with the DOT load test trucks. The maximum longitudinal strain reveals similarity in loadings, and the web gap strain reveals similar responses of the web gap for those loadings.



a. All bolts tight.

b. All bolts loose.

Figure 64. Maximum G1 web gap strains and G2 longitudinal strains for individual truck loadings.

The maximum strains in the G1 web gap are approximately 200 micro strain with the bolts tight. The four months following bolt loosening show approximately 20 micro strain, and show no signs of changing over time. Slight variations in the web gap values are partially due to slightly different weights of the ambient truck loadings. The correlation between load and gap strain is illustrated in Fig. 64. Occasionally the value of the longitudinal strain and web gap strain did not match the general trend, this can be accounted to unknown truck type and small variations that occur from test to test. No two trucks had

exactly the same longitudinal strain value. Regardless of slight variations in the strain data, the overall strain reduction was effective and strain in the web gaps had no tendency to change over time following retrofit installation.

Conclusions

The test results show that the bolt loosening retrofit reduces the strain in the web gap and the diaphragms. The near complete reduction of strain in the web gap indicates that the force in the diaphragms caused by differential deflection is nearly eliminated. The forces in these diaphragms cause the out-of-plane displacement in the web gaps which result in fatigue cracking. The lack of diaphragm force, which results in the illustrated reduction of strain and displacement in the web gaps, proves that this retrofit is effective in stopping fatigue cracking.

Long-term testing of an in-service bridge with the bolt loosening retrofit installed on a small-scale show that the retrofit remains effective after months of use. Settlement or binding of the connection does not occur over time and the reduced strain results remain stable. This further promotes the suitability of this retrofit for the elimination of web gap fatigue cracking in in-service bridges.

The Campbell Scientific DAS in these test performed well. It was rugged and capable of withstanding the harsh environment associated with remote installation. The system recorded only data of importance and reduced storage space and data manipulation time. The remote connection to the system allowed data to be downloaded from a remote computer and also provides real-time plots of sensor values. Important gages can be plotted for quick review of key aspects of a bridge's performance. The triggered data storage also makes collection of peak events possible. General statistical information about response to ambient loading could be collected from the data obtained with this system. Improvements in technology and continued research could lead to combined video and graphical output from a bridge available real-time or collected from peak values. The system could also be programmed to set off alarms if safe thresholds are exceeded, which be especially useful in large, heavily used bridges where inspection is difficult and hazardous.

Implementation Issues

The bolt loosening retrofit provides an inexpensive solution to web gap fatigue cracking provided diaphragm adjustments are acceptable on the bridge in question. Before this retrofit is installed on in-service bridges, a few key points need to be addressed on an individual bridge basis.

Lateral support for the girders and stability of the structure with the diaphragms needs to be addressed for each bridge retrofitted. Bracing for lateral torsional buckling is important in the negative moment region and the larger girders in the negative moment region generally provide adequate strength over the unbraced length. This usually allows for removal of diaphragms in the negative moment region, but the engineer must determine the girders are satisfactorily braced before implementing the retrofit. A check of stability was performed on this bridge using AASHTO LRFD specifications. It was calculated that the diaphragms could be removed from the negative moment regions of the bridge without affecting the moment capacity of the girders.

Lateral load distribution regarding diaphragms is also a concern. The change in lateral load distribution of the bridge was not thoroughly tested in this research, but other researchers have found that most bridges show little change in lateral load distribution with the diaphragms removed. The bolt loosening retrofit relieves the force in the diaphragms and is equivalent to diaphragm removal concerning lateral load distribution. The engineer should determine that the bridge has a satisfactory rating to safely carry up to 15 percent more strain in the maximum strain girder.

A system must be devised to ensure that the bolts remain in place so that the diaphragms are not at risk of falling. The nuts on the bolts may reverse due to bolt vibration under traffic load allowing the bolts to fall out. The method of connection was not researched, but a lock nut or double nut technique may be a solution. It was noted during long-term testing of the retrofit that longer bolts might need to be installed to provide room for nut locking techniques. A liquid thread locker was used in this research and may be another option. Any solution implemented should be periodically inspected to insure that it is functioning properly.

Each bridge must meet the listed requirements and any other requirements determined by the engineer before the retrofit is installed. The effects of the retrofit must be monitored closely until the engineer is convinced the bridge is stable and the diaphragms are safely secured to the stiffeners.

References

1. T.J. Wipf, and L.F. Greimann, A. Khalil. Preventing Cracking at Diaphragm/Plate Girder Connections in Steel Bridges. Ames, Iowa: Center for Transportation Research and Education, Iowa DOT Project HR-393, Iowa State University, 1998.
2. A. Khalil. "Aspects in Nondestructive Evaluation of Steel Plate Girder Bridges", Dissertation, Iowa State University, Ames, Iowa, 1998.
3. J.W. Fisher, and P.B. Keating. "Distortion-Induced Fatigue Cracking of Bridge Details with Web Gaps." Journal of Constructional Steel Research, Vol. 12, pp. 215-228, ASCE, 1989.
4. J.M. Stallings, and T.E. Cousins. "Fatigue Cracking in Bolted Diaphragm Connections." Proceedings of the 15th Structures Congress 1997 Portland, Vol. 1, pp. 36-40, New York: ASCE, 1997.
5. T.E. Cousins, J.M. Stallings, and T.E. Stafford. "Removal of Diaphragms from 3-Span Steel Girder Bridge." Journal of Bridge Engineering, Vol. 4, No. 1, pp. 63-70, ASCE, Feb. 1999.
6. A. Azizimini, S. Kathol; and M. Beachman. "Effects of Cross Frames on Behavior of Steel Girder Bridges." 4th International Bridge Engineering Conference Proceedings, pp. 117-124, Washington, D.C.: TRB, 1995.
7. M.J. Chajes, H.W. Shenton III, and D. O'Shea. "Bridge-Condition Assessment and Load Rating Using Nondestructive Evaluation Methods." Transportation Research Record, Vol. 2, No. 1969, pp. 83-91, Washington, D.C.: TRB, National Research Council, 1998.
8. A.E. Aktan, K.A. Grimmelsman, and R.A. Barrish. "Structural Identification of a Long-Span Truss Bridge." Transportation Research Record, Vol. 2, No. 1696, pp. 210-218, Washington, D.C.: TRB, National Research Council, 2000.

Chapter 5. General Conclusions

General Discussion

The previous papers describe extensive testing on the bolt loosening retrofit. Bridges with I-beam, channel, and X-type diaphragms were tested for the effectiveness of the retrofit and the results were positive.

Loosening the bolts in the diaphragm/girder connection reduced the strain in the girder web gaps by more than 70 percent in most cases. The exterior girders showed the largest reductions in strain in the web gap. The out-of-plane displacement of these web gaps was reduced almost as much as the web gap strain, approximately 50 percent. The strain in the diaphragms also reduced significantly, nearly 100 percent in the bridges tested, suggesting that the forces created in the diaphragms by differential deflection of the girders had been eliminated by the retrofit. The forces in the diaphragms have been linked directly to out-of-plane displacement of the web gap, and the elimination of these forces suggests the retrofit was effective.

Long-term testing of the X-type diaphragm bridge also showed promising results. A bridge was monitored for eight months, four months without the retrofit and four months with the retrofit. The strain and displacement values recorded from the bridge showed no indication of altering over time. The results acquired from short-term testing of the bolt loosening retrofit can therefore be applied to bridges with confidence that traffic loading effects over time will not have adverse affects on strain and displacement in the web gaps.

As a result of the long-term testing a remote monitoring system was developed for use by the Iowa DOT. The system is capable of monitoring strain, displacement, temperature gages, and many other sensor types in a remote location over a long period of time. The DAS can be programmed to collect continuously or only peak data, as selected by a designated trigger gage, for a predetermined period of time. This allows useful data to be collected, while the remainder of the ambient data is discarded. Another essential component of the DAS is its communication abilities. Engineers can collect data from the unit without physically being in the field. No site visit is necessary to download data from the DAS memory as modem communication allows office computers to access the system. This

communication ability also provides for real time monitoring of instrumentation at the site. Readings can be viewed at the time they are collected. This system has many possible applications in future DOT bridge monitoring programs.

Implementation of the retrofit will need to be monitored closely on tests bridges. A bolt fastening technique was not researched and will need to be devised to ensure that the bolts and diaphragms stay in place on the bridge. Strain in the girders indicating lateral load distribution and lateral torsional buckling should also be investigated on any bridge fitted with the retrofit. Essentially, bridges selected for retrofit should be monitored after all bolts are loose and should be periodically checked for diaphragm fastening and girder strain.

Recommendations for Future Research

A thorough investigation of the bridge behavior could be conducted using FEM. Bridges that have undergone field testing of the retrofit should be modeled with the diaphragm bolts loose or removed to better understand the behavior of the structure. Global and local results of the FEM analysis are of interest. The global deflection of each span and the tendency towards lateral torsional buckling should be investigated. The response of the bridge to high winds or a lateral impact should also be looked at. The local deflection of the web gap and diaphragm in the area of the fatigue cracking are important. A comprehensive model of the strains and deflections in the web gap would be helpful in understanding web gap fatigue cracking and the strain results obtained from field testing. Strain and deflection data acquired from field tests could also be used to calibrate the FEM.

More comprehensive stability calculations should be performed on the effects of lateral torsional buckling of the girders following installation of the retrofit. General calculations were completed using AASHTO criteria, but a more accurate calculation should be completed that accounts for small movements in the girders before the diaphragms begin to support the girders. FEM could also be used to model this behavior. The difficult part of the research involves quantification of the amount of freedom the girders actually have when the bolts are loose.

A full-scale test of the retrofit on an in-service bridge should also be performed. A test bridge should have all the diaphragms retrofitted and many aspects of the bridge monitored to ensure that the retrofit is functioning properly. Strain and displacement in

individual web gaps could be documented, and strains and displacements in the girders, vertical and horizontal, could also be monitored. Initial load tests should be run after installation of the retrofit, however, testing should continue on the bridge with ambient loading until the stability of the structure is assured.

Many have researched the effects of diaphragms on lateral load distribution, however, the affects of lateral load distribution was not investigated in the bridges tested. Instrumentation on a full-scale retrofit could focus on the deflection or strains of individual girders before and after the retrofit, showing changes due to loosening the diaphragms and lateral load distribution.

The DAS used in the long-term testing could be very useful in future bridge monitoring research. Sensors could be set up to monitor a critical joint or member on a bridge expected to experience distress. The system can monitor the critical point twenty-four hours a day, seven days a week and record the slightest change in the connection, alerting maintenance crews when there may be a problem. This type of system would be especially useful in bridges that are difficult to inspect at regular intervals. An example would be a critical connection in the middle of a busy span crossing the Mississippi River. Inspection could only be done with the aid of a snooper and traffic control. This disruption in traffic and resources may be in vain if no problem is discovered. The continuous monitoring DAS is ideal in this situation. It would reduce the number of human operated inspection trips and would alert proper personnel in the event of any significant change in the bridge. In the future, after some upgrading, visual data could also be collected by the system using digital cameras. As more technology becomes available the perceivable uses of this system will grow. This system, and those like it, are the future of remote bridge monitoring.

References

1. T.J. Wipf, and L.F. Greimann, A. Khalil. Preventing Cracking at Diaphragm/Plate Girder Connections in Steel Bridges. Ames, Iowa: Center for Transportation Research and Education, Iowa DOT Project HR-393, Iowa State University, 1998.
2. A. Khalil. "Aspects in Nondestructive Evaluation of Steel Plate Girder Bridges", Dissertation, Iowa State University, Ames, Iowa, 1998.
3. J.W. Fisher. Fatigue and Fracture in Steel Bridges, Case Studies. New York: John Wiley and Sons, 1984.
4. J.W. Fisher, B.T. Yen, and D.C. Wagner. "Review of Field Measurements for Distortion Induced Fatigue Cracking in Steel Bridges." Transportation Research Record, No. 1118, pp. 49-55, Washington, D.C.: TRB, National Research Council, 1987.
5. J.W. Fisher, and P.B. Keating. "Distortion-Induced Fatigue Cracking of Bridge Details with Web Gaps." Journal of Constructional Steel Research, Vol. 12, pp. 215-228, ASCE, 1989.
6. J.W. Fisher. Executive Summary: Fatigue Cracking in Steel Bridge Structures. Bethlehem, Pennsylvania: Advanced Technology for Large Structural Systems, Report No. 89-03, Lehigh University, 1989.
7. C.E. Demers, and J.W. Fisher. A Survey of Localized Cracking in Steel Bridges 1981 to 1988. Bethlehem, Pennsylvania: Advanced Technology for Large Structural Systems, Report No. 89-01, Lehigh University, 1989.
8. P.B. Keating. "Focusing on Fatigue." Civil Engineering, Vol. 64, No. 11, pp. 54-57, New York: ASCE, 1994.
9. T.E. Cousins, and J.M. Stallings. "Calculation of Steel Diaphragm Behavior", Journal of the Structural Division, Vol. 102, No. ST7, pp. 1411-1430, ASCE, July 1976.

10. J.M. Stallings, and T.E. Cousins, and T.E. Stafford. "Effects of Removing Diaphragms from Steel Girder Bridge", Transportation Research Record, Vol. 1541, pp. 183-188, Washington, D.C.: TRB, National Research Council, 1996.
11. J.M. Stallings, and T.E. Cousins. "Fatigue Cracking in Bolted Diaphragm Connections." Proceedings of the 15th Structures Congress 1997 Portland, Vol. 1, pp. 36-40, New York: ASCE, 1997.
12. J.M. Stallings, and T.E. Cousins. "Evaluation of Diaphragm Requirements in Existing Bridges." Proceedings of the 15th Structures Congress 1997 Portland, Vol. 2, pp. 1494-1498, New York: ASCE, 1997.
13. T.E. Cousins, and J.M. Stallings. "Laboratory Tests of Bolted Diaphragm-Girder Connection." Journal of Bridge Engineering, Vol. 3, No. 2, pp. 56-63, ASCE, May 1998.
14. T.E. Cousins, J.M. Stallings, and T.E. Stafford. "Removal of Diaphragms from 3-Span Steel Girder Bridge." Journal of Bridge Engineering, Vol. 4, No. 1, pp. 63-70, ASCE, Feb. 1999.
15. A. Azizimini. "Steel Bridge Design Using AASHTO LRFD Bridge Design Specifications (1999 Interim)." Proceedings of National Bridge Research Organization Short Course, Kansas City: NaBRO, November 1999.
16. A. Azizimini, S. Kathol; and M. Beachman. "Effects of Cross Frames on Behavior of Steel Girder Bridges." 4th International Bridge Engineering Conference Proceedings, pp. 117-124, Washington, D.C.: TRB, 1995.
17. C. Miki, H. Takenouchi, T. Mori, and S. Ohkawa. "Repair of Fatigue Damage in Cross Bracing Connections in Steel Girder Bridges." Structural Engineering/Earthquake Engineering, Vol. 6, No. 1, pp. 31s-39s, Tokyo, Japan: JSCE, April 1989.
18. F.S. Zwerneman, A.B. West, and K.S. Lim. "Fatigue Damage to Steel Bridge Diaphragms." Journal of Performance of Constructed Facilities, Vol. 7, No. 4, pp. 207-225, ASCE, Nov. 1993.

19. M.J. Chajes, H.W. Shenton III, and D. O'Shea. "Bridge-Condition Assessment and Load Rating Using Nondestructive Evaluation Methods." Transportation Research Record, Vol. 2, No. 1969, pp. 83-91, Washington, D.C.: TRB, National Research Council, 1998.
20. H.W. Shenton III, M.J. Chajes, and E.S. Holloway. "A System for Monitoring Live Load Strain in Bridges." Structural Materials Technology IV Conference Proceedings, pp. 89-94, Atlantic City, New Jersey: FHWA, 2000.
21. A.E. Aktan, K.A. Grimmelsman, and R.A. Barrish. "Structural Identification of a Long-Span Truss Bridge." Transportation Research Record, Vol. 2, No. 1696, pp. 210-218, Washington, D.C.: TRB, National Research Council, 2000.

Acknowledgements

The author of this paper wishes to thank everyone who contributed to the research presented and to the completion of this thesis. Special thanks go to my major professors Terry J. Wipf and Lowell F. Greimann. I would also like to thank Lester W. Shmerr for serving on my committee and Brent Phares for reviewing my reports. Thanks are also due to the Iowa Department of Transportation for sponsoring the research and assisting in load testing of the bridges presented.

The experimental portion of this project would not have been possible without the help of Doug Wood, Manager of the Structural Engineering Laboratory. The following Structural Engineering graduate students graciously volunteered time to help with load testing: J. Scott Ingersoll, Brian Kempers, Travis Konda, and A.J. Samuelson. I would also like to thank the following Civil Engineering undergraduates for all of their assistance in the field testing: Ben Drier, Ken Hoevelkamp, and Karla Troester.

Appendix

Appendix 1: I-80 AASHTO Stability Calculations

AASHTO Calculations for Lateral Bracing Adequacy of I-80 Bridge Assuming Diaphragms Removed

AASHTO calculations on the I-80 bridge were performed using the maximum live plus dead load moment in the negative moment region. All girder shape properties calculated assuming composite structure with the bridge deck. Some tests had factored maximum moment calculated prior to insertion into the calculation spreadsheet, while others included summing and factoring of individual moment components.

Maximum Loading:

- Dead Load of Superstructure and Deck
- Live Load Lane Loading, 0.64 kips
- Live Load Truck Loading, 2 trucks 50 ft apart centered over pier

Modeling:

- STAAD computer analysis performed on a single girder using AASHTO load distribution factors
- QConBridge₁ computer analysis used to double check particular calculations
- Moment data used in mathematical checks labeled as Tests 1 to 11 below

Test 1:

- Span 2 near Pier 2 considered
- Calculations considering large girder cross section (see attached table) the entire length to the splice
- L_b is considered to the splice, conservative assumption for zero moment under maximum moment shown
- The section passes AASHTO buckling checks

Test 2:

- Span 2 near Pier 2 considered
- Calculations considering medium girder cross section (see attached table) the entire length to the splice
- L_b is considered to the splice, conservative assumption for zero moment under maximum moment shown
- The section fails AASHTO buckling, use Tests 3 and 4 instead

Test 3:

- Span 2 near Pier 2 considered
- Calculations considering large cross section to the section change distance from the pier
- C_b value is affected, as the moment at the end is no longer considered zero as shown in the on the moment diagram at the splice location
- L_b is considered to the live and dead load inflection point on the plot
- The section passes AASHTO buckling checks

Test 4:

- Span 2 near Pier 2 considered
- Calculations considering medium cross section from the section change to the inflection point on the plot
- C_b value is maximum in this case as moment is zero at one end
- L_b is considered to the live and dead load inflection point on the plot
- The section passes AASHTO buckling checks

Test 5:

- Span 3 near Pier 2 considered
- Calculations considering large girder cross section the entire length to the splice
- L_b is considered to the splice, conservative assumption for zero moment under maximum moment shown
- The section passes AASHTO buckling checks

Test 6:

- Span 3 near Pier 2 considered
- Calculations considering medium girder cross section the entire length to the splice
- L_b is considered to the splice, conservative assumption for zero moment under maximum moment shown
- The section fails AASHTO buckling, use Tests 7 and 8 instead

Test 7:

- Span 3 near Pier 2 considered
- Calculations considering large cross section to the section change distance from the pier
- C_b value is affected, as the moment at the end is no longer considered zero as shown in the on the moment diagram at the splice location (M_1 and M_2 on plot)
- L_b is considered to the live and dead load inflection point on the plot
- The section passes AASHTO buckling checks

Test 8:

- Span 3 near Pier 2 considered
- Calculations considering medium cross section from the section change to the inflection point on the plot
- C_b value is maximum in this case as moment is zero at one end (M_2 and M_3 on plot)
- L_b is considered to the live and dead load inflection point on the plot
- The section passes AASHTO buckling checks

Test 9:

- Span 1 near Pier 1 considered
- Calculations considering large cross section to the section change distance from the pier
- C_b value is affected, as the moment at the end is no longer considered zero as shown in the on the moment diagram at the splice location

- L_b is considered to the live and dead load inflection point on the plot
- The section passes AASHTO buckling checks

Test 10:

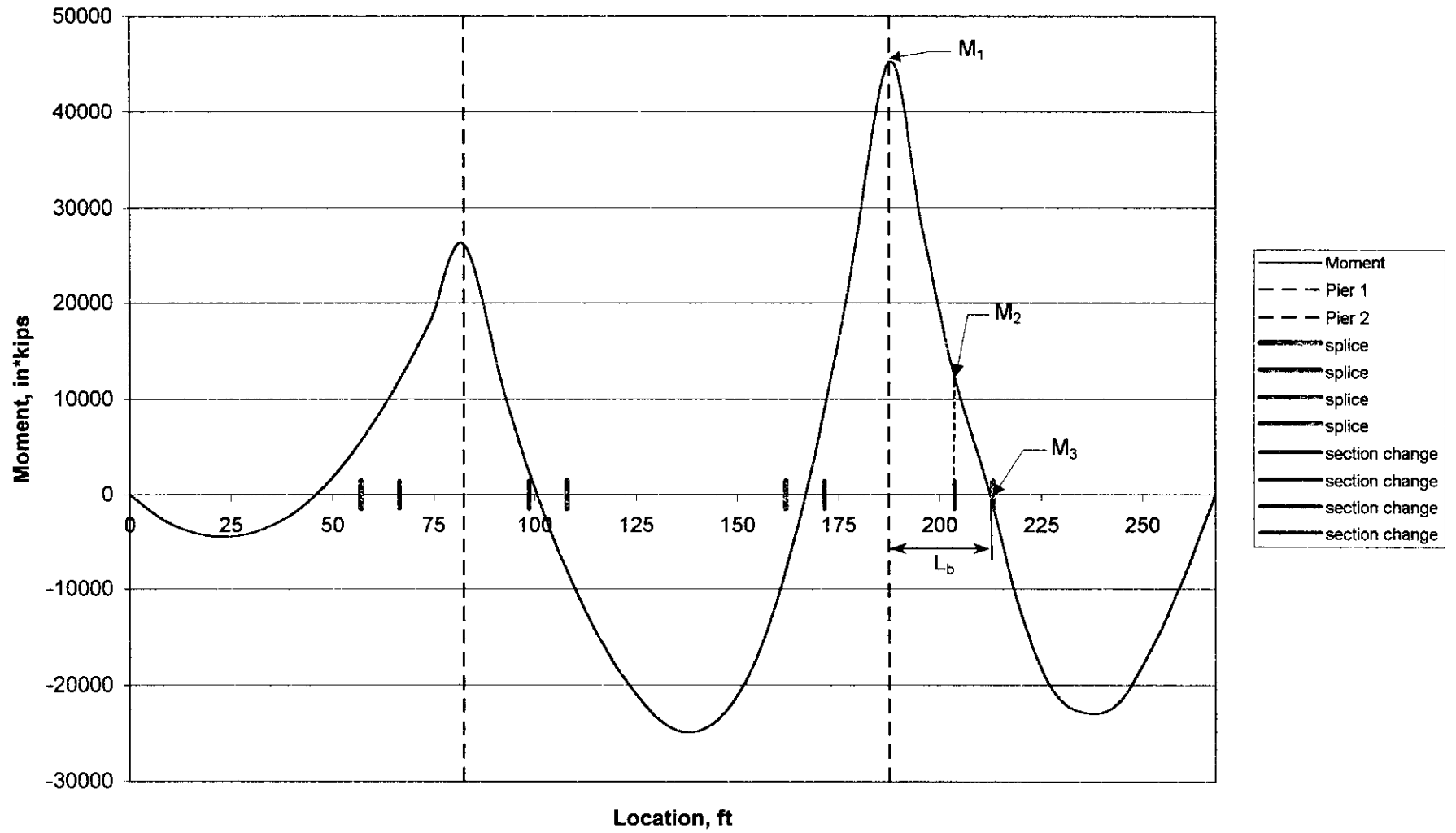
- Span 1 near Pier 1 considered
- Calculations considering medium cross section to the section change distance from the pier
- C_b value is affected, as the moment at the end is no longer considered zero as shown in the on the moment diagram at the splice location
- L_b is considered to the live and dead load inflection point on the plot
- The section passes AASHTO buckling checks

Test 11:

- Span 1 near Pier 1 considered
- Calculations considering small cross section to the section change distance from the pier
- C_b value is affected, as the moment at the end is no longer considered zero as shown in the on the moment diagram at the splice location
- L_b is considered to the live and dead load inflection point on the plot
- The section passes AASHTO buckling checks

¹ QConBridge is an AASHTO bridge analysis program created by the Washington Department of Transportation. It can be downloaded at http://www.wsdot.wa.gov/eesc/bridge/software/index.cfm?fuseaction=download&software_id=48

AASHTO Strength I Live and Dead Load I-80



Stability Tests run for I-80 bridge

Test specifics and results

Test Number	Span	Unbraced Length (L_b)		Cross Section	Section Length ft	Section Type	Maximum Moment	Minimum Moment	Result
		ft	in				in*kips	in*kips	
1	2	25.5	306	Large	25.5	Non-compact	44431	0	PASS
2	2	25.5	306	Medium	25.5	Non-compact	43406	0	FAIL
3	2	21.5	258	Large	16	Non-compact	45200	5620	PASS
4	2	21.5	258	Medium	9.5	Non-compact	5620	0	PASS
5	3	25.5	306	Large	25.5	Non-compact	44431	0	PASS
6	3	25.5	306	Medium	25.5	Non-compact	43406	0	FAIL
7	3	25.5	306	Large	16	Non-compact	45200	17200	PASS
8	3	25.5	306	Medium	9.5	Non-compact	17200	0	PASS
9	1	36.67	440.04	Large	36.67	Non-compact	26088	0	PASS
10	1	36.67	440.04	Medium	36.67	Non-compact	26088	0	PASS
11	1	36.67	440.04	Small	36.67	Non-compact	26088	0	PASS

Cross Section Dimensions

Cross Section	Bottom Flange (in)		Web (in)		Top Flange (in)	
	thickness	length	thickness	length	thickness	length
Large	2	16	0.375	46	2	16
Medium	1.5	12	0.375	46	1.5	12
Small	1.5	12	0.375	46	1.25	10

TEST 1

AASHTO CALCS FOR STABILITY OF GIRDERS 4/15/02 DAVID TARRIES

3 cross section dimensions are available for the interior and exterior girder
the interior girder is checked here

Large girder section, span 2, composite with 8 inch deck. Consider stability with whole
girder same size.

$$F_y := 36 \text{ ksi} \quad f_c := 3.5 \text{ ksi} \quad E_s := 29000 \text{ ksi} \quad E_c := 3375 \text{ ksi}$$

Limit state

6.5.4

$$\phi_f := 1$$

assume L_b is to the dead load inflection point (splice)

$$L_b := 306 \text{ in}$$

Spans

$$L_1 := 80.5 \text{ ft} \quad L_2 := 105 \text{ ft} \quad L_3 := 81.5 \text{ ft}$$

use largest span and estimate the effective span between dead load
inflection points

$$L := L_2 \cdot 0.8 \quad L = 84 \text{ ft}$$

Average girder spacing

$$s_g := 9.67 \text{ ft}$$

Deck

$$t_s := 8 \text{ in}$$

Section Dimensions: (b is base dimension and h is height dimension)

if cross section is not double
symmetric then check calcs

units : INCHES

section 1	section 2	section 3
bottom flange	web	top flange

$$b_1 := 16 \quad b_2 := \frac{3}{8} \quad b_3 := 16$$

$$h_1 := 2 \quad h_2 := 46 \quad h_3 := 2$$

4.6.2.6.1

$$\text{one} := .25 \cdot L \cdot 12$$

$$\text{one} = 252$$

$$\text{two} := 12 \cdot t_s + \begin{cases} (.5 \cdot h_3) & \text{if } .5 \cdot h_3 \leq b_2 \\ b_2 & \text{otherwise} \end{cases} \quad \text{two} = 96.375$$

$$\text{three} := s_g \cdot 12$$

$$\text{three} = 116.04$$

$$b_{\text{eff}} := \begin{cases} \text{one} & \text{if } \begin{cases} \text{one} \leq \text{two} \\ \text{one} \leq \text{three} \end{cases} \\ \text{two} & \text{if } \text{two} \leq \text{three} \\ \text{three} & \text{otherwise} \end{cases} \quad b_{\text{eff}} = 96.375 \quad \text{in}$$

slab top steel

slab bottom steel

6.10.1.2

$$a_4 := \frac{2}{3} \cdot .01 \cdot b_{\text{eff}} \cdot t_s$$

$$a_5 := \frac{1}{3} \cdot .01 \cdot b_{\text{eff}} \cdot t_s$$

$$a_4 = 5.14 \quad \text{in}^2$$

$$a_5 = 2.57 \quad \text{in}^2$$

$$d_4 := 55.5 \quad \text{in}$$

$$d_5 := 52.5 \quad \text{in}$$

Centroid Calculation

from bottom of girder

$$y_c := \frac{\left(b_1 \cdot h_1 \cdot \frac{h_1}{2} \right) + \left[b_2 \cdot h_2 \cdot \left(\frac{h_2}{2} + h_1 \right) \right] + b_3 \cdot h_3 \cdot \left(\frac{h_3}{2} + h_2 + h_1 \right) + a_4 \cdot d_4 + a_5 \cdot d_5}{b_1 \cdot h_1 + b_2 \cdot h_2 + b_3 \cdot h_3 + a_4 + a_5}$$

$$y_c = 27.557 \quad \text{in}$$

$$A_c := h_1 \cdot b_1 + h_2 \cdot b_2 + h_3 \cdot b_3 + a_4 + a_5 \quad A_c = 88.96 \quad \text{in}^2$$

Plastic moment compression web depth

6.10.5.1.4b-2

$$D_{cp} := \frac{h_2}{2 \cdot F_y \cdot h_2 \cdot b_2} \left[F_y \cdot b_3 \cdot h_3 + F_y \cdot b_2 \cdot h_2 + F_y \cdot (a_4 + a_5) - F_y \cdot b_1 \cdot h_1 \right]$$

$$D_{cp} = 33.28 \text{ in}$$

Elastic moment compression web depth

$$D_c := y_c - h_1$$

$$D_c = 25.557 \text{ in}$$

Moment of Inertia Calculations (Second Moment of Area)

$$I_{xx} := \frac{1}{12} \cdot b_1 \cdot h_1^3 + b_1 \cdot h_1 \cdot \left(y_c - \frac{h_1}{2} \right)^2 + \left[\frac{1}{12} \cdot b_3 \cdot h_3^3 + b_3 \cdot h_3 \cdot \left(-y_c + h_1 + h_2 + \frac{h_3}{2} \right)^2 \right] \dots$$

$$+ \left[\frac{1}{12} \cdot b_2 \cdot h_2^3 + b_2 \cdot h_2 \cdot \left(\frac{h_2}{2} + h_1 - y_c \right)^2 + a_4 \cdot (d_4 - y_c)^2 + a_5 \cdot (d_5 - y_c)^2 \right]$$

$$I_{xx} = 46070.619727 \text{ in}^4$$

$$S := \frac{I_{xx}}{y_c}$$

$$S = 1671.848 \text{ in}^3$$

Radius of gyration for compression T

$$w_d := \frac{D_c}{3} \quad w_d = 8.519 \text{ in}$$

$$I_{rt} := \frac{1}{12} \cdot w_d \cdot b_2^3 + \frac{1}{12} \cdot h_1 \cdot b_1^3 \quad I_{rt} = 682.704 \text{ in}^4$$

$$A_T := w_d \cdot b_2 + h_1 \cdot b_1 \quad A_T = 35.195 \text{ in}^2$$

$$r_t := \sqrt{\frac{I_{rt}}{A_T}} \quad r_t = 4.404 \text{ in}$$

AASSTO factored moments

Assume Strength I determines max negative moments

Table 3.4.1-1 Strength I load factors

$$DC := 1.25$$

$$DW := 1.5$$

$$LL := 1.75$$

Dynamic load allowance

3.6.2.1-1

$$DA := .33$$

elastic analysis moments with AASHTO loading (STAAD)
2 trucks 50 ft apart over pier

$$M_{DC1} := 1957.64 \text{ in} \cdot \text{kips} \quad \text{steel dead load}$$

$$M_{DC2} := 9867.07 \text{ in} \cdot \text{kips} \quad \text{deck dead load}$$

$$M_{DW} := 525.17 \text{ in} \cdot \text{kips} \quad \text{wearing surface}$$

$$M_{LL} := 23484 \text{ in} \cdot \text{kips} \quad \text{Qcon live load}$$

Live load distribution factor

4.6.2.2.1-1

$$s_g = 9.67 \quad 3.5 \leq s \leq 16 \quad \text{ft}$$

$$t_s = 8 \quad 4.5 \leq t_s \leq 12 \quad \text{in}$$

$$L_2 = 105 \quad 20 \leq L \leq 240 \quad \text{ft}$$

$$n := \frac{E_s}{E_c} \quad n = 8.593$$

$$e_g := s_g \cdot 12 \quad e_g = 116.04 \text{ in}$$

$$A_c = 88.96 \text{ in}^2$$

$$K_g := n \cdot (I_{xx} + A_c \cdot e_g^2)$$

$$K_g = 10688687.424 \text{ in}^4$$

$$LDF := .06 + \left(\frac{s_g}{14} \right)^4 \cdot \left(\frac{s_g}{L_2} \right)^3 \cdot \left(\frac{K_g}{12 \cdot L_2 \cdot t_s^3} \right)^{.1}$$

$$LDF = 0.618$$

Final factored moment

$$M_{uu} := DC \cdot (M_{DC1} + M_{DC2}) + DW \cdot M_{DW} + LL \cdot M_{LL} \cdot LDF \cdot (1 + DA)$$

$$M_{uu} = 49367.912 \text{ in-kips}$$

Moment redistribution

6.10.2.2

$$M_u := .9 \cdot M_{uu}$$

$$M_u = 44431.121 \text{ in-kips}$$

Composite section check

Table 6.10.5.2.1-1

$$\text{compact} := \begin{cases} \text{"yes"} & \text{if } \frac{2 \cdot D_{cp}}{b_2} \leq 3.76 \cdot \sqrt{\frac{E_s}{F_y}} \\ \text{"no"} & \text{otherwise} \end{cases}$$

$$\text{compact} = \text{"no"}$$

Non composite beam so use section 6.10.5.3.3 for negative flexure

Nominal Flexural Resistance

6.10.5.3.3a

$$\lambda_b := 5.76 \quad \text{since comp flange} \geq \text{tens flange}$$

$$R_b := \begin{cases} 1 & \text{if } \frac{2 \cdot D_c}{b_2} \leq \lambda_b \cdot \sqrt{\frac{E_s}{F_y}} \\ \text{"use 6.10.5.4.2a-2"} & \text{otherwise} \end{cases}$$

$$R_b = 1 \quad \text{Load shedding factor}$$

$$M_y := F_y \cdot S$$

$$M_y = 60186.512 \text{ in}\cdot\text{kips}$$

$$M_{yr} := M_y \quad \text{since not hybrid}$$

$$R_h := \frac{M_{yr}}{M_y}$$

$$R_h = 1 \quad \text{Hybrid Factor}$$

$$F_{n1} := R_b \cdot R_h \cdot F_y$$

$$F_{n1} = 36 \text{ ksi}$$

Web Slenderness

6.10.5.3.3b

$$\text{webslend} := \begin{cases} \text{"okay"} & \text{if } \frac{2 \cdot D_c}{b_2} \leq 6.77 \cdot \sqrt{\frac{E_s}{F_y}} \\ \text{"check"} & \text{otherwise} \end{cases}$$

$$\text{webslend} = \text{"okay"} \quad \text{So } F_{n1} \text{ is okay}$$

Compression flange slenderness

$$\text{compslend} := \begin{cases} \text{"okay"} & \text{if } \frac{b_1}{2 \cdot h_1} \leq 1.38 \cdot \sqrt{\frac{E_s}{F_y \cdot \sqrt{\frac{2 \cdot D_c}{b_2}}}} \\ \text{"check"} & \text{otherwise} \end{cases}$$

$$\text{compslend} = \text{"okay"} \quad \text{So } F_{n1} \text{ is okay}$$

Compression flange Bracing

6.10.5.3.3d

$$\text{compbrace} := \begin{cases} \text{"okay"} & \text{if } L_b \leq 1.76 \cdot r_t \cdot \sqrt{\frac{E_s}{F_y}} \\ \text{"check"} & \text{otherwise} \end{cases}$$

compbrace = "check"

therefore use 6.10.5.5

Lateral torsional bending

6.10.5.5

$P_l := 0$ PI is 0 because it is at an inflection point

$$\sigma := \frac{\frac{M_u}{S} + \frac{M_u}{S} \cdot \left(1 - \frac{h_l}{y_c}\right)}{2}$$

average stress in comp flange

$$\sigma = 25.612$$

$$P_h := \frac{\sigma}{b_l \cdot h_l}$$

$$P_h = 0.8$$

$$C_b := 1.75 - 1.05 \cdot \left(\frac{P_l}{P_h}\right) + .3 \cdot \left(\frac{P_l}{P_h}\right)^3$$

$$C_b = 1.75$$

$$F_{nc} := \begin{cases} C_b \cdot R_b \cdot R_h \cdot F_y \cdot \left[1.33 - .187 \cdot \frac{L_b}{r_t} \cdot \sqrt{\frac{F_y}{E_s}} \right] & \text{if } L_b \leq 4.44 \cdot r_t \cdot \sqrt{\frac{E_s}{F_y}} \\ C_b \cdot R_b \cdot R_h \cdot \left[\frac{9.86 \cdot E_s}{\left(\frac{L_b}{r_t}\right)^2} \right] & \text{if } L_b > 4.44 \cdot r_t \cdot \sqrt{\frac{E_s}{F_y}} \end{cases}$$

$$F_{nc} = 54.951 \text{ ksi}$$

$$4.44 \cdot r_t \cdot \sqrt{\frac{E_s}{F_y}} = 555.021$$

$$F_{n2} := \begin{cases} R_b \cdot R_h \cdot F_y & \text{if } R_b \cdot R_h \cdot F_y \leq F_{nc} \\ F_{nc} & \text{otherwise} \end{cases}$$

$$F_{n2} = 36 \text{ ksi}$$

Failure check

$$\text{check} := \begin{cases} \text{"lat tors"} & \text{if } F_{n2} < F_{n1} \\ \text{"other"} & \text{otherwise} \end{cases}$$

$$\text{check} = \text{"other"}$$

Final nominal stress

$$F_n := \begin{cases} F_{n2} & \text{if } F_{n2} \leq F_{n1} \\ F_{n1} & \text{otherwise} \end{cases}$$

$$F_n = 36 \quad \text{ksi}$$

$$F_r := F_n \cdot \phi_f$$

$$F_r = 36 \quad \text{ksi}$$

$$F_u := \frac{M_u}{S}$$

$$F_u = 26.576 \quad \text{ksi}$$

$$\text{stability} := \begin{cases} \text{"Fail"} & \text{if } F_u > F_r \\ \text{"Pass"} & \text{otherwise} \end{cases}$$

$$\text{stability} = \text{"Pass"}$$

Therefore the girder is stable considering the large cross section from the bearing to the splice.

Appendix 2: I-35 AASHTO Stability Calculations

AASHTO Calculations for Lateral Bracing Adequacy of I-35 Bridge Assuming Diaphragms Removed

AASHTO calculations on the I-35 bridge were performed using the maximum live plus dead load moment in the negative moment region. All girder shape properties calculated assuming composite structure with the bridge deck. Some tests had factored maximum moment calculated prior to insertion into the calculation spreadsheet, while others included summing and factoring of individual moment components.

Maximum Loading:

- Dead Load of Superstructure and Deck
- Live Load Lane Loading, 0.64 kips
- Live Load Truck Loading, 2 trucks 50 ft apart centered over pier

Modeling:

- STAAD computer analysis performed on a single girder using AASHTO load distribution factors
- QConBridge₁ computer analysis used to double check particular calculations
- Moment data used in mathematical checks labeled as Tests 1 to 3 below

Test 1:

- Span 2 near Pier 2 considered
- Calculations considering large girder cross section (see attached table) the entire length to the splice (there is no section change here)
- L_b is considered to the splice, conservative assumption for zero moment under maximum moment shown
- The section passes AASHTO buckling checks

Test 2:

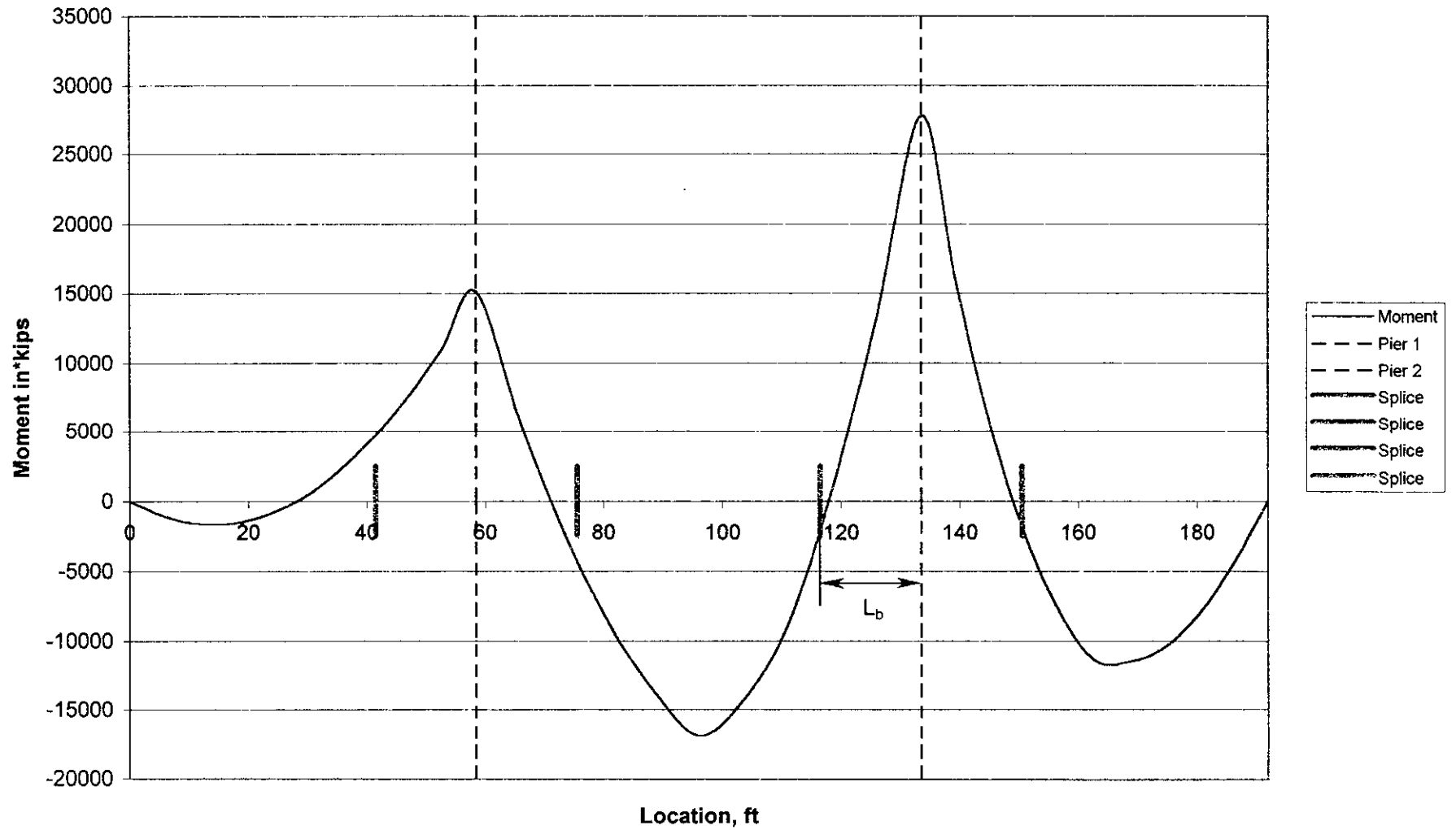
- Span 1 near Pier 1 considered
- Calculations considering large cross section to the section change (the splice in this case) distance from the pier
- C_b value is affected, as the moment at the end is no longer considered zero as shown in the on the moment diagram at the splice location
- L_b is considered to the live and dead load inflection point on the plot
- The section passes AASHTO buckling checks

Test 3:

- Span 1 near Pier 1 considered
- Calculations considering small cross section from the section change (the splice in this case) to the inflection point on the plot
- C_b value is maximum in this case as moment is zero at one end
- L_b is considered to the live and dead load inflection point on the plot
- The section passes AASHTO buckling checks

¹ QConBridge is an AASHTO bridge analysis program created by the Washington Department of Transportation. It can be downloaded at http://www.wsdot.wa.gov/eesc/bridge/software/index.cfm?fuseaction=download&software_id=48

AASHTO Strength I Live and Dead Load I-35



Stability Tests run for I-35 bridge

Test specifics and results

Test Number	Span	Unbraced Length (L_b)		Cross Section	Section Length	Section Type	Maximum Moment	Minimum Moment	Result
		ft	in				in*kips	in*kips	
1	2	17	204	Large	17	Compact	32000	0	PASS
2	1	29.4	352.8	Large	17	Non-compact	15100	4500	PASS
3	1	29.4	352.8	Small	12.4	Non-compact	4500	0	PASS

Cross Section Dimensions

Cross Section	Bottom Flange (in)		Web (in)		Top Flange (in)	
	thickness	length	thickness	length	thickness	length
Large	1.75	12	0.5	32	1.75	12
Small	0.8125	12	0.625	33.875	0.8125	12

TEST 1

AASHTO CALCS FOR STABILITY OF GIRDERS 4/15/02 DAVID TARRIES

2 cross section dimensions are available for the interior and exterior girder
the interior girder is checked here

large cross section, mid span section, composite with 8 inch deck, consider the large section
for the whole unbraced length (which is how the bridge was designed and built).

$$F_y := 36 \quad f_c := 3 \quad \text{ksi} \quad E_s := 29000 \quad E_c := \frac{57000 \cdot \sqrt{f_c \cdot 1000}}{1000} \quad E_c = 3122.019$$

Limit state

6.5.4

$$\phi_f := 1$$

assume L_b is to inflection point of dead loaded beam (splice)

$$L_b := 204 \quad \text{in}$$

Spans

$$L_1 := 58.5 \quad \text{ft} \quad L_2 := 75 \quad \text{ft} \quad L_3 := 58.5 \quad \text{ft}$$

use largest span and estimate the effective span between dead load
inflection points

$$L := L_2 \cdot 0.8 \quad L = 60 \quad \text{ft}$$

Average girder spacing

$$s_g := 9.5 \quad \text{ft}$$

Deck

$$t_s := 8 \quad \text{in}$$

Section Dimensions: (b is base dimension and h is height dimension)

if cross section is not double
symmetric then check calcs

units : INCHES

section 1	section 2	section 3
bottom flange	web	top flange

$$b_1 := 12 \quad b_2 := .5 \quad b_3 := 12$$

$$h_1 := 1.75 \quad h_2 := 32 \quad h_3 := 1.75$$

4.6.2.6.1

$$\text{one} := .25 \cdot L \cdot 12 \quad \text{one} = 180 \quad \text{in}$$

$$\text{two} := 12 \cdot t_s + \begin{cases} (.5 \cdot h_3) & \text{if } .5 \cdot h_3 \leq b_2 \\ b_2 & \text{otherwise} \end{cases} \quad \text{two} = 96.5 \quad \text{in}$$

$$\text{three} := s_g \cdot 12 \quad \text{three} = 114 \quad \text{in}$$

$$b_{\text{eff}} := \begin{cases} \text{one} & \text{if } \begin{cases} \text{one} \leq \text{two} \\ \text{one} \leq \text{three} \end{cases} \\ \text{two} & \text{if } \text{two} \leq \text{three} \\ \text{three} & \text{otherwise} \end{cases} \quad b_{\text{eff}} = 96.5 \quad \text{in}$$

slab top steel

slab bottom steel

6.10.1.2

$$a_4 := \frac{2}{3} \cdot .01 \cdot b_{\text{eff}} \cdot t_s \quad a_5 := \frac{1}{3} \cdot .01 \cdot b_{\text{eff}} \cdot t_s$$

$$a_4 = 5.147 \quad \text{in}^2 \quad a_5 = 2.573 \quad \text{in}^2$$

$$d_4 := 37.55 \quad \text{in} \quad d_5 := 41.55 \quad \text{in}$$

Centroid Calculation

from bottom of girder

$$y_c := \frac{\left(b_1 \cdot h_1 \cdot \frac{h_1}{2} \right) + \left[b_2 \cdot h_2 \cdot \left(\frac{h_2}{2} + h_1 \right) \right] + b_3 \cdot h_3 \cdot \left(\frac{h_3}{2} + h_2 + h_1 \right) + a_4 \cdot d_4 + a_5 \cdot d_5}{b_1 \cdot h_1 + b_2 \cdot h_2 + b_3 \cdot h_3 + a_4 + a_5}$$

$$y_c = 20.232 \quad \text{in}$$

$$A_c := h_1 \cdot b_1 + h_2 \cdot b_2 + h_3 \cdot b_3 + a_4 + a_5 \quad A_c = 65.72 \quad \text{in}^2$$

Plastic moment compression web depth

6.10.5.1.4b-2

$$D_{cp} := \frac{h_2}{2 \cdot F_y \cdot h_2 \cdot b_2} \left[F_y \cdot b_3 \cdot h_3 + F_y \cdot b_2 \cdot h_2 + F_y \cdot (a_4 + a_5) - F_y \cdot b_1 \cdot h_1 \right]$$

$$D_{cp} = 23.72 \quad \text{in}$$

Elastic moment compression web depth

$$D_c := y_c - h_1$$

$$D_c = 18.482 \quad \text{in}$$

Moment of Inertia Calculations (Second Moment of Area)

$$I_{xx} := \frac{1}{12} \cdot b_1 \cdot h_1^3 + b_1 \cdot h_1 \cdot \left(y_c - \frac{h_1}{2} \right)^2 + \left[\frac{1}{12} \cdot b_3 \cdot h_3^3 + b_3 \cdot h_3 \cdot \left(-y_c + h_1 + h_2 + \frac{h_3}{2} \right)^2 \right] + \left[\frac{1}{12} \cdot b_2 \cdot h_2^3 + b_2 \cdot h_2 \cdot \left(\frac{h_2}{2} + h_1 - y_c \right)^2 + a_4 \cdot (d_4 - y_c)^2 + a_5 \cdot (d_5 - y_c)^2 \right]$$

$$I_{xx} = 16406.529653 \quad \text{in}^4$$

$$S := \frac{I_{xx}}{y_c}$$

$$S = 810.9 \quad \text{in}^3$$

Radius of gyration for compression T

$$w_d := \frac{D_c}{3} \quad w_d = 6.161 \quad \text{in}$$

$$I_{rt} := \frac{1}{12} \cdot w_d \cdot b_2^3 + \frac{1}{12} \cdot h_1 \cdot b_1^3 \quad I_{rt} = 252.064 \quad \text{in}^4$$

$$A_T := w_d \cdot b_2 + h_1 \cdot b_1 \quad A_T = 24.08 \quad \text{in}^2$$

$$r_t := \sqrt{\frac{I_{rt}}{A_T}} \quad r_t = 3.235 \quad \text{in}$$

AASHTO factored moments

Assume Strength I determines max negative moments

Table 3.4.1-1 Strength I load factors

$$DC := 1.25$$

$$DW := 1.5$$

$$LL := 1.75$$

Dynamic load allowance

3.6.2.1-1

$$DA := .33$$

elastic analysis moments with AASHTO loading (STAAD)
2 trucks 50 ft apart over pier

$$M_{DC1} := 735.214 \text{ in} \cdot \text{kips} \quad \text{steel dead load}$$

$$M_{DC2} := 5100 \text{ in} \cdot \text{kips} \quad \text{deck dead load}$$

$$M_{DW} := 294.1 \text{ in} \cdot \text{kips} \quad \text{wearing surface}$$

$$M_{LL} := 14250 \text{ in} \cdot \text{kips} \quad \text{Live load (2 trucks)}$$

Live load distribution factor

4.6.2.2.1-1

$$s_g = 9.5 \quad 3.5 \leq s \leq 16$$

$$t_s = 8 \quad 4.5 \leq t_s \leq 12$$

$$L_2 = 75 \quad 20 \leq L \leq 240$$

$$n := \frac{E_s}{E_c} \quad n = 9.289$$

$$e_g := s_g \cdot 12 \quad e_g = 114 \text{ in}$$

$$A_c = 65.72 \text{ in}^2$$

$$K_g := n \cdot (I_{xx} + A_c \cdot e_g^2)$$

$$K_g = 8085988.347 \text{ in}^4$$

$$LDF := .06 + \left(\frac{s_g}{14}\right)^4 \cdot \left(\frac{s_g}{L_2}\right)^3 \cdot \left(\frac{K_g}{12 \cdot L_2 \cdot t_s^3}\right)^1$$

$$LDF = 0.674$$

$$LDF := .85$$

Final factored moment

$$M_{uu} := DC \cdot (M_{DC1} + M_{DC2}) + DW \cdot M_{DW} + LL \cdot M_{LL} \cdot LDF \cdot (1 + DA)$$

$$M_{uu} = 35927.011$$

Moment redistribution

6.10.2.2

$$M_u := .9 \cdot M_{uu}$$

$$M_u = 32334.31$$

Composite section check

Table 6.10.5.2.1-1

$$\text{compact} := \begin{cases} \text{"yes"} & \text{if } \frac{2 \cdot D_{cp}}{b_2} \leq 3.76 \cdot \sqrt{\frac{E_s}{F_y}} \\ \text{"no"} & \text{otherwise} \end{cases}$$

$$\text{compact} = \text{"yes"}$$

$$\text{compact2} := \begin{cases} \text{"yes"} & \text{if } \frac{b_1}{2 \cdot h_1} \leq .382 \cdot \sqrt{\frac{E_s}{F_y}} \\ \text{"no"} & \text{otherwise} \end{cases}$$

$$\text{compact2} = \text{"yes"}$$

composite beam so use section 6.10.5.3.2 for negative flexure

weak axis moment of inertia

$$x_c := \frac{\left(h_1 \cdot b_1 \cdot \frac{b_1}{2}\right) + \left(h_3 \cdot b_3 \cdot \frac{b_1}{2}\right) + \left(h_2 \cdot b_2 \cdot \frac{b_1}{2}\right)}{h_1 \cdot b_1 + h_2 \cdot b_2 + h_3 \cdot b_3}$$

$$x_c = 6 \text{ in}$$

$$I_{yy} := \frac{1}{12} \cdot h_1 \cdot b_1^3 + b_1 \cdot h_1 \cdot \left(\frac{b_1}{2} - x_c \right)^2 + \frac{1}{12} \cdot h_3 \cdot b_3^3 + b_3 \cdot h_3 \cdot \left(\frac{b_1}{2} - x_c \right)^2 \dots$$

$$+ \left[\frac{1}{12} \cdot h_2 \cdot b_2^3 + h_2 \cdot b_2 \cdot \left(\frac{b_1}{2} - x_c \right)^2 \right]$$

$$I_{yy} = 504.33 \text{ in}^4$$

$$r_y := \sqrt{\frac{I_{yy}}{A_c}}$$

$$r_y = 2.77 \text{ in}$$

$$Z_x := b_1 \cdot h_1 \cdot \left(y_c - \frac{h_1}{2} \right) + b_3 \cdot h_3 \cdot \left(h_2 - y_c - h_1 + \frac{h_3}{2} \right) \dots$$

$$+ \left[\left(h_2 - y_c - h_1 \right) \cdot b_2 \cdot \left(\frac{h_2 - y_c - h_1}{2} \right) + \left(y_c - h_1 \right) \cdot b_2 \cdot \left(\frac{y_c - h_1}{2} \right) \right]$$

$$Z_x = 745.738 \text{ in}^3$$

$$Z_y := 2 \cdot \left(\frac{b_1}{4} \cdot \frac{b_1}{2} \cdot h_1 \right) + 2 \cdot \frac{b_3}{4} \cdot \frac{b_3}{2} \cdot h_3$$

$$Z_y = 126 \text{ in}^3$$

$$M_1 := 0 \quad \text{since other end of Lb is an inflection point}$$

Table A6.1-2

6.10.5.1.3

$$Y := \frac{h_2}{2} \cdot \left(\frac{F_y \cdot h_1 \cdot b_1 - F_y \cdot h_3 \cdot b_3 - F_y \cdot a_4 - F_y \cdot a_5}{F_y \cdot b_2 \cdot h_2} + 1 \right)$$

$$d_{rb} := -(h_1 + h_2 - Y - d_4) \quad d_{rb} = 12.08$$

$$d_{rt} := -(h_1 + h_2 - Y - d_5) \quad d_{rt} = 16.08$$

$$d_c := \frac{h_1}{2} + h_2 - Y \quad d_c = 24.595$$

$$d_t := -\left(\frac{-h_3}{2} - Y\right) \quad d_t = 9.155$$

$$M_p := \begin{cases} \frac{F_y \cdot b_2 \cdot h_2}{2 \cdot h_2} \left[Y^2 + (h_2 - Y)^2 \right] \dots & \text{if } (F_y \cdot h_1 \cdot b_1 + F_y \cdot b_2 \cdot h_2 \geq F \\ + (F_y \cdot h_1 \cdot b_1 \cdot d_c + F_y \cdot h_3 \cdot b_3 \cdot d_t + F_y \cdot a_4 \cdot d_{rb} + F_y \cdot a_5 \cdot d_{rt}) \\ \text{"bad"} & \text{otherwise} \end{cases}$$

$$M_p = 34923.605 \text{ in-kips}$$

$$\text{compact3} := \begin{cases} \text{"yes"} & \text{if } L_b \leq \left(.124 - .0759 \cdot \frac{M_1}{M_p} \right) \cdot \frac{r_y \cdot E_s}{F_y} \\ \text{"no"} & \text{otherwise} \end{cases}$$

$$\text{compact3} = \text{"yes"}$$

Nominal Flexural Resistance

6.10.5.2.3a

$$M_n := M_p$$

$$M_n = 34923.605 \text{ in-kips}$$

Web Slenderness

6.10.5.2.3b

$$\text{webslend} := \begin{cases} \text{"okay"} & \text{if } \frac{2 \cdot D_{cp}}{b_2} \leq 3.76 \cdot \sqrt{\frac{E_s}{F_y}} \\ \text{"check"} & \text{otherwise} \end{cases}$$

$$\text{webslend} = \text{"okay"}$$

So Mp is okay

Compression flange slenderness

$$\text{compslend} := \begin{cases} \text{"okay"} & \text{if } \frac{b_1}{2 \cdot h_1} \leq .382 \cdot \sqrt{\frac{E_s}{F_y}} \\ \text{"check"} & \text{otherwise} \end{cases}$$

$$\text{compslend} = \text{"okay"}$$

Mp Equation continued:

$$y \cdot h_3 \cdot b_3 + F_y \cdot a_4 + F_y \cdot a_5)$$

Compression flange Bracing

6.10.5.3.3d

$$\text{compbrace} := \begin{cases} \text{"okay"} & \text{if } L_b \leq .124 - .0759 \cdot \frac{M_1}{M_p} \cdot \frac{r_y \cdot E_s}{F_y} \\ \text{"check"} & \text{otherwise} \end{cases}$$

compbrace = "okay"

Lateral torsional bending

Final nominal stress

$$M_r := M_n \cdot \phi_f$$

$$M_r = 34923.605 \text{ in}\cdot\text{kips}$$

$$M_u = 32334.31 \text{ in}\cdot\text{kips}$$

$$\text{stability} := \begin{cases} \text{"Fail"} & \text{if } M_u > M_r \\ \text{"Pass"} & \text{otherwise} \end{cases}$$

stability = "Pass"

Therefore the large section is capable of supporting maximum AASHTO Strength I loading without the diaphragms in the negative moment region.

Appendix 3: IA-17 AASHTO Stability Calculations

AASHTO Calculations for Lateral Bracing Adequacy of IA-17 Bridge Assuming Diaphragms Removed

AASHTO calculations on the IA-17 bridge were performed using the maximum live plus dead load moment in the negative moment region. All girder shape properties calculated assuming composite structure with the bridge deck. Some tests had factored maximum moment calculated prior to insertion into the calculation spreadsheet, while others included summing and factoring of individual moment components.

Maximum Loading:

- Dead Load of Superstructure and Deck
- Live Load Lane Loading, 0.64 kips
- Live Load Truck Loading, 2 trucks 50 ft apart centered over pier

Modeling:

- STAAD computer analysis performed on a single girder using AASHTO load distribution factors
- QConBridge₁ computer analysis used to double check particular calculations
- Moment data used in mathematical checks labeled as Tests 1 to 7 below

Test 1:

- Span 2 near Pier 2 considered
- Calculations considering large girder cross section (see attached table) the entire length to the splice
- L_b is considered to the splice, conservative assumption for zero moment under maximum moment shown
- The section passes AASHTO buckling checks

Test 2:

- Span 2 near Pier 2 considered
- Calculations considering medium girder cross section (see attached table) the entire length to the splice
- L_b is considered to the splice, conservative assumption for zero moment under maximum moment shown
- The section fails AASHTO buckling, use Tests 3 and 4 instead

Test 3:

- Span 2 near Pier 2 considered
- Calculations considering large cross section to the section change distance from the pier
- C_b value is affected, as the moment at the end is no longer considered zero as shown in the on the moment diagram at the splice location (M_1 and M_2 on plot)
- L_b is considered to the live and dead load inflection point on the plot
- The section passes AASHTO buckling checks

Test 4:

- Span 2 near Pier 2 considered
- Calculations considering medium cross section from the section change to the inflection point on the plot
- C_b value is maximum in this case as moment is zero at one end (M_2 and M_3 on plot)
- L_b is considered to the live and dead load inflection point on the plot
- The section passes AASHTO buckling checks

Test 5:

- Span 1 near Pier 1 considered
- Calculations considering large cross section to the section change distance from the pier
- C_b value is affected, as the moment at the end is no longer considered zero as shown in the on the moment diagram at the splice location
- L_b is considered to the live and dead load inflection point on the plot
- The section passes AASHTO buckling checks

Test 6:

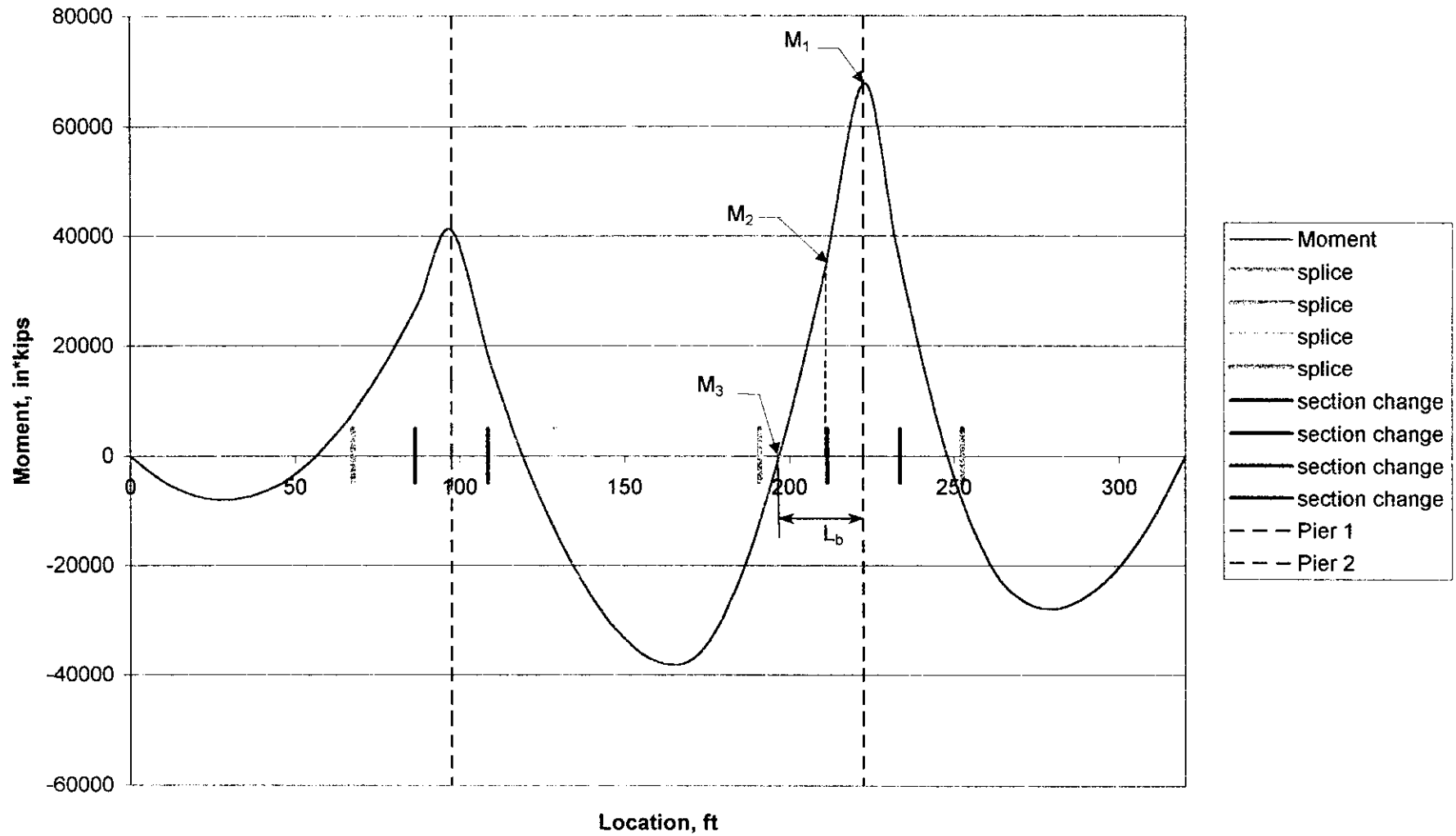
- Span 1 near Pier 1 considered
- Calculations considering medium cross section to the section change distance from the pier
- C_b value is affected, as the moment at the end is no longer considered zero as shown in the on the moment diagram at the splice location
- L_b is considered to the live and dead load inflection point on the plot
- The section passes AASHTO buckling checks

Test 7:

- Span 1 near Pier 1 considered
- Calculations considering small cross section to the section change distance from the pier
- C_b value is affected, as the moment at the end is no longer considered zero as shown in the on the moment diagram at the splice location
- L_b is considered to the live and dead load inflection point on the plot
- The section passes AASHTO buckling checks

¹ QConBridge is an AASHTO bridge analysis program created by the Washington Department of Transportation. It can be downloaded at http://www.wsdot.wa.gov/eesc/bridge/software/index.cfm?fuseaction=download&software_id=48

AASHTO Strength I Live and Dead Load IA-17



Stability Tests run for IA-17 bridge

Test specifics and results

Test Number	Span	Unbraced Length (L_b)		Cross Section	Section Length	Section Type	Maximum Moment	Minimum Moment	Result
		ft	in		ft		in*kips	in*kips	
1	2	31.5	378	Large	31.5	Non-compact	64998	0	PASS
2	2	31.5	378	Medium	31.5	Non-compact	64076	0	FAIL
3	2	25	300	Large	11	Non-compact	67738	37300	PASS
4	2	25	300	Medium	20.5	Non-compact	37300	0	PASS
5	1	41	492	Large	11	Non-compact	41136	29000	PASS
6	1	41	492	Medium	19	Non-compact	29000	9500	PASS
7	1	41	492	Small	11	Non-compact	9500	0	PASS

Cross Section Dimension

Cross Section	Bottom Flange (in)		Web (in)		Top Flange (in)	
	thickness	length	thickness	length	thickness	length
Large	1.5	22	0.375	59.5	1.5	22
Medium	1.5	15	0.375	59.5	1.5	15
Small	1	15	0.375	60.75	0.75	12

TEST 1

AASHTO CALCS FOR STABILITY OF GIRDERS 4/15/02 DAVID TARRIES

3 cross section dimensions are available for the interior and exterior girder
the interior girder is checked here

Section 1 (large) at maximum moment side of span 2 considering only one cross section of girder

$$F_y := 36 \quad f_c := 3.5 \text{ ksi} \quad E_s := 29000 \quad E_c := \frac{57000 \cdot \sqrt{f_c \cdot 1000}}{1000} \quad E_c = 3372.165$$

Limit state

6.5.4

$$\phi_f := 1$$

assume L_b is to inflection point of dead loaded beam, splice point

$$L_b := 378 \text{ in}$$

Spans

$$L_1 := 97.5 \text{ ft} \quad L_2 := 125 \text{ ft} \quad L_3 := 97.5 \text{ ft}$$

use largest span and estimate the effective span between dead load inflection points

$$L := L_2 \cdot 0.8 \quad L = 100 \text{ ft}$$

Average girder spacing

$$s_g := 10 \text{ ft}$$

Deck

$$t_s := 8 \text{ in}$$

Section Dimensions: (b is base dimension and h is height dimension)

if cross section is not double symmetric then check calcs

units : INCHES

section 1	section 2	section 3
bottom flange	web	top flange

$$\begin{array}{lll}
 b_1 := 22 & b_2 := .375 & b_3 := 22 \\
 h_1 := 1.5 & h_2 := 59.5 & h_3 := 1.5
 \end{array}$$

girder dimensions in inches

4.6.2.6.1

$$\begin{array}{ll}
 \text{one} := .25 \cdot L \cdot 12 & \text{one} = 300 \\
 \text{two} := 12 \cdot t_s + \begin{cases} (.5 \cdot h_3) & \text{if } .5 \cdot h_3 \leq b_2 \\ b_2 & \text{otherwise} \end{cases} & \text{two} = 96.375 \\
 \text{three} := s_g \cdot 12 & \text{three} = 120
 \end{array}$$

$$b_{\text{eff}} := \begin{cases} \text{one} & \text{if } \begin{cases} \text{one} \leq \text{two} \\ \text{one} \leq \text{three} \end{cases} \\ \text{two} & \text{if } \text{two} \leq \text{three} \\ \text{three} & \text{otherwise} \end{cases}$$

$b_{\text{eff}} = 96.375 \text{ in}$

slab top steel

slab bottom steel

6.10.1.2

$$\begin{array}{ll}
 a_4 := \frac{2}{3} \cdot .01 \cdot b_{\text{eff}} \cdot t_s & a_5 := \frac{1}{3} \cdot .01 \cdot b_{\text{eff}} \cdot t_s \\
 a_4 = 5.14 \text{ in}^2 & a_5 = 2.57 \text{ in}^2 \\
 d_4 := 65.5 \text{ in} & d_5 := 69.5 \text{ in}
 \end{array}$$

Centroid Calculation

from bottom of girder

$$y_c := \frac{\left(b_1 \cdot h_1 \cdot \frac{h_1}{2} \right) + \left[b_2 \cdot h_2 \cdot \left(\frac{h_2}{2} + h_1 \right) \right] + b_3 \cdot h_3 \cdot \left(\frac{h_3}{2} + h_2 + h_1 \right) + a_4 \cdot d_4 + a_5 \cdot d_5}{b_1 \cdot h_1 + b_2 \cdot h_2 + b_3 \cdot h_3 + a_4 + a_5}$$

$$y_c = 34.107 \text{ in}$$

$$A_c := h_1 \cdot b_1 + h_2 \cdot b_2 + h_3 \cdot b_3 + a_4 + a_5 \quad A_c = 96.022 \text{ in}^2$$

Plastic moment compression web depth

6.10.5.1.4b-2

$$D_{cp} := \frac{h_2}{2 \cdot F_y \cdot h_2 \cdot b_2} \left[F_y \cdot b_3 \cdot h_3 + F_y \cdot b_2 \cdot h_2 + F_y \cdot (a_4 + a_5) - F_y \cdot b_1 \cdot h_1 \right]$$

$$D_{cp} = 40.03 \text{ in}$$

Elastic moment compression web depth

$$D_c := y_c - h_1$$

$$D_c = 32.607 \text{ in}$$

Moment of Inertia Calculations (Second Moment of Area)

$$I_{xx} := \frac{1}{12} \cdot b_1 \cdot h_1^3 + b_1 \cdot h_1 \cdot \left(y_c - \frac{h_1}{2} \right)^2 + \left[\frac{1}{12} \cdot b_3 \cdot h_3^3 + b_3 \cdot h_3 \cdot \left(-y_c + h_1 + h_2 + \frac{h_3}{2} \right)^2 \right] \dots$$

$$+ \left[\frac{1}{12} \cdot b_2 \cdot h_2^3 + b_2 \cdot h_2 \cdot \left(\frac{h_2}{2} + h_1 - y_c \right)^2 + a_4 \cdot (d_4 - y_c)^2 + a_5 \cdot (d_5 - y_c)^2 \right]$$

$$I_{xx} = 76997.296362 \text{ in}^4$$

$$S := \frac{I_{xx}}{y_c}$$

$$S = 2257.514 \text{ in}^3$$

Radius of gyration for compression T

$$w_d := \frac{D_c}{3} \quad w_d = 10.869 \text{ in}$$

$$I_{rt} := \frac{1}{12} \cdot w_d \cdot b_2^3 + \frac{1}{12} \cdot h_1 \cdot b_1^3 \quad I_{rt} = 1331.048 \text{ in}^4$$

$$A_T := w_d \cdot b_2 + h_1 \cdot b_1 \quad A_T = 37.076 \text{ in}^2$$

$$r_t := \sqrt{\frac{I_{rt}}{A_T}} \quad r_t = 5.992 \text{ in}$$

AASHTO factored moments

Assume Strength I determines max negative moments

Table 3.4.1-1 Strength I load factors

$$DC := 1.25$$

$$DW := 1.5$$

$$LL := 1.75$$

Dynamic load allowance

3.6.2.1-1

$$DA := .33$$

elastic analysis moments with AASHTO loading (STAAD)
2 trucks 50 ft apart over pier

$$M_{DC1} := 4540 \quad \text{in*kips} \quad \text{steel dead load}$$

$$M_{DC2} := 15300 \quad \text{in*kips} \quad \text{deck dead load}$$

$$M_{DW} := 833 \quad \text{in*kips} \quad \text{wearing surface}$$

$$M_{LL} := 32964 \quad \text{in*kips} \quad \text{Live load (QCON Program AASHTO Live Load)}$$

Live load distribution factor

4.6.2.2.1-1

$$s_g = 10 \quad 3.5 \leq s \leq 16$$

$$t_s = 8 \quad 4.5 \leq t_s \leq 12$$

$$L_2 = 125 \quad 20 \leq L \leq 240$$

$$n := \frac{E_s}{E_c} \quad n = 8.6$$

$$e_g := s_g \cdot 12 \quad e_g = 120$$

$$A_c = 96.022$$

$$K_g := n \cdot (I_{xx} + A_c \cdot e_g^2)$$

$$K_g = 12553333.427$$

$$LDF := .06 + \left(\frac{s_g}{14} \right)^4 + \left(\frac{s_g}{L_2} \right)^3 + \left(\frac{K_g}{12 \cdot L_2 \cdot t_s^3} \right)^1$$

$$LDF = 0.602$$

Final factored moment

$$M_{uu} := DC \cdot (M_{DC1} + M_{DC2}) + DW \cdot M_{DW} + LL \cdot M_{LL} \cdot LDF \cdot (1 + DA)$$

$$M_{uu} = 72219.586 \text{ in} \cdot \text{kip}$$

Moment redistribution

6.10.2.2

$$M_u := .9 \cdot M_{uu}$$

$$M_u = 64997.627 \text{ in} \cdot \text{kip}$$

Composite section check

Table 6.10.5.2.1-1

$$\text{compact} := \begin{cases} \text{"yes"} & \text{if } \frac{2 \cdot D_{cp}}{b_2} \leq 3.76 \cdot \sqrt{\frac{E_s}{F_y}} \\ \text{"no"} & \text{otherwise} \end{cases}$$

$$\text{compact} = \text{"no"}$$

Non composite beam so use section 6.10.5.3.3 for negative flexure

Nominal Flexural Resistance

6.10.5.3.3a

$$\lambda_b := 5.76 \quad \text{since comp flange} \geq \text{tens flange}$$

$$f_c := \frac{M_u}{S} \quad f_c = 28.792 \text{ ksi}$$

$$A_{fc} := h_3 \cdot b_2$$

$$a_r := \frac{2 \cdot D_c \cdot b_2}{A_{fc}}$$

$$R_b := \begin{cases} 1 & \text{if } \frac{2 \cdot D_c}{b_2} \leq \lambda_b \cdot \sqrt{\frac{E_s}{f_c}} \\ 1 - \left(\frac{a_r}{1200 + 300 \cdot a_r} \right) \cdot \left(\frac{2 \cdot D_c}{b_2} - \lambda_b \cdot \sqrt{\frac{E_s}{f_c}} \right) & \text{otherwise} \end{cases}$$

$$R_b = 1 \quad \text{Load shedding factor}$$

$$M_y := F_y \cdot S$$

$$M_y = 81270.507 \quad \text{ksi}$$

$$M_{yr} := M_y \quad \text{since not hybrid}$$

$$R_h := \frac{M_{yr}}{M_y}$$

$$R_h = 1 \quad \text{Hybrid Factor}$$

$$F_{n1} := R_b \cdot R_h \cdot F_y$$

$$F_{n1} = 36 \quad \text{ksi}$$

Web Slenderness

6.10.5.3.3b

$$\text{webslend} := \begin{cases} \text{"okay"} & \text{if } \frac{2 \cdot D_c}{b_2} \leq 6.77 \cdot \sqrt{\frac{E_s}{F_y}} \\ \text{"check"} & \text{otherwise} \end{cases}$$

$$\text{webslend} = \text{"okay"} \quad \text{So } F_{n1} \text{ is okay}$$

Compression flange slenderness

$$\text{compslend} := \begin{cases} \text{"okay"} & \text{if } \frac{b_1}{2 \cdot h_1} \leq 1.38 \cdot \sqrt{\frac{E_s}{F_y \cdot \sqrt{\frac{2 \cdot D_c}{b_2}}}} \\ \text{"check"} & \text{otherwise} \end{cases}$$

compslend = "okay"

So Fn1 okay

Compression flange Bracing

6.10.5.3.3d

$$\text{compbrace} := \begin{cases} \text{"okay"} & \text{if } L_b \leq 1.76 \cdot r_t \cdot \sqrt{\frac{E_s}{F_y}} \\ \text{"check"} & \text{otherwise} \end{cases}$$

compbrace = "check"

therefore use 6.10.5.5

Lateral torsional bending

6.10.5.5

$P_1 := 0$

PI is 0 because it is at an inflection point

$$\sigma := \frac{\frac{M_u}{S} + \frac{M_u}{S} \cdot \left(1 - \frac{h_l}{y_c}\right)}{2}$$

average stress in comp flange

$$\sigma = 28.159 \text{ ksi}$$

$$P_h := \frac{\sigma}{b_l \cdot h_l}$$

$$P_h = 0.853 \text{ kip}$$

$$C_b := 1.75 - 1.05 \cdot \frac{P_l}{P_h} + 0.3 \cdot \frac{P_l^3}{P_h^3}$$

$$C_b = 1.75$$

$$F_{nc} := \begin{cases} C_b \cdot R_b \cdot R_h \cdot F_y \cdot \left[1.33 - 0.187 \cdot \frac{L_b}{r_t} \cdot \sqrt{\frac{F_y}{E_s}} \right] & \text{if } L_b \leq 4.44 \cdot r_t \cdot \sqrt{\frac{E_s}{F_y}} \\ C_b \cdot R_b \cdot R_h \cdot \left[\frac{9.86 \cdot E_s}{\left(\frac{L_b}{r_t}\right)^2} \right] & \text{if } L_b > 4.44 \cdot r_t \cdot \sqrt{\frac{E_s}{F_y}} \end{cases}$$

$$F_{nc} = 57.604 \quad \text{ksi}$$

$$4.44 \cdot r_t \cdot \sqrt{\frac{E_s}{F_y}} = 755.06$$

$$F_{n2} := \begin{cases} R_b \cdot R_h \cdot F_y & \text{if } R_b \cdot R_h \cdot F_y \leq F_{nc} \\ F_{nc} & \text{otherwise} \end{cases}$$

$$F_{n2} = 36 \quad \text{ksi}$$

Failure check

$$\text{check} := \begin{cases} \text{"lat tors"} & \text{if } F_{n2} < F_{n1} \\ \text{"other"} & \text{otherwise} \end{cases}$$

$$\text{check} = \text{"other"}$$

Final nominal stress

$$F_n := \begin{cases} F_{n2} & \text{if } F_{n2} \leq F_{n1} \\ F_{n1} & \text{otherwise} \end{cases}$$

$$F_n = 36 \quad \text{ksi}$$

$$F_r := F_n \cdot \phi_f$$

$$F_r = 36 \quad \text{ksi}$$

$$F_u := \frac{M_u}{S}$$

$$F_u = 28.792 \quad \text{ksi}$$

$$\text{stability} := \begin{cases} \text{"Fail"} & \text{if } F_u > F_r \\ \text{"Pass"} & \text{otherwise} \end{cases}$$

$$\text{stability} = \text{"Pass"}$$

Therefore structure is capable of having negative moment diaphragms removed